Direct Synthesis of Hydrogen Peroxide from Hydrogen and Oxygen over Catalysts Containing Gold

Thesis submitted in accordance with the requirements of the University
of Cardiff for the degree of Doctor of Philosophy by
Jennifer Kelly Edwards

October 2006

UMI Number: U584968

UMI

Dissertation Publishing

ProQuest

Abstract (microfiche)

The direct synthesis of hydrogen peroxide from hydrogen and oxygen over supported gold, palladium and gold palladium catalysts was studied in a high-pressure stirred autoclave containing a stabiliser-free solvent system. The rate of H_2O_2 synthesis for supported Au catalysts was found to be lower than that of the Pd only catalysts. However, carbon, titania, iron oxide and alumina supported Au-Pd catalysts are significantly more active and selective for H_2O_2 synthesis than the monometallic catalysts. For silica supported gold-palladium catalysts, the activity was found to scale directly with palladium content and no synergy was observed with gold-palladium catalysts. Gold-palladium catalysts prepared on iron oxide, alumina and titania were all found to form core-shell structures on calcination consisting of a gold core surrounded by a palladium shell. However, on silica and activated carbon the bimetallic catalysts formed homogenous alloys. The activity and selectivity of the catalyst was found to be highly dependant on the reaction conditions employed; factors such as catalyst mass, solvent composition, catalyst composition and reaction length had significant effects on the catalyst activity. Modification of the support with a dilute acid prior to metal deposition led to gold-palladium catalysts with >98% selectivity to H_2O_2 when compared to catalysts prepared on the unmodified support. This increase in catalytic performance corresponded to an increase in metal particle size - indicating that smaller gold-palladium catalysts are highly active and selective for the direct synthesis of hydrogen peroxide. Acid pre-treatment of silica prior to metal deposition led to bimetallic catalysts where the activity did not scale with the palladium content.

Abstract

The direct synthesis of hydrogen peroxide from hydrogen and oxygen over supported gold, palladium and gold-palladium catalysts was studied in a high-pressure stirred autoclave. All prepared catalysts were evaluated for H_2O_2 synthesis using reaction conditions optimised in previous work, namely 10mg catalyst, water : methanol solvent system, 1200rpm stirring at 30 bar pressure (using dilute gases) for 30 min at 2°C. te reaction medium was free of any promoters or stabilisers.

The preparation method was shown to be very important in the formation of highly active catalysts. The impregnation method produced catalysts with large Au particles when supported on TiO_2 and Al_2O_3 and these catalysts were found to be active for the formation of H_2O_2 but inactive (due to large particle size) for CO oxidation. Preparation of Au-Pd core shell particles (on Fe_2O_3, Al_2O_3 and TiO_2) by calcination at 400°C for 3 hours in static air of the fresh, impregnated catalyst produced stable catalysts highly active and selective for the direct synthesis of H_2O_2. Catalysts supported on SiO_2 and activated carbon formed homogenous alloys when treated in the same manner.

The activity of Au-Pd catalysts on the metal oxide and carbon supports was much higher than the analogous Pd only catalyst, with the exception of the silica support catalysts. The Au-Pd bimetallic catalysts all displayed lower H_2 conversion than the Pd catalyst, however the selectivity towards H_2O_2 was much higher. For example, a calcined 5%Pd/TiO_2 catalyst has an activity of 32 mol/h-kg$_{cat}$ with a H_2 conversion of 29% and 21% selectivity towards H_2O_2. The calcined 2.5wt%Au-2.5wt%Pd/TiO_2 catalyst had an activity of 64mol/ h-kg$_{cat}$ with 21% H_2 conversion and 61% selectivity towards H_2O_2. The SiO_2 supported Au-Pd catalysts were more active than any other supported catalyst, however the catalytic activity scales directly with Pd content when using the SiO_2 as provided.

Modification of the standard reaction using different solvent compositions, reaction length, catalyst mass and temperature were investigated. It was found that

the activity and selectivity of the catalyst was highly dependant on these variables. Longer reaction times were detrimental to the selectivity of the catalyst as the hydrogenation reaction becomes more facile, and the same was true of high (>2°C) reaction temperatures. The Au:Pd ratio was also found to be an important variable, although the optimum concentration varied depending on the support. Storing a 2.5wt%Au-2.5wt%Pd/Al_2O_3 catalyst for 12 months led to agglomeration of the Au-Pd particles, with an increase in the particle size distribution (from STEM analysis) corresponding to a 3 fold increase in the catalyst activity.

All experiments were conducted in the absence of any stabilisers in the reaction medium. Investigation into support pre-treatment by washing with dilute acid prior to the metal impregnation resulted in Au and Au-Pd catalysts more active and more selective for H_2O_2 synthesis due to stabilisation of H_2O_2 *in-situ* and the "switching off" of the hydrogenation reaction. This effect did not originate from the removal of a poison from the support but seems to have its origin in a change in the Au-Pd and Au particle size distribution, with the treated catalysts having a smaller particle size distribution and no particles >30nm. However, supported Pd catalysts were not affected by support pre-treatment. The most active pre-treated catalyst had an activity of 170mol/h-kg_{cat} with >99% selectivity towards H_2O_2. Pre-treated catalysts allowed higher reaction temperatures (2-40°C) and H_2O_2 concentrations to be achieved; these catalysts are also exceptionally active in a water only solvent system.

Acknowledgements

Table of Contents

Chapter One

Chapter 1 : Introduction

1.1   Catalysis

The term catalysis was first coined in 1835 by Jöns Jakob Berzelius[1], who noted from his study of Döberenier's experiments into the combustion of hydrogen and oxygen over platinum at ambient temperatures that the presence of certain "compound bodies" in a reaction had the ability to speed up the reaction whilst they remain unaltered during the reaction. This first period of catalytic activity was followed by much research into reactions which could make use of a catalyst (most of the work by Faraday[2] and Philips[3] revolving around Pt based catalysts), and also into understanding how these compound bodies worked. The first development was by Wilhelmy in 1850 who demonstrated that the rate at which sugar cane was reversed was dependant on the concentration of the sugar used[4]. The thermodynamics of catalysis were first elucidated by Lemoine in 1877, who showed that the equilibrium of a chemical reaction cannot be changed by the addition of a catalyst, only the rate at which it is reached[5].

There are three distinct groups of catalyst, namely heterogeneous, homogenous and enzymatic. A heterogeneous catalyst is one that is in a different phase to the reactants, and the reaction takes place at the phase boundary. This occurs when there is a distinct phase present that is liquid-solid or gas-solid, where the solid is the catalyst. A homogenous catalyst is where the catalyst is dissolved into a liquid phase and is hence in the same phase as the reactants. Enzymes are "natural catalysts" and are present in the metabolic pathway of most living creatures.

All catalysts work by lowering the energy required for the transition state of the reaction to form, hence lowering the activation energy of the reaction (figure 1)
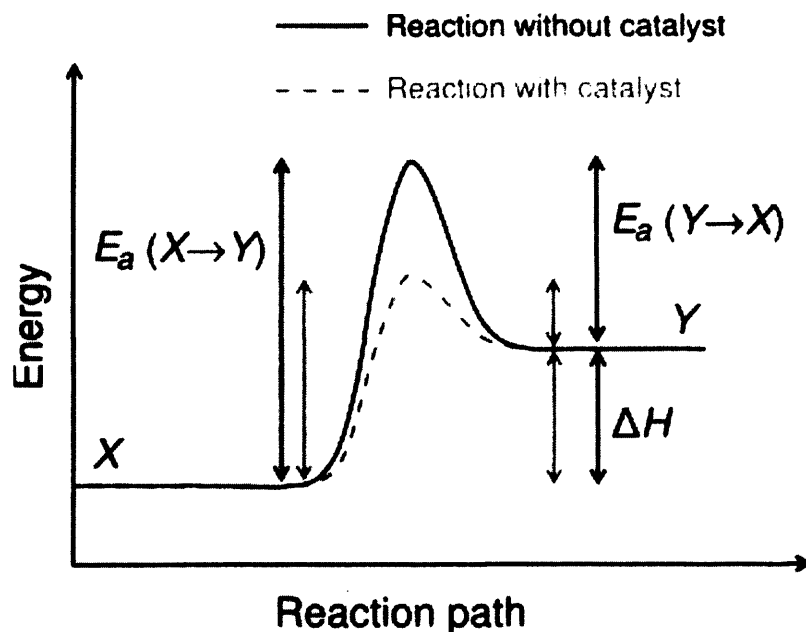
Figure 1   The relationship between activation energy (Ea) and enthalpy of formation (ΔH) with and without a catalyst. The highest energy position (peak position) represents the transition state. With the catalyst, the energy required to enter the transition state decreases, thereby decreasing the energy required to initiate the reaction and making the reaction more facile[6]

The shift in catalysis from laboratory experiments to reactions that were driven from an industrial point of view came with the arrival of the Great War in Europe.   One of the most famous catalytic processes, the Haber Process for ammonia production, was developed in 1903 by Haber who noted high pressures and temperatures were required for high activity and equilibrium.   Haber's use of an iron based catalyst, plus the input of Carl Bosch of BASF led to the first large-scale industrial process for ammonia synthesis in Ludwigshafen in 1910.

Currently, catalytic processes account for nine tenths of all chemical manufacturing, from the synthesis of plastics to margarine production.   Many industrial catalytic processes, with the advent of legislation for cleaner technology, have yet to be fully optimised which means the field of catalysis is as widely researched as it has ever been.

1.2 Hydrogen Peroxide

Hydrogen peroxide (H_2O_2) is a very simple inorganic molecule, with roles within the fine chemical industry and within the home. Bleaches and hair dyes typically contain around 5wt% H_2O_2 and in lower concentrations (around 3wt%) it can be used medically to clean wounds. In the pulp and paper bleaching industry[7] hydrogen peroxide is used in place of chlorine containing bleaching agents, *i.e* chlorine dioxide or sodium chlorate, and in 1994 this application accounted for 50% of the H_2O_2 produced globally. Further industrial uses for hydrogen peroxide include wastewater treatment, hydrogen peroxide will oxidize hydrogen sulphide to elemental sulphur liberating water and in the chemical industry for the synthesis of fine and bulk chemicals[8-11]. One of the benefits of using hydrogen peroxide to do such oxidations is that the only by-product from the oxidation is water. Thus the process is inherently green, especially if it can be used in place of bulky stoichiometric oxygen donors (e.g., sodium perborate, sodium percarbonate, metallic peroxides, organic hydroperoxides, percarboxylic acids), which inherently exhibit poor atom efficiency[12-15]. The discovery of the titanium silicalite TS-1[16] and its application for the oxidation of propene to propene oxide and the ammoxidation of cyclohexanone to its oxime using hydrogen peroxide, has further increased the interest in using hydrogen peroxide for the synthesis of chemical intermediates.

1.2.1 Chemical and physical properties of hydrogen peroxide

Hydrogen peroxide is a clear colourless non-flammable liquid that is one oxygen atom heavier than water. Due to increased hydrogen bonding hydrogen peroxide has a higher boiling point than water. Water and hydrogen peroxide do not form an azetropic mixture and are 100% miscible, hence can be separated by distillation. Table 1 contains some important physical properties of H_2O_2 compared with water.

Table 1.1 Physical properties of hydrogen peroxide and water[17]

Property	Hydrogen peroxide	Water
Melting point (°C)	-0.43	0
Boiling point (°C)	150.2	100
Heat of melting (J/g)	368	334
Heat of vaporisation ($Jg^{-1}K^{-1}$)		
25°C	1519	2443
b.p.	1387	2258
Specific heat ($Jg^{-1}K^{-1}$)		
liquid (25°C)	2.629	4.128
Gas (25°C)	1.352	1.865
Relative density (g cm^{-3})		
0°C	1.4700	0.9998
20°C	1.4500	0.9980
25°C	1.4425	0.9971
Viscosity (mPa s)		
0°C	1.819	1.792
20°C	1.249	1.002
Critical temperature (°C)	457	374.2
Critical temperature (MPa)	20.99	21.44

The redox potential of hydrogen peroxide is 1.76 V for the half reaction as shown in scheme 1.1

$$H_2O_2 + 2H^+ + 2e^- \rightarrow 2H_2O \quad E^0 = 1.76V$$
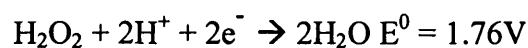
Scheme 1.1 Half-reaction of hydrogen peroxide to water.

This value of E^0 would lead one to expect that H_2O_2 would be a powerful oxidising agent; however, it is a relatively weak oxidising agent and although will oxdise some reactions unaided, for faster reactions addition of an activating agent, *i.e.* Fentons reagent[18], is required.

Hydrogen peroxide possesses both nucleophillic and electrophillic properties. The polarisation of the O-O bond contributes to the electrophillic nature. The nucleophillic nature of hydrogen peroxide allows it to readily add to carbonyls giving peracetals and perketals, albeit slowly. In alkaline solution H_2O_2 dissociates forming the perhydroxyl anion, HO_2^-, which is a powerful nucleophile which will react readily with aldehydes and electron deficient olefins. If the nucleophile is mixed with species such as electron deficient acyl compounds or nitriles, even stronger oxidants can be produced *in situ*. In a highly acidic medium H_2O_2 can become protonated, forming $H_3O_2^+$. When H_2O_2 is utilised as a reducing agent oxygen is always evolved. The ability of H_2O_2 to reduce chlorine and hypochlorite leads to its use in wastewater treatment[19]. The electrophillic form can also be utilised for phenol hydroxylation.

Hydrogen peroxide is an unstable molecule, especially at elevated concentrations and temperatures. The decomposition of hydrogen peroxide is summarised in figure 1.3.
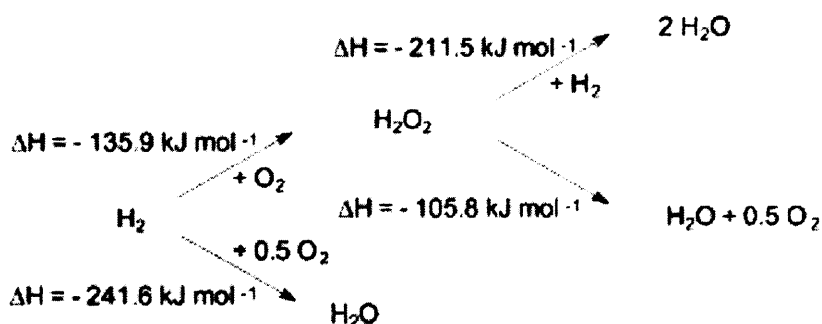
Figure 1.3 Hydrogen peroxide decomposition and hydrogenation to water[20].

1.2.2 Uses

As mentioned previously hydrogen peroxide is a green oxidant which has many applications. It is very important in the fine chemical industry for a number of reactions; the epoxidation of alkenes as exemplified by the production of epoxidised soya bean oil (ESBO) or epoxidised linseed oil *via* the formation of the perboxylic or performic acid *in situ* on addition of H_2O_2 to a carboxylic acid or

formic acid[17, 21]; hydroxylation of olefins such as cyclohexene or dodecane (*via* percarboxylic acid formation); and for the oxidation of alcohols *via* a suitable catalyst like a heteropolyacid complex.

1.2.3   Manufacture

Hydrogen peroxide was isolated by L. J. Thenard in 1818, following his experiments reacting barium peroxide with nitric acid[22]. Addition of HCl to the reaction medium increased the H_2O_2 yield and also helped prevent H_2O_2 decomposition (scheme 1.2)

$$BaO_2 + 2HCl \rightarrow BaCl_2 + H_2O_2$$

$$BaCl_2 + H_2SO_4 \rightarrow BaSO_4 + 2HCl$$

$$BaO_2 + H_2SO_4 \rightarrow BaSO_4 + H_2O_2$$
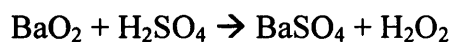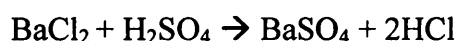
Scheme 1.2 Synthesis of H_2O_2 from HCl and BaO_2. Note the regeneration of the HCl and BaO_2. $BaCl_2$ is removed by precipitation with H_2SO_4.

This process was commercialised 60 years later, and produced 2000 metric tonnes of H_2O_2 from 10,000 metric tonnes of $BaSO_4$[23] at the turn of the century. This process has it drawbacks as only 3wt% H_2O_2 solutions were formed, the process was expensive and the resulting H_2O_2 contained impurities from the reactants, which subsequently affected the H_2O_2 stability.

In 1853 Meidinger developed an electrolytic process for forming H_2O_2 from aqueous sulphuric acid[24] *via* the production of a preoxodisulphuric acid intermediate[25] (scheme 1.3), and the first electro-chemical process went online in 1908. This process helped alleviate some of the problems encountered by Thenard, however further research by Reidel and Lowenstein in 1924 using ammonium sulphate in place of sulphuric acid (producing ammonium peroxodisuphate which

is subsequently hydrolysed to H_2O_2) resulted in a process producing 35,000 metric tonnes of 100% *m/m* H_2O_2 per annum[26].

$$2H_2SO_4 \rightarrow H_2S_2O_8 + H_2$$

$$H_2S_2O_8 + H_2O \rightarrow H_2SO_5 + H_2SO_4$$

$$H_2SO_5 + H_2O \rightarrow H_2O_2 + H_2SO_4$$

$$2H_2O \rightarrow H_2O_2 + H_2$$
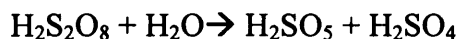
Scheme 1.3 Electrochemical manufacture of aqueous hydrogen peroxide

Currently, the majority of the world's hydrogen peroxide is made *via* the anthraquinone cycle (AQ). This process, developed by Hans-Joachim Riedl and George Pfleiderer in 1939[27-30] involves the hydrogenation of a substituted anthraquinone over a nickel or palladium catalyst, forming the diol. The subsequent oxidation of anthraquinol in air (or oxygen enriched air) reforms the original anthraquinone, and produces hydrogen peroxide. This process was developed from work carried out previously by Manchot who noted in 1901 that hydroquinone and hydrazobenzenes have the ability to undergo auto-oxidation under alkaline solutions producing peroxides[31]. The first AQ pilot plant produced around 30 metric tonnes of H_2O_2 per month. Concentrations of hydrogen peroxide between 0.8-35wt% can be obtained using this method, depending on the solvent system and the choice of hydrogenation catalyst - after refinement hydrogen peroxide concentrations can exceed 70wt%. Indeed, the Dupont de Nemours plant commissioned in 1953 has produced 1.3 x 10^6 *m/m* tonnes of H_2O_2 annually (figures from 1996).

The chemistry of the autoxidation method for producing H_2O_2 is relatively straight forward, and illustrated in figure 1.6.
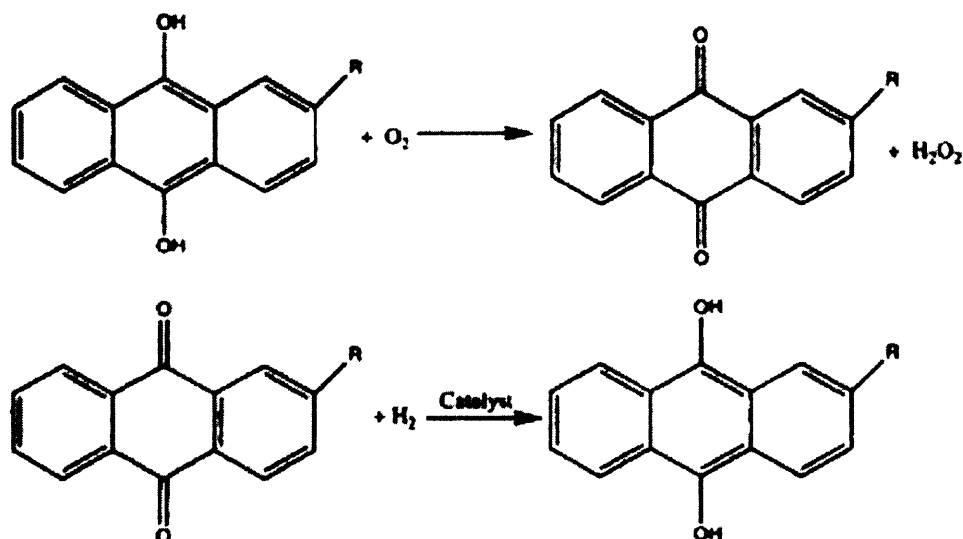
Figure 1.6 Anthrahydroquinone autoxidation processs for the manufacture of hydrogen peroxide[17]

A 2-alkylanthraquinone (usually 2-ethyl or 2-pentyl) is dissolved in a suitable solvent system (working solution), then catalytically hydrogenated to the 2-alkylanthrahydroquinone. The working solution containing the 2-alkylanthrahydroquinone is separated from the hydrogenation catalyst and aerated with oxygen containing gas (compressed air), reforming the original anthraquinone and forming the hydrogen peroxide. The reaction is carried out between 30-60°C, at up to 10 atmospheres pressure. A schematic for the AO process is shown in figure 1.7.
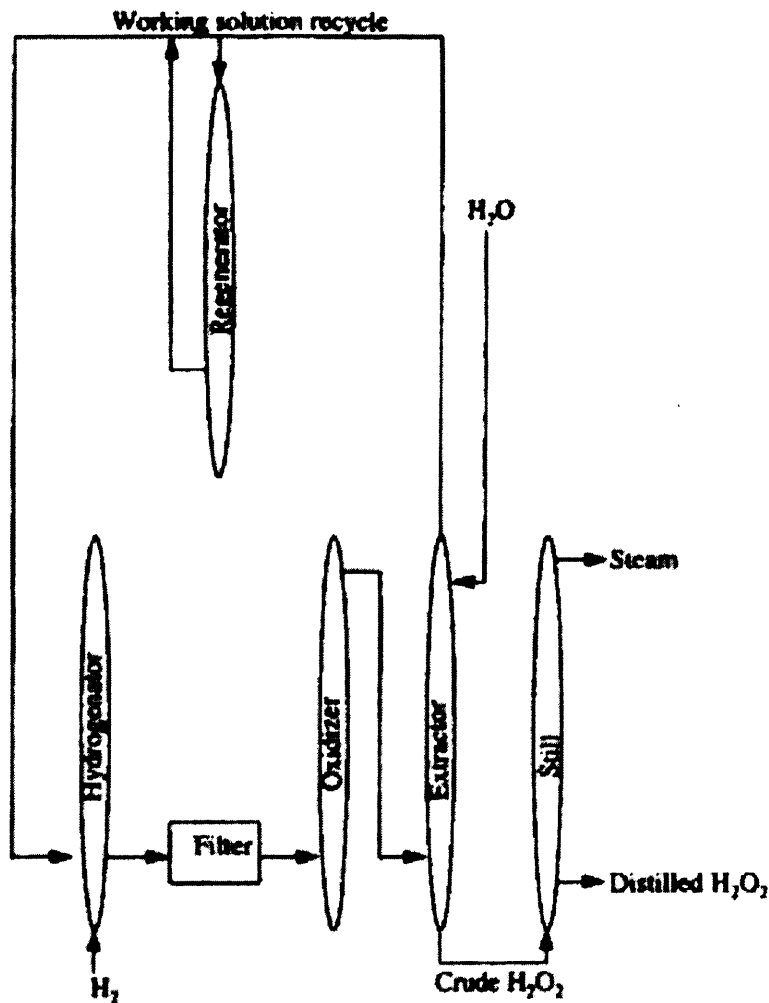
Figure 1.7 Schematic for the autoxidation process[17]

However, there are drawbacks to this method for producing hydrogen peroxide, including the cost of solvent system, and degradation of the anthraquinone. The removal of degraded anthraquinone (figure 1.8) formed during the hydrogenation step (which can clog the reactor and poison the hydrogenation catalyst) increases the production cost, and means that the capacity of the process is between 85-90%. There is also significant cost in the refinement and separation of the hydrogen peroxide. As the hydrogenation and oxidation steps of the reaction are carried out sequentially, oxygen and hydrogen do not come into direct contact, which is highly advantageous as H_2 and O_2 are explosive over a large range of compositions.
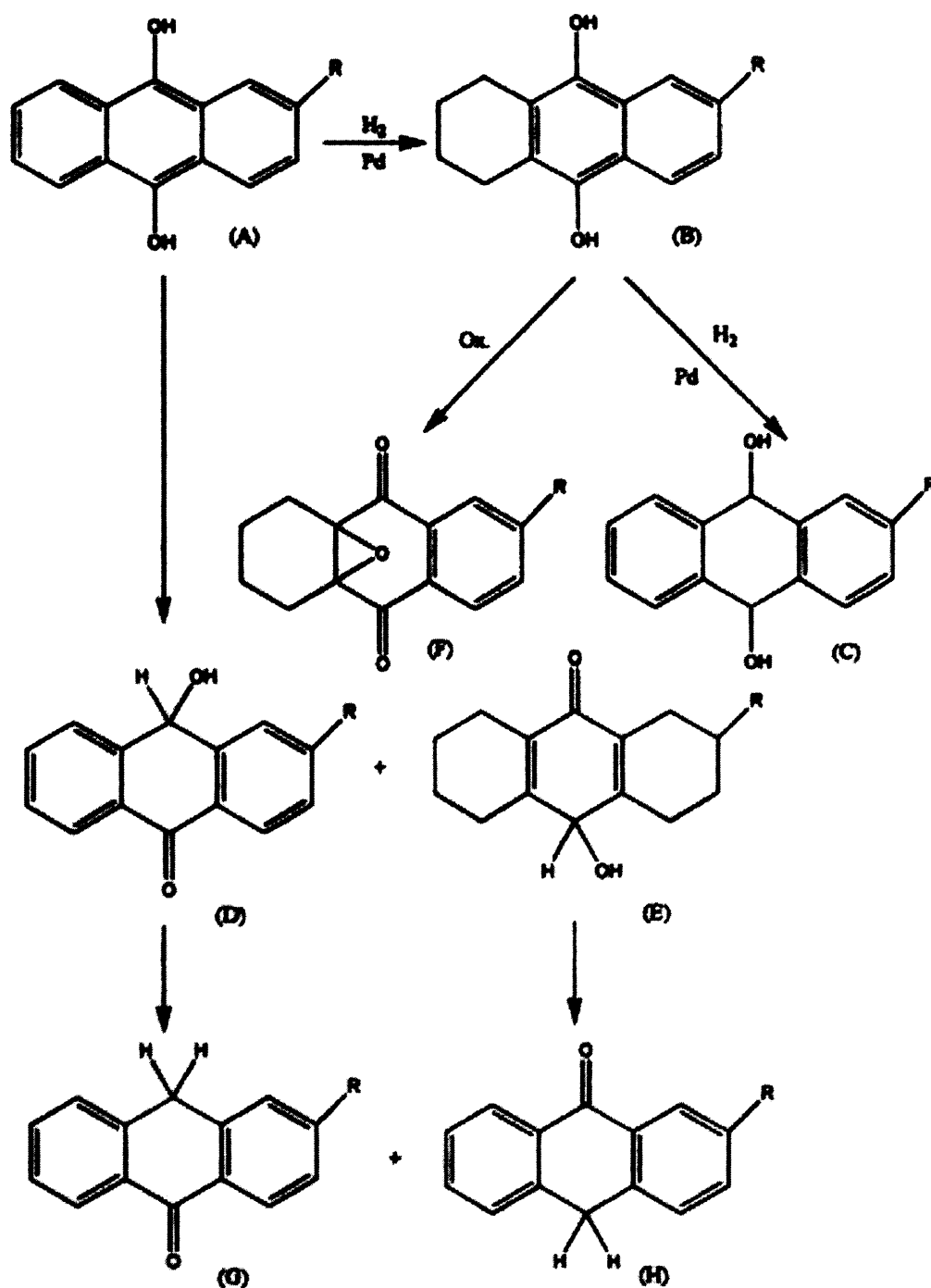
Figure 1.8 Secondary reactions taking place in the presence of (A) 2-alkylanthrahydroquinones (B = ring reduction, C= octa-product, D, E = hydroxyanthrones from tautomerism, F =epoxide product G, H = anthrones)

Although steps have been made to improve the efficiency of the anthraquinone cycle as a method of producing H_2O_2, the current impetus on green chemistry leads one to look for alternative methods for its production.

1.3 Gold catalysis

1.3.1 Gold catalysts for selective oxidation

The selective oxidation of substrates is essential to the fine chemical industry, however it remains a challenging unit process. Many oxidation processes for fine chemicals and pharmaceuticals utilise stoichiometric oxygen donors. Many would prefer a catalytic process using dioxygen from air as the oxidising species, and pressure for development along these lines is being applied from the need to develop green chemical technology. In contrast to selective oxidation, many hydrogenation reactions utilise catalysts with molecular hydrogen. There is one essential difference between catalytic hydrogenation and oxidation. Under most reaction conditions, the hydrogen molecule has to be activated by chemisorption on a catalyst surface before it can be reacted with a substrate for hydrogenation to occur. At the relatively low temperatures at which catalytic hydrogenation reactions are carried out, hydrogen activation *via* a radical pathway is not feasible. This is not the case with selective oxidation. Dioxygen in its ground state is a diradical triplet species. This presents the possibility of competing non-catalysed gas or liquid phase reactions in which triplet dioxygen reacts directly with the substrate without the intervention of a catalyst. Fortunately, most organic substrates of interest are in singlet states in their ground states and so this effect can be minimised. However, it is a factor which can complicate matters. It is clear that there is a need to develop new oxidation catalysts and, surprisingly, supported gold catalysts have been found to be particularly effective for the epoxidation of alkenes and the oxidation of alcohols. Interestingly there are some studies suggesting that C-H activation may be feasible with supported gold catalysts. Further details are contained in the following section.

1.3.1.1 Epoxidation

Most research has focussed on the oxidation of propene to propene oxide which is a major research target, as this is a commodity chemical used in the manufacture of polyurethane and polyols. The epoxidation of ethene with dioxygen is a commercial process which operates using a supported silver catalyst [32] obtaining selectivities in excess of 90%. However, the oxidation of propene has proved to be much more problematic and typically selectivities lower than 10% are observed with many catalysts - Lambert and co-workers [33] have shown that supported catalysts can give selectivities of *ca.* 50% at 0.25% conversion, but the selectivity declines rapidly with increasing conversion.

Haruta and co-workers were the first to demonstrate the potential of supported gold catalysts for the epoxidation of propene with oxygen in the presence of H₂. The H₂ acting as a sacrificial reactant permits the activation of O_2 at relatively low temperatures permitting the selective oxidation of propene to occur [34-36]. Haruta found that Au/TiO₂, prepared by deposition precipitation, was selective for propene epoxidation and the catalysis was associated with the contact between hemi-spherical gold nano-crystals (2-5 nm in diameter) and the TiO₂ support as revealed by high-angle annular dark field transmission electron microscopy. Initially the selectivities were low but by using different titanium-containing supports including TS-1, Ti-zeolite β, Ti-MCM-41 and Ti-MCM-48 improvements were seen[6-27].

These studies clearly demonstrate that with H₂ as a sacrificial reactant present Au/TiO₂ catalysts are very effective for the epoxidation of propene. Many early studies concentrated on the use of TS-1 as a support as it is known that this material is selective for the epoxidation of propene with H₂O₂ as the oxidising species [37]. Haruta and co-workers [38] found the Au/TS-1 catalysts produced more propanal than propene oxide. In contrast, Moulijn [39] and co-workers clearly showed that Au/TS-1 catalysts could be very selective to the formation of propene oxide, and that the catalysts were stable under reaction conditions. Recent mechanistic studies by Moulijn and co-workers [40] show that a bidentate propoxy species is formed as an intermediate, and Delgass and co-workers [41, 42] have confirmed these findings. In particular, gold loading requires careful tuning, as had

previously been noted by Haruta and co-workers [43], to obtain high selectivity and activity and when normalised for gold content propene oxide yields of 350 g/h-g_{Au} are achievable at 200°C for a 0.01 wt% Au/TS-1 catalyst with a Si/Ti ratio of 500[44]. In these catalysts the active species are considered to be gold clusters with diameters much smaller than 2 nm.

The challenge of poor H_2 utilisation has been addressed by Haruta who has shown that using mesoporous titanoslicates as a support [45] reasonably efficient H_2 consumption was attained together with high propene oxide yields (93g/h-kg_{cat} at 160°C) and propene oxide selectivities of >90%, The conversion observed was relativiely low at *ca.* 7%, however the H_2 efficiency was 40% [46] . These catalysts showed relatively short lifetimes but could be reactivated, and these catalysts have commercial potential.

Very recently, trimethylamine has been identified as a gas-phase promoter for the epoxidation of propene with supported gold catalysts [47]. This is an important observation, since the epoxidation of ethene is greatly enhanced by a complex mixture of gas-phase promoters and so this could provide a very valuable new line for research activity.

Supported gold catalysts has been shown to be active for the epoxidation of alkanes in the absence of sacrificial H_2 in a recent study by Hughes et al. [48]. In this study it was shown that catalytic amounts of peroxides could initiate the oxidation of alkenes with oxygen. A range of substrates were used to show that the effect was a general one. Very high selectivities of the epoxides were observed with cyclohexene, styrene, *cis*-stilbene and cyclooctene. The selectivity was shown to be highly dependent on the solvent and the best results were achieved with substituted benzenes. However, these catalysts were also effective in the absence of solvent which coupled with the mild reaction temperatures certainly addresses the possibility of a new green technology. The yields of epoxides obtained under these solvent-free conditions were similar to those obtained for supported gold catalysts using sacrificial H_2 [45, 46].

1.3.1.2. Oxidation of alcohols and aldehydes

The oxidation of alcohols and polyols to chemical intermediates represents a demanding target. Supported platinum and palladium nanoparticles are generally acknowledged to be effective catalysts for the oxidation of polyols, for example in carbohydrate chemistry for the oxidation of glucose to gluconic acid and the oxidation of glycerol to glyceric acid. Although these well established catalysts have good activity, they exhibit poor selectivity with complex substrates which is a potential problem. Rossi and Prati with co-workers [32-45] have shown in their seminal studies that supported gold nanoparticles can be very effective catalysts for the oxidation of alcohols, including diols in the presence of a base. The base is considered to be essential for the first hydrogen abstraction, unlike Pd and Pt catalysts that are effective in acidic as well as basic conditions. The catalysts were Au/carbon and they were observed to be effective for a range of substrates. These catalysts were also shown to be effective with gas phase reactants and in this case no base addition is required [49]. These studies have been expanded to the oxidation of sugars and similar high catalytic efficiency for the oxidation of glucose and sorbitol has been observed [50, 51]. In recent studies they have reported the synergistic effect of the addition of Pd or Pt to the Au/carbon catalysts for the selective oxidation of D-sorbitol to gluconic and gulonic acids [52].

Carrettin *et al.* [53-55] have shown that Au supported on graphite can oxidise glycerol to glycerate with 100% selectivity using dioxygen as the oxidant under relatively mild conditions with yields approaching 60%. It was observed that the selectivity to glyceric acid and the glycerol conversion were very dependent upon the glycerol/NaOH ratio. In general, with high concentrations of NaOH, exceptionally high selectivities to glyceric acid can be observed. However, decreasing the glycerol concentration, and increasing the mass of the catalyst and the concentration of oxygen, leads to the formation of tartronic acid *via* consecutive oxidation of glyceric acid. Careful control of the reaction conditions can produce 1 wt% Au/C catalysts with 100% selectivity towards glyceric acid. Under comparable conditions, supported Pd/C and Pt/C always gave other C_3 and C_2 products in addition to glyceric acid and, in particular, also gave some C_1 by-products. Subsequent studies by Prati and co-workers [56] have shown further

aspects of this complex oxidation. Recently Basheer *et al.* [57] have shown that a simple capillary reactor can be used for the selective oxidation of glucose, showing that oxidations in a flow reactor using a supported gold catalyst are feasible.

It is known for a number of reactions that the support-catalyst interaction is a crucial factor controlling reactivity. Interestingly, Rossi and co-workers [58] have shown that gold colloidal particles can be very effective catalysts for the oxidation of glucose to gluconic acid. The demonstration that the initial rates for these un-supported particles was identical to the rates observed with Au/carbon catalysts (operated under the same conditions) confirms that the support is of limited importance in the origin of the catalyst activity in these oxidation reactions. The support-catalyst interaction is, however, essential for the observation of a stable catalyst system. Subsequently Martens *et al.* [59, 60] have also shown that colloidal gold can catalyse the oxidation of 1,2-diols. Recently, Tsunoyama *et al*[61] have shown that benzyl alcohol can be oxidised using oxygen in aqueous media with gold nanoclusters stabilised on polymers.

One of the most significant advances in the field of alcohol oxidation has been the observations of Corma and co-workers [62, 63] showing that an Au/CeO$_2$ catalyst is active for the selective oxidation of alcohols to aldehydes and ketones and the oxidation of aldehydes to acids. This catalyst is active at relatively mild conditions, without the addition of a solvent, using O$_2$ as oxidant without the requirement for the addition of NaOH to achieve high activity. The results were shown to be comparable to, or higher than, the highest activities that had been previously observed with supported Pd catalysts [64]. The catalytic activity was thought to be due to the Au/CeO$_2$ catalyst stabilising a reactive peroxy intermediate from O$_2$. Enache *et al.* [65] showed that alloying Pd with the Au in supported Au/TiO$_2$ catalysts enhanced the activity for alcohols under solvent free conditions by a factor of over 25. With these reactive catalysts primary alcohols and diols can be readily oxidised, further extending the scope of selective oxidation reactions that are possible with gold catalysts.

1.3.1.3 C-H bond activation

Another commercially interesting reaction i the activation of C-H bonds in alkanes. As supported nano-crystalline gold catalysts have been shown to be effective for the selective oxidation of alkenes and alcohols, it is not surprising that attention is now being given to the oxidation of C-H bonds. In this respect attention has so far been focused on cyclohexene activation under mild conditions. One of the most important alkane activation processes currently operated industrially is the oxidation of cyclohexane to cyclohexanol and cyclohexanone, which in a recent review has been acknowledged to be a reaction that continues to be a significant challenge [66]. The aerobic oxidation of cyclohexane is central to the production of nylon-6 and nylon-6,6 and the worldwide production exceeds 10^6 tonnes per annum. Commercially the process is operated at 150–160°C with cobalt naphthenate as an initiator for the radical oxidation process that gives 70–85% selectivity at 4% conversion. Operation at high conversions leads to total oxidation and consequently this large-scale commercial process has been designed to operate at low conversion. There is clearly scope to produce a more efficient process but given the current focus on green chemistry the main scope is to design a system that gives 100% specificity. Ratnasamy and co-workers [67] have shown that μ_3-oxo-bridged Co/Mn cluster complexes are very selective as homogeneous catalysts, but it is generally recognised that a heterogeneous catalyst is preferred as these present less problems with removal. Recently, Nowotny *et al.* [68] have investigated immobilization of cobalt complexes but leaching occurs under reaction conditions and subsequently the catalyst loses activity. Thomas and co-workers [69] have shown that aluminophosphates substituted with Mn(III), Co(III) and Fe(III) could give very high selectivities when operated at 130°C. It is against the background of these recent initiatives that potential gold-based systems need to be assessed.

The use of gold catalysis for this application has been initiated by Zhao *et al.* [70, 71] who have shown that gold can be active for the activation of cyclohexane at 150 °C using an Au/ZSM-5 catalyst selectivities of >90% can be achieved, and >90% for a Au/MCM-41 catalyst although an initial induction period was apparent with these catalysts. It was also shown that these gold catalysts can be re-used but

the activity gradually declines and the selectivity shifts from cyclohexanone to cyclohexanol. These studies show that supported gold catalysts are indeed active for the activation of C–H bonds and that high selectivities can be achieved.

A recent study by Xu *et al.* [72] has investigated the potential oxidation of cyclohexane at temperatures well below 100°C, using oxygen as oxidant, with a gold catalyst, since, at this temperature higher selectivities might be expected. In this study Au/carbon catalysts were contrasted with supported Pt and Pd catalysts. The Au/carbon catalysts were identical to those that were found to be highly effective for the epoxidation of alkenes [41]. In this study, a reaction inhibitor was also investigated (1,4-difluorobenzene). The selectivity to cylohexanone and cyclohexanol observed was very high at low conversion, but this declined rapidly with enhanced conversion at longer reaction times. However, the gold catalysts were found to give identical performance to the Pt and Pd catalysts and in general the selectivity observed was just a function of cyclohexene conversion.

1.4   Direct synthesis of hydrogen peroxide from hydrogen and oxygen

As discussed previously, hydrogen peroxide is a noted green oxidant that has widespread applications in many large-scale processes such as bleaching and as a disinfectant, as mentioned previously. Such uses account for the majority of the H_2O_2 material manufactured. Its use in the fine chemical industry accounts for a much lower fraction of its consumption, *e.g.* epoxidised oils, catechol, hydroquinone, peracetic acid and caprolactone, and tends to require only small amounts of hydrogen peroxide. At present, hydrogen peroxide is produced by the sequential hydrogenation and oxidation of an alkyl anthraquinone [73]. However, there are problems associated with the anthraquinone route which include the cost of the quinone solvent system and the requirement for periodic replacement of anthraquinone due to hydrogenation. In addition, the process is only economically viable on a relatively large scale (4-6 x 10^4 tpa), and this necessitates the transportation and storage of concentrated solutions of hydrogen peroxide when required for use in the fine chemicals industry since only relatively small amounts

are required at any one time. Hence the development of a new, highly efficient and smaller scale manufacturing process for H_2O_2 is of significant commercial interest.

The identification of a direct route for the synthesis of hydrogen peroxide from the reaction of oxygen and hydrogen would be highly beneficial, since this presents the possibility of small scale distributed synthesis. At present, no commercial process exists for the direct process, even though there has been considerable research effort on this topic for over 90 years[74-82]. The first patent for the direct synthesis method was filed by Henkel and Weber on 25th August 1914[74] detailing the use of a Palladium lined pipe submerged in oxygen rich water, forming hydrogen peroxide on subsequent aeration with hydrogen. However, until recently the topic has attracted limited interest from the academic community. There are numerous problems associated with the direct route for H_2O_2 synthesis from its elements-the reaction scheme outlined in figure 1.3 demonstrates the numerous other reactions that can occur during synthesis, all of which are thermodynamically preferred. The formation of these side products can be minimized by careful control of reaction conditions, choice of catalyst and the addition of stabilizers in the reaction medium.

1.4.1 Direct synthesis of hydrogen peroxide using supported Pd catalysts.

Until 2002 the catalysts used in the investigations into the direct synthesis of hydrogen peroxide have been based on Pd. Since it is important to try to achieve the highest rate of product formation, most of these earlier studies used H_2/O_2 mixtures in the explosive region, and solutions of over 35 wt% hydrogen peroxide have been made by reacting H_2/O_2 over Pd catalysts at elevated pressures [78]. However, the commercial operation of such a process in the explosive region is extremely dangerous, and more recently studies have concentrated on carrying out the reaction with dilute H_2/O_2 mixtures well away from the explosive regime [20, 83]. Alternatively, a catalytic membrane can be employed to prevent the contact of hydrogen and oxygen during the reaction-and in this case pure gases can be used thus obtaining higher yields of H_2O_2[84, 85].

The seminal studies by Pospelova in 1961[86-88] showed that supported Pd catalysts work well in the presence of an aqueous acidic reaction medium (HCl,

HNO_3) due to the decreased decomposition of H_2O_2. The activity of the catalysts was also highly dependant on the $H_2 : O_2$ composition and the reaction temperature. Fu *et al*[89] showed that the direct synthesis of H_2O_2 using a fluorinated, hydrophobic Pd/carbon catalyst could be achieved in a stirred autoclave. The activity of the catalyst was dependant on its hydrophobicity. The most active catalyst has very low selectivity to H_2O_2 (8.7%) although the conversion was high (41%). In this case, H_2SO_4 was chosen as a stabilizer.

The extensive work of Lunsford[90-96] has shown that supported Pd catalysts can be highly active for the direct formation of hydrogen peroxide. However, the catalysts are only active with halides present in the reaction medium. High concentrations of HCl (0.1-1M) were used in the reaction medium leading to the formation of $PdCl_4^{2-}$ and colloidal Pd when $PdCl_2$ or reduced Pd/SiO_2 were used as a catalyst[94, 96]. Indeed, high concentrations of HCl led to dissolution of Pd from the supported catalyst[94], and the high activity was attributed to the formation of colloidal Pd as, the reaction medium remained active for the formation of H_2O_2 on removal of the catalyst. A recent study from this group using a Pd/SiO_2 catalyst has elucidated many of the controlling factors for H_2O_2 synthesis[90]. The presence of bromide ions in acidified reaction medium limited the dissolution of Pd from the support and led to catalysts highly selective for the direct synthesis reaction. Indeed, in the absence of such promoters only water is formed *via* the combustion reaction. In aqueous acidified ethanol, containing 2×10^{-5} M Br⁻ ions, at a O_2/H_2 ratio of 15, selectivity towards H_2O_2 of 80% was achieved. The reaction was found to be first order with respect to H_2 and zero order with respect to O_2, and was not mass transport limited under the batch reactor conditions used. Lunsford's investigations into the role of chloride ions in the reaction medium show that addition of 4×10^{-4} M Cl⁻ gives 45% selectivity towards H_2O_2, and appears to prevent O-O cleavage[91]. This is advantageous two-fold; it prevents the initial combustion of H_2 and O_2 and also helps prevent the decomposition of hydrogen peroxide after it has formed.

Choudhary *et al*. have also studied supported Pd catalysts for the direct synthesis of hydrogen peroxide[97-105]. Initial studies with a range of supports found that reduced Pd catalysts were inactive for the direct synthesis of H_2O_2 but

subsequent washing with an oxidising agent formed highly active catalysts, attributed to the presence of PdO on the surface[104, 105]. It was observed later that an increase in selectivity can be achieved by the brominating the reduced catalyst[102], which was achieved by impregnation of the calcined Pd with the corresponding ammonium bromide, followed by drying. Once again, an aqueous acidic reaction medium is required for good catalytic activity. The assignment of PdO as the species is in direct contrast by the work of Burch who demonstrated that metallic Pd was responsible for good selectivity and conversion[106].

Table 1.3 summarises the research into the direct synthesis reaction using supported Pd catalysts.

1.4.2 Direct synthesis of hydrogen peroxide using supported Au catalysts.

Hutchings and co-workers were the first to show that gold containing catalysts (in this case Au/Al_2O_3) were active for the direct synthesis of hydrogen peroxide. However, the key discovery was the observation that the direct synthesis of H_2O_2 was significantly enhanced by using Au-Pd alloys supported on alumina and these catalysts gave significant improvements in the rate of hydrogen peroxide formation when compared with the Pd or Au only catalysts [20, 83]. However, in common with pure Pd catalysts, these Al_2O_3-supported Au-Pd alloys gave low selectivity based on H_2 and in these initial studies selectivities of only *ca.* 14 % were observed. Selectivity is the key problem with this reaction since the conditions that are required to produce hydrogen peroxide also promote (i) its decomposition to oxygen and water, (ii) its hydrogenation to water or (iii) the direct non-selective formation of water (figure 1.3).

Subsequently, Haruta and coworkers [105] have shown that Au/SiO_2 catalysts were also effective for this reaction using temperatures of 10°C. They concluded that the activity of the catalyst was related to the size of the metal particles, which larger Au nano-crystals formed on calcination being less active for the direct synthesis reaction.

Work by Ishihara[107] also demonstrated that gold could be effective for the direct synthesis of hydrogen peroxide, although the activity of the catalyst was

dependant on the support used. Addition of Pd to the Au again led to an increase in the rate of formation, and the maximum selectivity towards H_2O_2 achieved using an Au-Pd catalyst was 30%.

Table 1.4 summarises the research into the direct synthesis reaction using supported Au and Au-Pd catalysts.

Table 1.3 Hydrogen peroxide synthesis over Pd based catalysts

Catalyst	Promoter	Reaction Conditions	Remarks	Reference
Supported Pd catalysts (SiO$_2$, alumina, carbon)	Aqueous Acidic (HCl, H$_2$SO$_4$)	3-35°C 300-400 vibrations per minute	H$_2$: O$_2$ 1:1 optimum High H$_2$O$_2$ concentrations at lower temperatures H$_2$ adsorption on Pd initiates reaction H bond cleavage is responsible for the decomposition with Pd based catalysts. Pd$_2$ responsible for H$_2$O$_2$ synthesis Acid decreases H$_2$O$_2$ decomposition	84, 85, 86
Pd/Carbon (hydrophobic/hydrophilic)	H$_2$SO$_4$	25°C Batch reactor 0.65Mpa	High conversion (41%) Low selectivity (8.7%) High fluorine content in support leads to high conversion	87
Pd supported on a membrane	0.1M HCl	25°C Ambient pressure	100% conversion O$_2$: H$_2$ 1:1 optimum No hydrogen or oxygen contact due to membrane	83
Supported Pd catalysts on various metal oxides (impregnation)	0.02M H$_2$SO$_4$	22°C Ambient pressure	Reduced Pd catalysts show low selectivity towards H$_2$O$_2$ and are highly active for H$_2$O$_2$ decmposition Oxidation of catalyst leads to improvement – PdO is the active species for H$_2$O$_2$ synthesis	103

22

Catalyst	Promoter	Reaction Conditions	Remarks	Reference
Pd containing zeolite catalysts	0.016M (acid or halide)	22°C Ambient pressure	Reduced Pd catalysts show low selectivity towards H_2O_2 and are highly active for H_2O_2 decomposition Oxidation of catalyst leads to improvement – PdO is the active species for H_2O_2 synthesis Reaction is less selectivie in water only medium	102
PdCl$_2$ or Pd/SiO$_2$	1 – 0.1M HCl	22°C Ambient pressure	HCl leads to the formation of colloidal Pd which is the active phase for H_2O_2 synthesis 65% selectivity towards H_2O_2	90
Pd supported on various metal oxides and carbon	1.6M H$_3$PO$_4$ NaBr	22°C 3.4 MPa	Bromide containing promoters most effective for H_2O_2 synthesis Reduced Pd is the active metal species Low metal loading is beneficial (1wt%)	
Pd/SiO$_2$	0.1M HCl 0.01 M Br-	10°C Ambient pressure	Reduced Pd catalysts show low selectivity towards H_2O_2 and are highly active for H_2O_2 decomposition Mechanistic study 2wt% H_2O_2 90% selective towards H_2O_2 Combustion prevented by Br-	93

23

Catalyst	Promoter	Reaction Conditions	Remarks	Reference
Pd/SiO$_2$	0.12M H$_2$SO$_4$ HCl	Ethanol 22°C Ambient pressure	With zero Cl- present H$_2$O$_2$ formation is low 4 x 10^{-4} M Cl- 45% selectivity towards H$_2$O$_2$ Cl- on the surface inhibits O-O bond cleavage (in H$_2$O$_2$ and O$_2$) Cl- prevents dissolution of Pd into solution	88
Pd/SiO$_2$	0.12M H$_2$SO$_4$ HCl /KCl NaBr	Ethanol 22°C Ambient	H$^+$ ions prevent combustion reaction H$_2$O$_2$ selectivity of 80% achieved using 2 x 10^{-5} M Br- Br- limits Pd loss from the catalyst Low synthesis rates at higher temperature	89

24

Table 1.4 Hydrogen peroxide synthesis over Au based catalysts

Catalyst	Promoter	Reaction Conditions	Remarks	Reference
Au/Al_2O_3 $Au-Pd/Al_2O_3$ Pd/Al_2O_3	None	Methanol : water solvent system $2^{\circ}C$	Addition of Pd to the Au catalyst increases rate of formation Au-Pd catalyst more active than Pd only catalysts	81
Au, Pd and Au-Pd catalysts supported on carbon and various metal oxides	None	Supercritical CO_2 used as solvent $35^{0}C$ 9.2MPa	Addition of Pd to the Au catalyst increases rate of formation Au-Pd catalyst more active than Pd only catalysts Au-Pd catalysts form a core shell structure, Au core surrounded by Pd shell Higher rate of formation at lower temperatures	80
Au/SiO_2	Reaction carried out at ph 6	$10^{\circ}C$ Stirring	SiO_2 and zeolite supported catalyst active for H_2O_2 formation $Au-Pd/SiO_2$ catalyst has higher rate of formation 30% selectivity towards H_2O_2	106
Au catalysts supported on various metal oxides	Reaction carried out at ph 6	0.1-1MPa $0-20^{\circ}C$	Low conversions Higher acidity / basic conditions resulted in lower rates of H_2O_2 formation Increasing calcination temperature decreased activity due to Au sintering	10

25

1.1   Aims of the project

Using a stirred autoclave the direct synthesis of hydrogen peroxide will be studied using various heterogenous gold catalysts to determine parameters which may allow for the industrialisation of this green catalytic reaction.

1.2   Objectives

1   Development of supported gold catalysts for the direct synthesis of hydrogen peroxide with high activity and selectivity from hydrogen and oxygen using dilute gases.

2   Development of a catalyst active for the direct synthesis of hydrogen peroxide in a medium that does not contain stabilisers.

3   Systematic study into the effect of reaction conditions on catalytic activity and selectivity.

4   Modification of the catalyst and reaction conditions to allow hydrogen peroxide formation under ambient conditions without compromising catalyst selectivity.

5   Elucidation of the active site of the catalyst to determine the optimum preparation route and catalyst composition.

6   *In-situ* utlisation of hydrogen peroxide as an oxidation intermediate for the synthesis of fine chemicals

Objectives 1 and 2 and 5 are dealt with in chapters 3,4 and 5, objectives 3 and 6 are dealt with in chapter 3 and objective 4 is dealt with in chapter 5.

1.6 References

[1]   J. J. Berzelius, *Edinburgh New Philosophical Journal*
       1836, *XXI*, 223

[2]   M. Faraday, *Phil. Trans.* **1834**, *124*, 55

[3]   Phillips, *GP6069* **1831**.

[4]   L. F. Wilhelmy, *Pogg Ann* **1850**, *81*, 413.

[5]   G. Lemoine, *Ann Chim Phys* **1877**, *12*, 145.

[6]   www.wikipedia.com.

[7]   P. B. Walsh, *Tappi Journal* **1991**, *74*, 81.

[8]   K. Sato, R. Noyori, *Kagaku to Kogyo (Tokyo)* **1999**, *52*, 1166.

[9]   S. E. Turnwald, M. A. Lorier, L. J. Wright, M. R. Mucalo, *Journal of Materials Science Letters* **1998**, *17*, 1305.

[10]   C. Esmelindro Maria, G. Oestreicher Enrique, H. Marquez-Alvarez, C. Dariva, M. S. Egues Silvia, C. Fernandes, J. Bortoluzzi Adailton, V. Drago, O. A. C. Antunes, *Journal of inorganic biochemistry* **2005**, *99*, 2054.

[11]   I. I. Vasilenko, A. N. Fedosova, E. Siniak Iu, *Kosmicheskaia biologiia i aviakosmicheskaia meditsina* **1991**, *25*, 52.

[12]   D. Enders, L. Wortmann, R. Peters, *Accounts of Chemical Research* **2000**, *33*, 157.

[13]   A. R. Vaino, *Journal of Organic Chemistry* **2000**, *65*, 4210.

[14]   P. Wadhwani, M. Mukherjee, D. Bandyopadhyay, *Journal of the American Chemical Society* **2001**, *123*, 12430.

[15]   S. Lee, P. L. Fuchs, *Journal of the American Chemical Society* **2002**, *124*, 13978.

[16]   G. Perego, M. Taramasso, B. Notari, (Snamprogetti SpA, Italy). Application: BE, **1981**, p. 18 pp.

[17]   C. W. Jones, *applications of hydrogen peroxide and derivatives*, RSC, **1999**.

[18]   C. Walling, K. Amarnath, *Journal of the American Chemical Society* **1982**, *104*, 1185.

[19]   M. L. Costa, G. Cowley, C. Pu, (Can.). Application: US, **2004**, p. 9 pp.

[20]   *Kirk Othmer's encyclopedia of chemical technology, Vol. 9*, **1994**.

[21]   L. J. Thenard, *Ann. Chym. Phys.* **1818**, *8*, 306

[22]   W. C. Schumb, C. N. Satterfield, R. L. Wentworth, *Hydrogen Peroxide*, Rheinhold Publ. Co, New York, **1955**.

[23]   H. Meidinger, *Ann. Chem. Pharm* **1853**, *88*, 57.

[24]   H. Berthelot, *C. R. Hebd. Seances Acad, Sci.* **1878**, *86*, 71.

[25]   W. M. Weigart, H. Delle, G. Kabish, *Chem.-ZTG.* **1975**, *99*, 101

[26]   G. Pfleiderer, H. J. Riedl, W. Deuschel, (Badische Anilin- & Soda-Fabrik (I. G. Farbenindustrie Akt.-Ges. \"In Auflosung\")). DE, **1951**.

[27]   G. Pfleiderer, H. J. Riedl, (Alien Property Custodian). US, **1945**.

[28]   H.-J. Riedl, G. Pfleiderer, (Duisberg, Walter H.). US, **1940**.

[29]   H.-J. Riedl, G. Pfleiderer, (I. G. Farbenindustrie AG). US, **1939**.

[30]   W. Manchot, *Leibigs. Ann. Chim* **1901**, *314*, 377.

[31]   G. Boxhoorn, (Shell Internationale Research Maatschappij B. V., Neth.). Application: EP, **1988**, p. 8 pp.

[32]   O. P. H. Vaughan, G. Kyriakou, N. Macleod, M. Tikhov, R. M. Lambert, *Journal of Catalysis* **2005**, *236*, 401.

[33]   M. Haruta, *Nature (London, United Kingdom)* **2005**, *437*, 1098.

[34]   T. Hayashi, K. Tanaka, M. Haruta, *Journal of Catalysis* **1998**, *178*, 566.

[35]   M. Haruta, M. Date, *Applied Catalysis, A: General* **2001**, *222*, 427.

[36]   T. A. Nijhuis, T. Visser, B. M. Weckhuysen, *Journal of Physical Chemistry B* **2005**, *109*, 19309.

[37]   B. S. Uphade, S. Tsubota, T. Hayashi, M. Haruta, *Chemistry Letters* **1998**, 1277.

[38]   T. A. Nijhuis, B. J. Huizinga, M. Makkee, J. A. Moulijn, *Industrial & Engineering Chemistry Research* **1999**, *38*, 884.

[39]   T. A. Nijhuis, T. Q. Gardner, B. M. Weckhuysen, *Journal of Catalysis* **2005**, *236*, 153.

[40]   N. Yap, R. P. Andres, W. N. Delgass, *Journal of Catalysis* **2004**, *226*, 156.

[41]   A. Zwijnenburg, M. Makkee, J. A. Moulijn, *Applied Catalysis, A: General* **2004**, *270*, 49.

[42]   C. Qi, T. Akita, M. Okumura, K. Kuraoka, M. Haruta, *Applied Catalysis, A: General* **2003**, *253*, 75.

[43]   B. Taylor, J. Lauterbach, W. N. Delgass, *Applied Catalysis, A: General* **2005**, *291*, 188.

[44]   A. K. Sinha, S. Seelan, S. Tsubota, M. Haruta, *Angewandte Chemie, International Edition* **2004**, *43*, 1546.

[45]   A. K. Sinha, S. Seelan, M. Okumura, T. Akita, S. Tsubota, M. Haruta, *Journal of Physical Chemistry B* **2005**, *109*, 3956.

[46]   B. Chowdhury, J. J. Bravo-Suarez, M. Date, S. Tsubota, M. Haruta, *Angewandte Chemie, International Edition* **2006**, *45*, 412.

[47]   M. D. Hughes, Y.-J. Xu, P. Jenkins, P. McMorn, P. Landon, D. I. Enache, A. F. Carley, G. A. Attard, G. J. Hutchings, F. King, E. H. Stitt, P. Johnston, K. Griffin, C. J. Kiely, *Nature (London, United Kingdom)* **2005**, *437*, 1132.

[48]   S. Biella, M. Rossi, *Chemical communications (Cambridge, England)* **2003**, 378.

[49]   M. Comotti, C. Della Pina, R. Matarrese, M. Rossi, A. Siani, *Applied Catalysis, A: General* **2005**, *291*, 204.

[50]   P. Beltrame, M. Comotti, C. Della Pina, M. Rossi, *Applied Catalysis, A: General* **2006**, *297*, 1.

[51]   N. Dimitratos, F. Porta, L. Prati, A. Villa, *Catalysis Letters* **2005**, *99*, 181.

[52]   S. Carrettin, P. McMorn, P. Johnston, K. Griffin, G. J. Hutchings, *Chemical Communications (Cambridge, United Kingdom)* **2002**, 696.

[53]   S. Carrettin, P. McMorn, P. Johnston, K. Griffin, C. J. Kiely, G. A. Attard, G. J. Hutchings, *Topics in Catalysis* **2004**, *27*, 131.

[54]   S. Carrettin, P. McMorn, P. Johnston, K. Griffin, C. J. Kiely, G. J. Hutchings, *Physical Chemistry Chemical Physics* **2003**, *5*, 1329.

[55]   F. Porta, L. Prati, *Journal of Catalysis* **2004**, *224*, 397.

[56]   C. Basheer, S. Swaminathan, H. K. Lee, S. Valiyaveettil, *Chemical Communications (Cambridge, United Kingdom)* **2005**, 409.

[57]   M. Comotti, C. Della Pina, R. Matarrese, M. Rossi, *Angewandte Chemie (International ed. in English)* **2004**, *43*, 5812.

[58]   P. G. N. Mertens, M. Bulut, L. E. M. Gevers, I. F. J. Vankelecom, P. A. Jacobs, D. E. De Vos, *Catalysis Letters* **2005**, *102*, 57.

[59]   P. G. N. Mertens, I. F. J. Vankelecom, P. A. Jacobs, D. E. De Vos, *Gold Bulletin (London, United Kingdom)* **2005**, *38*, 157.

[60]   H. Tsunoyama, H. Sakurai, Y. Negishi, T. Tsukuda, *Journal of the American Chemical Society* **2005**, *127*, 9374.

[61]   A. Abad, P. Concepcion, A. Corma, H. Garcia, *Angewandte Chemie,*
         International Edition **2005**, *44*, 4066.

[62]   A. Corma, M. E. Domine, *Chemical Communications (Cambridge, United*
         Kingdom) **2005**, 4042.

[63]   K. Mori, T. Hara, T. Mizugaki, K. Ebitani, K. Kaneda, *Journal of the*
         American Chemical Society **2004**, *126*, 10657.

[64]   D. I. Enache, J. K. Edwards, P. Landon, B. Solsona-Espriu, A. F. Carley, A.
         A. Herzing, M. Watanabe, C. J. Kiely, D. W. Knight, G. J. Hutchings,
         Science (Washington, DC, United States) **2006**, *311*, 362.

[65]   C. L. Hill, I. A. Weinstock, *Nature (London)* **1997**, *388*, 332.

[66]   S. A. Chavan, D. Srinivas, P. Ratnasamy, *Journal of Catalysis* **2002**, *212*, 39.

[67]   M. Nowotny, L. N. Pedersen, U. Hanefeld, T. Maschmeyer, *Chemistry--A*
         European Journal **2002**, *8*, 3724.

[68]   R. Raja, G. Sankar, J. M. Thomas, *Journal of the American Chemical Society*
         1999, *121*, 11926.

[69]   R. Zhao, D. Ji, G. Lu, G. Qian, L. Yan, X. Wang, J. Suo, *Chemical*
         Communications (Cambridge, United Kingdom) **2004**, 904.

[70]   G. Lue, R. Zhao, G. Qian, Y. Qi, X. Wang, J. Suo, *Catalysis Letters* **2004**, *97*,
         115.

[71]   Y.-J. Xu, P. Landon, D. Enache, A. F. Carley, M. W. Roberts, G. J.
         Hutchings, *Catalysis Letters* **2005**, *101*, 175.

[72]   H. T. Hess, I. Kroschwitz, M. Howe-Grant, **1995**, *13*, 961.

[73]   H. Henkel, W. Weber, US, **1914**.

[74]   G. A. Cook, (Carbide & Carbon Chemicals Corp.). US, **1945**.

[75]   M. Nystrom, J. Wanngard, W. Herrmann, (Akzo Nobel N.V., Neth.; Eka
         Chemicals AB). Application: WO, **1999**, p. 17 pp.

[76]   J. Van Weynbergh, J. P. Schoebrechts, J. C. Colery, (Interox International
         S.A., Belg.). Application: WO, **1992**, p. 19 pp.

[77]   B. Zhou, L.-K. Lee, (Hydrocarbon Technologies, Inc., USA). Application:
         US, **2001**, p. 11 pp.

[78]   R. Moritz, FR, **1918**.

[79]   L. W. Gosser, (du Pont de Nemours, E. I., and Co., USA). Application: EP,
         1985, p. 15 pp.

[80] L. W. Gosser, (du Pont de Nemours, E. I., and Co., USA). Application: EP, **1989**, p. 6 pp.

[81] L. W. Gosser, J. A. T. Schwartz, (du Pont de Nemours, E. I., and Co., USA). Application: US, **1989**, p. 9 pp.

[82] P. Landon, P. J. Collier, A. F. Carley, D. Chadwick, A. J. Papworth, A. Burrows, C. J. Kiely, G. J. Hutchings, *Physical Chemistry Chemical Physics* **2003**, *5*, 1917.

[83] P. Landon, P. J. Collier, A. J. Papworth, C. J. Kiely, G. J. Hutchings, *Chemical Communications (Cambridge, United Kingdom)* **2002**, 2058.

[84] S. Abate, S. Melada, G. Centi, S. Perathoner, F. Pinna, G. Strukul, *Catalysis Today* **2006**, *117*, 193.

[85] V. R. Choudhary, A. G. Gaikwad, S. D. Sansare, *Angewandte Chemie, International Edition* **2001**, *40*, 1776.

[86] T. A. Pospelova, N. I. Kobozev, *Zhurnal Fizicheskoi Khimii* **1961**, *35*, 1192.

[87] T. A. Pospelova, N. I. Kobozev, *Zhurnal Fizicheskoi Khimii* **1961**, *35*, 535.

[88] T. A. Pospelova, N. I. Kobozev, E. N. Eremin, *Zhurnal Fizicheskoi Khimii* **1961**, *35*, 298.

[89] F. Fu, K. T. Chuang, R. Fiedorow, *Stud. Surf. Sci. Catal* **1992**, *72*, 33.

[90] Q. Liu, J. H. Lunsford, *Applied Catalysis, A: General* **2006**, *314*, 94.

[91] Q. Liu, J. H. Lunsford, *Journal of Catalysis* **2006**, *239*, 237.

[92] J. H. Lunsford, *Abstracts of Papers, 223rd ACS National Meeting, Orlando, FL, United States, April 7-11, 2002* **2002**, COLL.

[93] J. H. Lunsford, *Journal of Catalysis* **2003**, *216*, 455.

[94] D. P. Dissanayake, J. H. Lunsford, *Journal of Catalysis* **2002**, *206*, 173.

[95] S. Chinta, J. H. Lunsford, *Journal of Catalysis* **2004**, *225*, 249.

[96] D. P. Dissanayake, J. H. Lunsford, *Journal of Catalysis* **2003**, *214*, 113.

[97] V. R. Choudhary, C. Samanta, T. V. Choudhary, *Applied Catalysis, A: General* **2006**, *308*, 128.

[98] V. R. Choudhary, C. Samanta, P. Jana, (Council of Scientific & Industrial Research, India). Application: US, **2006**, p. 10 pp.

[99] V. R. Choudhary, C. Samanta, *Journal of Catalysis* **2006**, *238*, 28.

[100] V. R. Choudhary, C. Samanta, P. Jana, *Chemical Communications (Cambridge, United Kingdom)* **2005**, 5399.

[101] V. R. Choudhary, C. Samanta, *Catalysis Letters* **2005**, *99*, 79.

[102] V. R. Choudhary, C. Samanta, A. G. Gaikwad, *Chemical Communications (Cambridge, United Kingdom)* **2004**, 2054.

[103] V. R. Choudhary, A. G. Gaikwad, *Reaction Kinetics and Catalysis Letters* **2003**, *80*, 27.

[104] V. R. Choudhary, S. D. Sansare, A. G. Gaikwad, *Catalysis Letters* **2002**, *84*, 81.

[105] V. R. Choudhary, A. G. Gaikwad, S. D. Sansare, *Catalysis Letters* **2002**, *83*, 235.

[106] R. Burch, P. R. Ellis, *Applied Catalysis, B:Environmental* **2003**, *42*, 203.

[107] T. Ishihara, Y. Ohura, S. Yoshida, Y. Hata, H. Nishiguchi, Y. Takita, *Applied Catalysis, A: General* **2005**, *291*, 215.

Chapter Two

Chapter 2 : Experimental

2.1   Introduction

There are many preparative methods for synthesizing supported gold catalysts. An important aspect when attempting to prepare a supported metal catalyst is the dispersion and particle size of the metal on the support. Generally, high dispersion and small particle size result in high selectivity and conversion. The role of the support in catalyst preparation is also important-the support should promote dispersion and provide stability against sintering of the active metallic species. This is achieved by employing metal oxides (TiO_2, SiO_2, Al_2O_3) or activated carbons that have high melting points and are chemically inert.

Wet impregnation preparation requires aqueous solutions of metal salts that are deposited on a support under stirring. Wet impregnation deposits all the metal which is put in, but can result in large metal particles and an uneven dispersion of metals on the surface. Deposition precipitation is the preferred method for depositing active gold species on supports such as titania. The resulting highly dispersed nano sized gold particles are known to be very active for CO oxidation[1-6].

2.2   Support preparation

2.2.1   Preparation of FeO_x

FeO_x was precipitated from an aqueous solution of $Fe(NO_3)_3.9H_2O$ (25g in 100ml, Aldrich) at pH = 8.2 by drop-wise addition aqueous $Na_2 CO_3$ (0.25M, Aldrich) over 1 h. After filtration, the Fe_2O_3 was dried at 120°C for 16 h.

2.2.2   Support pre-treatment

Prior to metal deposition the support can be subjected to a pre-treatment described as follows:

The support (10g) was suspended in HNO_3, HCl, H_3PO_4, $NaNO_3$ (1N (unless otherwise stated) 100ml) under stirring for 3 hours (unless otherwise stated). After filtration the support was washed with water (typically 1L) until the washings achieved pH=7. The resulting paste was dried for 16 h at 80°C prior to metal deposition.

2.3   Catalyst preparation

2.3.1   Preparation of Au, Pd and Au-Pd supported catalysts by wet impregnation

A range of catalysts were prepared using (γ–Al_2O_3 (Condea SCF-140), TiO_2 (P25 Degussa), SiO_2 (Degussa, Johnson Matthey, Grace), Activated carbon (AC (Aldrich Darco G60)), Fe_2O_3 (Cardiff University) using a wet impregnation technique. 5 wt % Pd/support, 5 wt %Au/support, and a range of Au-Pd/supported catalysts were prepared by impregnation of the support *via* a wet impregnation method using aqueous solutions of $PdCl_2$ (Johnson Matthey) and/or $HAuCl_4.3H_2O$ (Johnson Matthey). For the 2.5 wt % Au-2.5 wt % Pd catalyst, the detailed procedure was as follows: an aqueous solution (10 ml) of $HAuCl_4.3H_2O$ (5 g in 250 ml of water) and an aqueous $PdCl_2$ solution (4.15 ml of a solution of 1 g in 25 ml of water) were simultaneously added to the support (3.8 g). The paste formed was ground and dried at 80°C for 16 h and finally calcined (500mg, 3 inch ceramic boat) in static air at 400 °C for 3 h with a temperature ramp of 20°C a minute. Other Au-Pd ratios were prepared by varying the amounts of reagents accordingly. The catalysts were pretreated using a range of conditions: drying at 80°C in air for 3 h, calcination in static air at 400 °C for 3 h. Catalysts were used fresh (i.e. within a few hours of synthesis).

2.3.2 Preparation of Au-Pd catalysts by deposition precipitation.

A range of Au/TiO$_2$ catalysts were prepared by deposition precipitation using NaOH as the precipitant. For 2.5wt%Au/TiO$_2$ the following method was employed:

An aqueous solution (26mL) of HAuCl$_4$.3H$_2$O (Johnson Matthey, 5g in 250mL) was added to a slurry of TiO$_2$ (Degussa P25) in water (300mL) and stirred at room temperature for 30 min. Aqueous NaOH (1g in 25ml, Aldrich) was prepared and added dropwise until the pH of the slurry reached 9. After 1 h the solution was filtered and washed until the pH of the washings reached 7. The resulting paste was dried at 80 °C for 16 h and finally calcined in static air at 400 °C for 3 h with a temperature ramp of 20°C/min.

Following the synthesis of an Au/TiO$_2$ catalyst by deposition precipitation, Pd was deposited *via* impregnation with PdCl$_2$. The impregnation step occurred before the calcination of the Au/TiO$_2$ catalyst. The resulting bimetallic catalyst is calcined in static air 400°C for 3 h.

2.3.3 Preparation of Au/FeO$_x$ by co-precipitaiton

Dilute aqueous solutions of HAuCl$_4$. 3H$_2$O (0.43g, Johnson Matthey) and Fe(NO$_3$)$_3$.9H$_2$O (25g, Aldrich) are mixed under vigorous stirring at 50°C for 30 minutes. Aqueous Na$_2$CO$_3$ (0.25mol l^{-1}) is added until pH=8.2 is obtained. The pH is maintained for 45 min. The resulting precipitate is left to cool and washed under suction with approx 1l demineralised H$_2$O and dried in an oven at 80°C for 16 h.

2.4 Catalyst evaluation

2.4.1 H_2O_2 synthesis – Standard reaction conditions.

Catalyst testing was performed using a Parr Instruments stainless steel autoclave with a nominal volume of 50 ml and a maximum working pressure of 14 MPa. The autoclave was equipped with an overhead stirrer (0 – 2000 rpm) and provision for measurement of temperature and pressure. Typically, the autoclave was charged with catalyst (0.01 g unless otherwise stated), solvent (5.6 g alcohol and 2.9 g H_2O) purged three times with CO_2 (3 MPa) and then filled with 5% H_2/CO_2 and 25% O_2/CO_2 to give a hydrogen to oxygen stoichiometry of 1 : 2, at a total pressure of 3.7 MPa at 2°C. Stirring (1200 rpm) was started on reaching the desired temperature, and experiments were run for 30 min. H_2O_2 yield was determined by titration of aliquots of the final filtered solution with acidified $Ce(SO_4)_2$ (7 x 10^{-3} mol/l). $Ce(SO_4)_2$ solutions were standardised against $(NH_4)_2Fe(SO_4)_2.6H_2O$ using ferroin as indicator. Wt% H_2O_2 is determined as follows

Wt H_2O_2 formed in reaction / 8.5g x 100%

Gas analysis for H_2 and O_2 was performed by gas chromatography using a thermal conductivity detector and a CP–Carboplot P7 column (25 m, 0.53 mm i.d.). Conversion of H_2 was calculated by gas analysis before and after reaction. Selectivity was calculated by using the equation:

H_2 Sel towards H_2O_2 = (H_2O_2 yield / H_2 conversion) x 100 %

A series of experiments were conducted varying the alcohol used in the reaction. An investigation into alcohol : water concentrations was also completed. Reactions at elevated temperatures and longer reaction times were also conducted to optimise the autoclave reaction conditions.

A further series of experiments were performed with KBr (6 x 10^{-4} M, Aldrich) and H_3PO_4 (1.6 M, Aldrich) present in the reaction medium to simulate industrial type conditions.

2.4.2 H_2O_2 decomposition studies

The autoclave was charged with catalyst (0.01 g), solvent (5.6 g Alcohol and 2.9 g H_2O) and H_2O_2 (0.5wt%) purged three times with CO_2 (3 MPa) and then filled with 5% H_2/CO_2 and 25% O_2/CO_2 to give a H_2 : O_2 ratio of 1 : 2, at a total pressure of 3.7 MPa at 2°C. Stirring (1200 rpm) was started on reaching 2°C, and experiments were run for 30 min. To determine the extent of decomposition over 30 minutes aliquots of the final filtered solution were titrated with acidified $Ce(SO_4)_2$ (7 x 10^{-3} mol/l). $Ce(SO_4)_2$ solutions were standardised against $(NH_4)_2Fe(SO_4)_2.6H_2O$ using ferroin as indicator.

2.4.3 Refresh Experiments

A series of experiments were undertaken to mimic industrial conditions by operating a semi-continuous batch reaction as follows.

The autoclave was charged with catalyst (0.01 g), solvent (5.6 g alcohol and 2.9 g H_2O) purged three times with CO_2 (3 MPa) and then filled with 5% H_2/CO_2 and 25% O_2/CO_2 to give a H_2 : O_2 molar ratio of 1 : 2, at a total pressure of 3.7 MPa at 2°C. Stirring (1200 rpm) was started on reaching 2°C, and experiments were carried out for 30 min. Following the reaction the autoclave was again purged three times with CO_2 (3 MPa) and then filled with again 5% H_2/CO_2 and 25% O_2/CO_2 to give a H_2 : O_2 molar ratio of 1 : 2, at a total pressure of 3.7 MPa at 2°C. Following this refresh of the reactant gases the autoclave was allowed to reach 2°C, then left to stir (1200rpm) for a further 30 minu. H_2O_2 yield was determined as before. The refresh was repeated up to 10 times.

2.4.4 *In-situ* capture of H_2O_2- oxidation of benzyl alcohol to benzaldehyde

Alcohol oxidation was performed using a Parr Instruments stainless steel autoclave with a nominal volume of 50 ml and a maximum working pressure of 14 MPa. The autoclave was equipped with an overhead stirrer (0 – 2000 rpm) and provision for measurement of temperature and pressure. Typically, the autoclave was charged with catalyst (0.1 g unless otherwise stated), solvent (5.6 g MeOH and 2.9 g H_2O) and benzyl alcohol (0.085 g) purged three times with CO_2 (3 MPa) and then filled with 5% H_2/CO_2 and 25% O_2/CO_2 to give a H_2 : O_2 molar ratio of 1 : 2, at a total pressure of 3.7 MPa at room temperature. Stirring at 1200 rpm was started on reaching the desired temperature, and experiments were run for 22 h (unless otherwise stated). After filtration the reaction mixture was analysed by GC using a DB-Wax column.

2.4.5 Catalyst Stability

A number of experiments were completed to ascertain the stability of catalysts calcined at various temperatures. The autoclave was charged with catalyst (0.1g), solvent (5.6 g alcohol and 2.9 g H_2O) purged three times with CO_2 (3 MPa) and then filled with 5% H_2/CO_2 and 25% O_2/CO_2 to give a H_2 : O_2 molar ratio of 1 : 2, at a total pressure of 3.7 MPa at 2°C. Stirring (1200 rpm) was started on reaching 2°C, and experiments were run for 30 min. After filtration, 0.01g of the catalyst was re-used as described previously, and the activity ascertained. If the catalyst exhibits lower activity on re-use the composition of the catalyst was determined by atomic absorption spectroscopy (AAS).

2.5 Catalyst Characterisation

2.5.1 Atomic Absorption Spectroscopy (AAS)

2.5.1.1 Background

Atomic-absorption spectroscopy uses the absorption of light to measure the concentration of gas-phase atoms. If the sample to be analysed is a liquid or solid, the analyte atoms or ions are vaporized in a flame or graphite furnace. In their elemental form, metals will absorb ultraviolet light when they are excited by heat. Each metal has a characteristic wavelength that will be absorbed. The AAS instrument looks for a particular metal by focusing a beam of UV light at a specific wavelength through a flame and into a detector. The sample of interest is aspirated into the flame. If that metal is present in the sample, it will absorb some of the light (corresponding to the excitement of an electron from its ground state), thus reducing the intensity of the beam. The instrument measures this change in intensity. A computer data system converts the change in intensity into an absorbance (figure 2.1). Concentration measurements are usually determined from a working curve after calibrating the instrument with standards of known concentration.
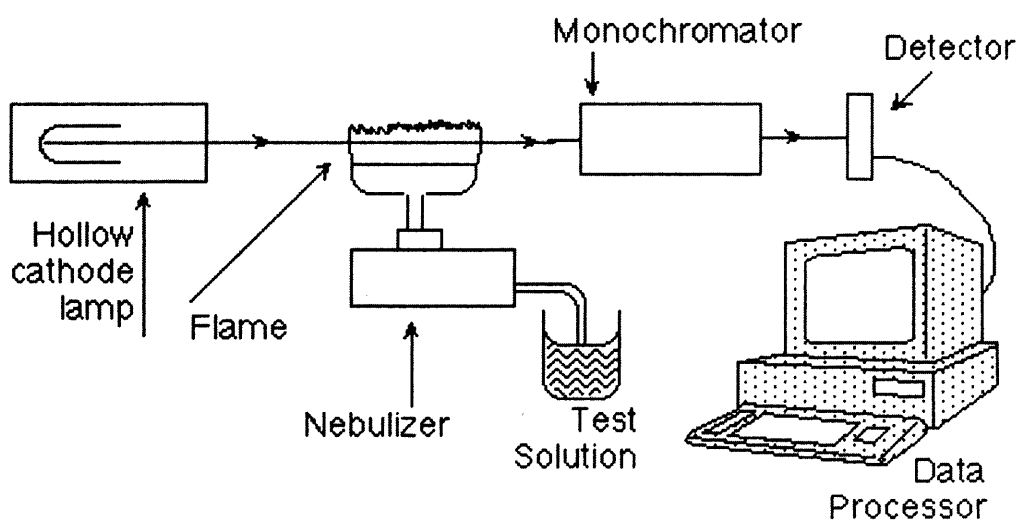
Figure 2.1 Schematic of an atomic absorption spectrophotometer

2.5.1.2 Experimental

Atomic absorption spectroscopy (AAS) was performed with a Perkin–Elmer 2100 Atomic Absorption spectrometer using an air–acetylene flame. Gold/palladium samples were examined at wavelengths 242.8 nm (Au) and 247.6 nm (Pd). Samples for analysis were prepared by dissolving an aliquot of the dried catalyst (0.1 g) in an aqua regia solution, followed by the addition of 250 ml deionised water to dilute the sample. AAS was used to determine the wt% of the metal incorporated into the support after impregnation, as well as the concentration (ppm) of Au or Pd that had leached out into solution during reaction, by determining the Au and Pd content of the used catalyst and comparing the value to that obtained for the fresh catalyst.

2.5.2   X-Ray photoelectron spectroscopy (XPS)

2.5.2.1 Background

X-ray Photoelectron Spectroscopy (XPS) is a quantitative spectroscopic technique that measures the empirical formula, chemical state and electronic state of the elements that exist within a material. XPS spectra are obtained by irradiating a material with a monochromatic beam of X-rays. The photons from the X-rays are absorbed by an atom in a molecule or solid, leading to ionization and the emission of a core (inner shell) electron (figure 2.2). The kinetic energy distribution of the emitted photoelectrons (i.e. the number of emitted photoelectrons as a function of their kinetic energy) can be measured using any appropriate electron energy analyser and a photoelectron spectrum can be recorded. For each and every element, there is a characteristic binding energy associated with each core atomic orbital *i.e.* each element will give rise to a characteristic set of peaks in the photoelectron spectrum at kinetic energies determined by the photon energy and the respective binding

energies. The presence of peaks at particular energies therefore indicates the presence of a specific element in the sample under study - furthermore, the intensity of the peaks is related to the concentration of the element within the sampled region.
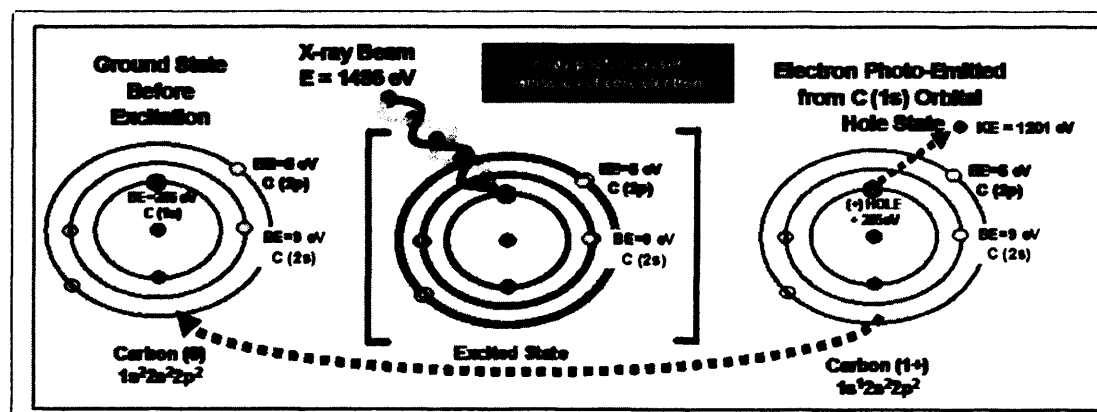
Figure 2.2 Photoemission during X-ray irradiation of carbon[4]

2.5.2.2 Experimental

X-Ray photoelectron spectroscopy (XPS) was performed using a VG EscaLab 220i spectrometer, using a standard Al-Kα X-ray source (300 W) and an analyser pass energy of 20 eV. Samples were mounted using double-sided adhesive tape, and binding energies were referenced to the C 1s binding energy of adventitious carbon contamination, which was taken to be 284.7 eV.

2.5.3   Scanning Transmission Electron Spectroscopy (STEM)

2.5.4.1 Background

A scanning transmission electron microscope (STEM) is a type of transmission electron microscope, an imaging technique whereby a beam of electrons is focused onto a specimen causing an enlarged version to appear on a fluorescent screen or layer of photographic film, or to be detected by a CCD camera.

With a STEM, a beam of primary electrons strike the surface and are inelastically scattered by atoms in the sample. Through these scattering events, the primary electron beam effectively spreads and fills a teardrop-shaped volume, known as the interaction volume, extending from less than 100 nm to around 5 µm into the surface. Interactions in this region lead to the subsequent emission of electrons which are then detected to produce an image. What makes a STEM different to a TEM is the electron beam is scanned in parallel lines across the sample. The results from this raster scan (which can be likened to an image cut up into successive samples called pixels, or picture elements across the line) can then be analysed by ADF (annular dark field) and EDX (energy dispersive X-ray) methods.

EDX identifies an element by detecting the precise amount of energy produced by an X-ray caused by the movement of an electron within the element. Consider the STEM electron beam displacing an inner shell electron. This vacancy is replaced by a higher energy outer shell electron, and produces an X-ray to lose the energy required to fill the vacancy. The amount of energy released by the transferring electron depends on which shell it is transferring from, as well as which shell it is transferring to. Furthermore, the atom of every element releases X-rays with unique amounts of energy during the transferring process. Thus, by measuring the amounts of energy present in the X-rays being released by a specimen during electron beam bombardment, the identity of the atom from which the X-ray was emitted can be established. If the electron beam scans the sample, EDX can be performed at every pixel of the raster scan, and a profile across a sample can be imaged.

A bright field image in electron microscopy is formed when the unscattered electrons of the incident beam combine with the scattered electrons as modified by passage through the objective aperture (figure 2.3). Dark areas in the image arise from specimen regions which scatter electrons widely and into the objective aperture. If the unscattered electrons are removed, the image is formed only from the scattered electrons (i.e. those which have interacted with the specimen) and a dark field image is produced. This imaging mode is called "dark-field" because the viewing screen is

dark unless there is specimen present to scatter electrons. Dark field images typically have considerably higher contrast than bright field images although the intensity is greatly reduced, therefore requiring longer photographic exposures. The Annular Dark Field (ADF) signal from the annular detector is also sensitive to the atomic number of the atoms - the greater the atomic number, the greater is the scattering intensity.
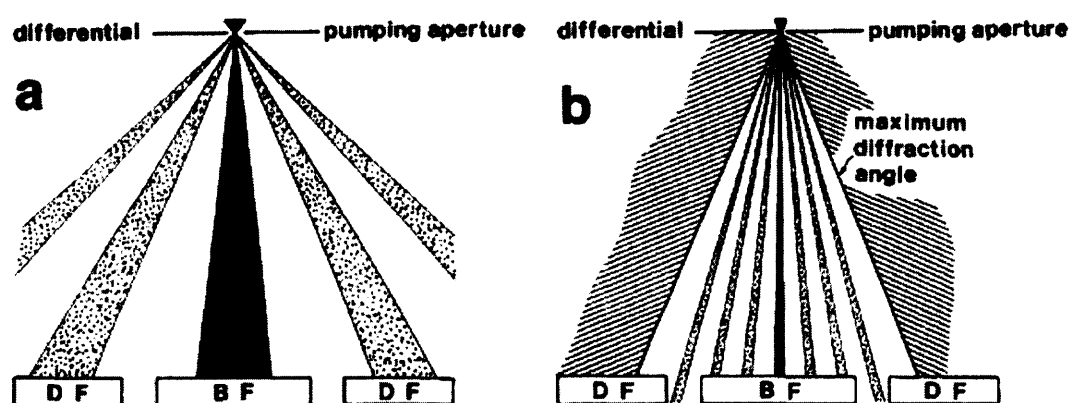
Fig. 1. Detector/camera length configurations for annular dark-field imaging (a) and high-angle annular dark-field imaging (b). At the camera length used for dark-field imaging (about 300 to 700 mm), the bright-field beam (solid ray path) falls on the central bright-field detector (BF), while Bragg beams (dotted ray paths) fall on the annular dark-field detector (DF). In high-angle annular dark-field im-

aging, the camera length is reduced to a small value (about 50 to 80 mm). This results in the bright-field and Bragg beams falling on the bright-field detector, while the Rutherford-scattered electrons at the edge of the diffraction pattern fall on the dark-field detector, generating the high-angle annular dark-field image.

Figure 2.3 Detector/camera length configuration for bright field (BF), dark field (DF) and high angle dark field images[7]

MSA is a group of processing techniques that can be used to identify specific features within large data sets such as X-ray spectrum images and to reduce random noise components in the data sets in a statistical manner[8]. MSA has recently been shown to be particularly useful for analysis of X-ray maps taken from nanoparticles[9]. This statistical technique performs a data smoothing calculation by portioning the EDS data using a probability density function

2.5.4.2 Experimental

Samples for characterisation by scanning transmission electron microscopy (STEM) were prepared by dispersing the catalyst powder in high-purity ethanol, then allowing a drop of the suspension to evaporate on a holey carbon film supported by a

300-mesh copper grid. Samples were then subjected to chemical microanalysis and annular dark-field imaging in a VG Systems HB603 STEM operating at 300 kV equipped with a Nion Cs corrector. The instrument was also fitted with an Oxford Instruments INCA TEM 300 system for energy-dispersive X-ray (XEDS) analysis.

2.7 References

[1] X.-Y. Wang, S.-P. Wang, S.-R. Wang, Y.-Q. Zhao, J. Huang, S.-M. Zhang, W.-P. Huang, S.-H. Wu, *Catalysis Letters* **2006**, *112*, 115.

[2] R. J. H. Grisel, B. E. Nieuwenhuys, *Journal of Catalysis* **2001**, *199*, 48.

[3] E. D. Park, S. H. Choi, J. S. Lee, *Journal of Physical Chemistry B* **2000**, *104*, 5586.

[4] Z. Suo, L. An, H. He, J. Shang, M. Jin, *Ranliao Huaxue Xuebao* **1999**, *27*, 451.

[5] H. Kita, H. Nakajima, K. Hayashi, *Journal of Electroanalytical Chemistry and Interfacial Electrochemistry* **1985**, *190*, 141.

[6] T. K. Gibbs, C. McCallum, D. Pletcher, *Electrochimica Acta* **1977**, *22*, 525.

[7] M. T. Otten, *Journal of electron microscopy technique* **1991**, *17*, 221.

[8] N. Bonnet, *Journal of Microscopy (Oxford)* **1998**, *190*, 2.

[9] M. Wanatabe, *Microscopy Microanalysis* **2004**, 468

Chapter Three

Chapter Three : Direct synthesis of H_2O_2 from H_2 and O_2 over Au, Pd and Au-Pd/TiO$_2$catalysts

---

3.1   Introduction

Hydrogen peroxide is a noted green oxidant that is useful in many large scale processes, such as bleaches and as a disinfectant, and also as an oxidant in the fine chemical industry. A catalytic, direct route for hydrogen peroxide synthesis is investigated, as an alternative the current process; the costly and non-green synthesis of hydrogen peroxide via the anthraquinone cycle.

Following on from the work of Landon *et al.*[1, 2] where Au and Au-Pd catalysts supported on alumina were shown to be active for the direct synthesis of hydrogen peroxide, a series of supported Au, Pd and Au-Pd alloyed catalysts were prepared and their activity for H_2O_2 synthesis evaluated. Titania (P25, Degussa) was used as the initial support as it has been shown previously that highly dispersed Au/TiO$_2$ catalysts exhibit high activity for CO oxidation[3-6] and have also shown to be active for the water gas shift reaction[7, 8].

3.2   Evaluation of Au/TiO$_2$, Pd/TiO$_2$ and Au-Pd/TiO$_2$ catalysts for H_2O_2 synthesis under standard reaction conditions as defined in chapter 2.

3.2.1   Comparison of Au/TiO$_2$ catalysts for H_2O_2 synthesis and CO oxidation.

A series of 5%Au/TiO$_2$ catalysts were prepared by impregnation (I) and deposition precipitation (DP) and tested for H_2O_2 synthesis and CO oxidation under standard reaction conditions. The results, shown in table 3.1, show that catalysts prepared by deposition precipitation exhibit high activity for CO oxidation and low activity for H_2O_2 synthesis, whereas catalysts prepared by impregnation show good activity for H_2O_2 synthesis but are inactive for CO oxidation.

Table 3.1 Effect of Au/TiO$_2$ preparation on CO oxidation and H$_2$O$_2$ synthesis

Catalyst	Preparation Method	Pre-treatment	Productivity (mol/kg/hr)	H$_2$O$_2$ (wt%)	CO conversion (%)
5%Au/TiO$_2$	DP	air 25 °C	0.229	0.002	85
5%Au/TiO$_2$	DP	air 120 °C	0.482	0.005	76
5%Au/TiO$_2$	DP	air, 400°C	0.388	0.004	40
5%Au/TiO$_2$	I	air, 400°C	7.1	0.014	<1

(H$_2$O$_2$ synthesis : 50mg catalyst in 5.6g Methanol 2.9g water at 2°C for 30 min, molar ratio H$_2$:O$_2$ 1:2, CO oxidation : 50mg catalyst, 25°C, 22.5ml min^{-1})

Calcination of the catalyst prepared by DP does not affect the activity of the catalyst with regards to H$_2$O$_2$ synthesis, but causes a 50% decrease in activity for CO oxidation.

3.2.2   Pd and Au-Pd/TiO$_2$ catalysts for CO oxidation and H$_2$O$_2$ synthesis

A 5%Pd/TiO$_2$ and 2.5%Au-2.5%Pd/TiO$_2$ catalyst were prepared by impregnation (I) and tested for H$_2$O$_2$ synthesis and CO oxidation under standard reaction conditions. For the catalysts prepared by impregnation and calcined at 400°C, the pure Au catalysts all generate H$_2$O$_2$ but at low rates (table 3.2). The addition of Pd to Au significantly enhances the catalytic performance for the synthesis of H$_2$O$_2$, and moreover it is interesting to note that there is an optimum Pd-Au composition where the rate of H$_2$O$_2$ production is much higher than for the pure Pd catalyst, which in itself is significantly more active than pure gold. The highest rates are observed when equal amounts by weight of Au and Pd are present. Furthermore, the 2.5 wt% Au/2.5

wt% Pd/TiO$_2$ catalyst gives remarkably higher selectivities than was found with alumina as a support.[1,2] In addition, the rates of hydrogen peroxide formation with the TiO$_2$ supported catalysts are generally a factor of three higher than the corresponding Al$_2$O$_3$-supported catalyst[1,2] demonstrating that the nature of the support plays an important role in the direct oxidation reaction.

Table 3.2 H$_2$O$_2$ synthesis over impregnated Au, Pd and Au-Pd catalysts

Catalyst	Pre-treatment	Productivity (mol/kg/hr)	H$_2$O$_2$ (wt%)	CO conversion (%)
5%Au/TiO$_2$	air, 400°C	7.1	0.014	<1
4%Au/1%Pd/TiO$_2$	air, 400°C	28	0.057	<1
2.5%Au/2.5%Pd/TiO$_2$	air, 400°C	64	0.128	<1
5%Pd/TiO$_2$	air, 400°C	31	0.061	<1

(H$_2$O$_2$ synthesis : 50mg catalyst Au only, 10mg Pd, Au-Pd otherwise as table 3.1;

CO oxidation – as table 3.1)

3.3   Optimisation of the standard reaction

3.3.1   Influence of catalytic mass and reaction time

The reaction time and amount of catalyst used are important variables in the direct synthesis reaction since there are a number of competing processes that lead to the decomposition of hydrogen peroxide even at 2°C. The effect of increasing reaction time in the autoclave is shown in Fig. 3.1 for the 2.5% Au/2.5% Pd/TiO$_2$ catalyst calcined at 400°C. Separate experiments were conducted for each reaction time and so the data present the amount of H$_2$O$_2$ formed as an average over the

reaction period. It is apparent that as the yield of H_2O_2 increases steadily with reaction time so the rate of formation decreases, and under our reaction conditions we have concluded that 30 min. gives a reasonable compromise between rate and overall yield of H_2O_2 for the purposes of comparing the catalytic performance of these catalysts.
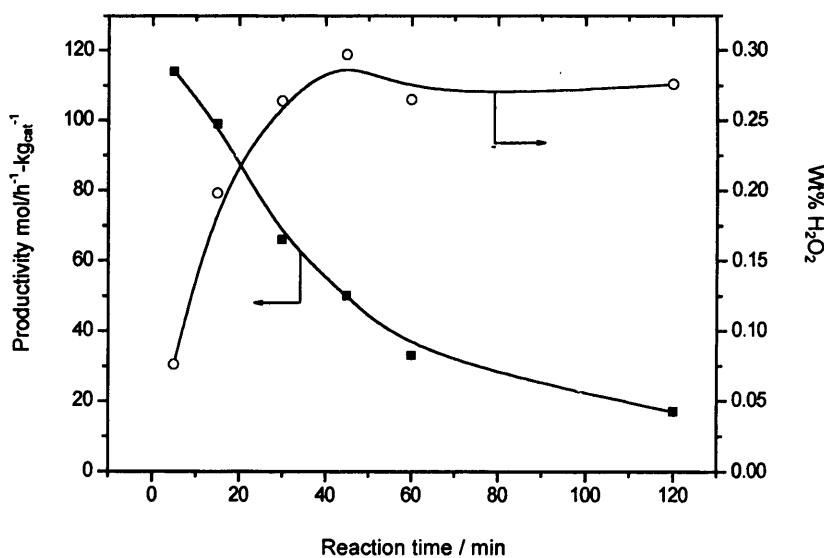
Figure 3.1 Effect of reaction time on yield and rate of H_2O_2 synthesis over 2.5wt%Au-2.5wt%Pd/TiO$_2$ calcined 400°C 3hours in static air under standard reaction conditions as detailed in chapter 2.

Using gas chromatography the hydrogen conversion and selectivity over the calcined 2.5wt%Au-2.5wt%Pd/TiO$_2$ was determined at different reaction times. The conversion was determined by measuring the hydrogen consumed during the reaction, and the selectivity determined from the hydrogen conversion and the yield of hydrogen peroxide. The results are shown in table 3.3.

Table 3.3 Influence of reaction time on the conversion of H_2 and selectivity to hydrogen peroxide synthesis

Reaction time	Productivity (mol/kg/hr)	H_2 conversion (%)	H_2O_2 selectivity (%)	Yield H_2O_2(%)
5	114	8	93	7.6
30	66	44	60	26.4
120	17	93	29	27.6

(20mg of the 400°C calcined 2.5% Au- 2.5%Pd/TiO₂ catalyst used, reaction conditions as table 3.1)

For the 2.5% Au/2.5% Pd/TiO₂ calcined at 400°C, the initial rate after 5 min reaction time is >100 mol Kg_{cat}^{-1} h^{-1} with a hydrogen selectivity of >90%. Increasing the length of the reaction decreases the selectivity to H_2O_2 as water, the preferential product for the reaction, is formed at high conversions.

3.3.2 Influence of catalyst mass

The effect of increasing the amount of catalyst in the autoclave is shown in Fig. 3.2 for the 2.5% Au/2.5% Pd/TiO₂ calcined at 400 °C. It is apparent that the yield of H_2O_2 produced increases as the amount of catalyst is increased in the water methanol system, indication that the reaction is not mass transport limited. However the rate of H_2O_2 synthesis is highest at lower catalyst masses.
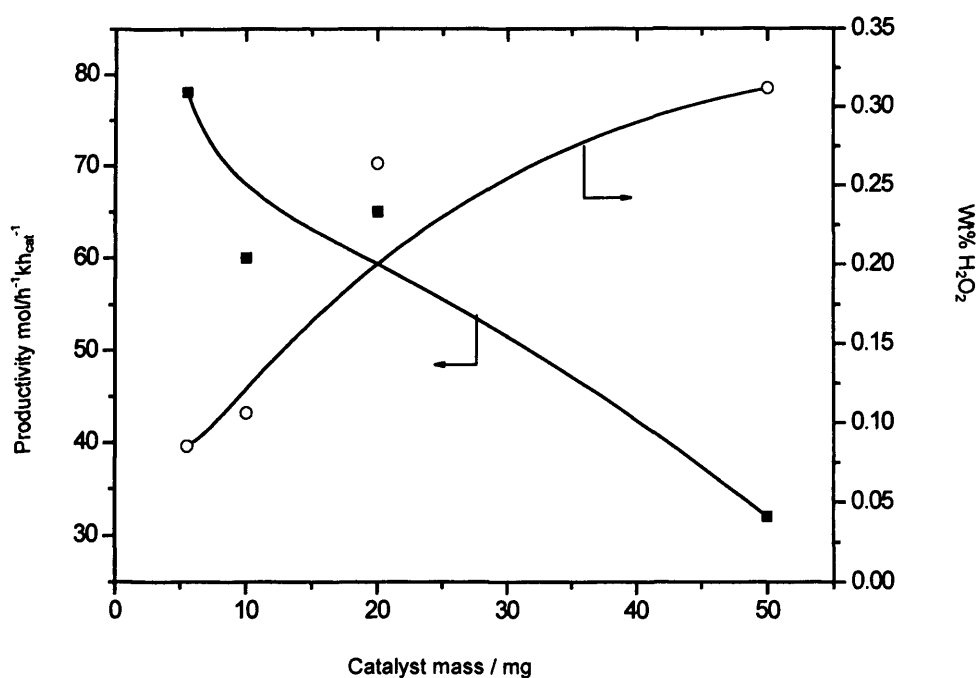
Figure 3.2   Effect of catalyst mass on the synthesis (■) and concentration (O) of hydrogen peroxide using a 2.5 wt%Au-2.5wt%Pd/TiO₂ catalyst 400°C 3hr air under standard conditions as detailed in chapter 2.

3.3.3   Influence of calcination and reduction

The effect of calcination and reduction on the optimum composition of the TiO₂ supported catalyst was investigated and the results are presented in Table 3.4. It is apparent that calcination either by itself or followed by reduction in H₂ leads to a significant decrease in the rate of H₂O₂ synthesis, determined as an average over the 30 min reaction period. The uncalcined bimetallic catalyst, *i.e.* a sample that has only been dried at 25°C, gives the highest rate of H₂O₂ synthesis (202 mol-H₂O₂/h/Kg$_{cat}$), H₂ conversion (46%) and H₂O₂ selectivity (89%). Increasing calcination temperature causes a decrease in selectivity, conversion and productivity of Pd only catalysts, and the bimetallic Au-Pd catalyst.

Table 3.4 The effect of catalyst calcination and/or reduction treatment on hydrogen peroxide synthesis for 2.5wt%Au-2.5wt%Pd/TiO₂ catalysts

Catalyst	Pretreatment	Productivity (mol/kg/hr)	H_2O_2 (Wt.%)	H_2 conversion (%)	H_2O_2 selectivity (%)
2.5%Pd/TiO₂	air, 25 °C,	90	0.180	38	48
5%Pd/TiO₂	air, 25 °C,	173	0.346	86	40
2.5%Au-2.5%Pd/TiO₂	air, 25 °C,	202	0.404	46	89
5%Pd/TiO₂	air, 200 °C, 3 h	99	0.198	42	47
2.5%Au-2.5%Pd/TiO₂	air, 200°C,3h	124	0.248	34	73
2.5%Pd/TiO₂	air, 400 °C, 3 h	24	0.048	19	25
5%Pd/TiO₂	air, 400 °C, 3 h	31	0.062	29	21
2.5%Au-2.5%Pd/TiO₂	air, 400°C, 3 h	64	0.128	21	61
2.5%Au-2.5%Pd/TiO₂	air, 400°C, 3 h + H₂ 500°C	32	0.064	Nd	Nd

(10 mg catalyst in 5.6g Methanol 2.9g water at 2°C, 30 min reaction, 1200 rpm stirring, molar ratio H₂ : O₂ 1 : 2, Nd Not determined)

Reduction of the bimetallic catalyst with H_2 at 500°C causes a further decrease in catalytic activity. The activity of the Au-Pd catalysts is higher that the mono metallic catalysts, regardless of calcination//temperature treatment. The selectivity of the Pd only catalysts is consistently lower than the Au-Pd catalysts, although the conversion of H_2 over the bimetallic catalysts is lower than over the pure Pd supported catalysts.

It can bee seen from figure 3.3 that the length of calcination can also have an effect on catalyst activity, catalysts calcined for 16 hours are markedly less active for H_2O_2 synthesis than catalysts which are calcined under standard conditions.
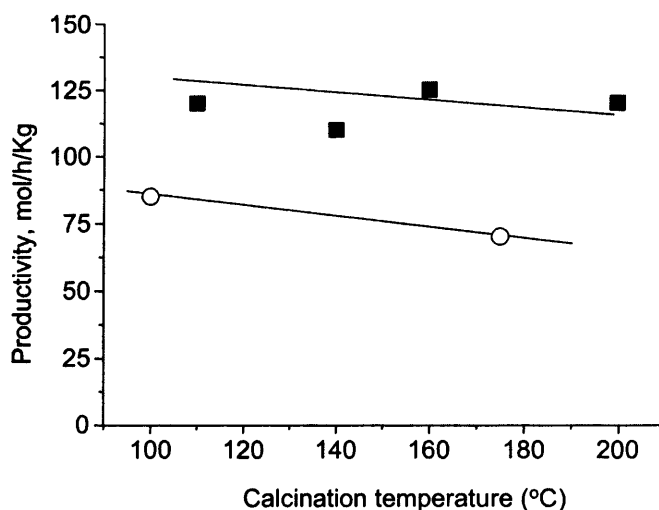
Figure 3.3   Effect of calcination duration on H_2O_2 synthesis for a 2.5wt%Au-2.5wt%Pd/TiO$_2$ catalyst (■ 3 hour calcination, O 16 hour calcination)

3.3.4   Influence of solvent system

Following on from the work of Landon[1, 2], a standard solvent system (5.6g methanol, 2.9g water) was employed to screen the catalysts under standard reaction conditions. A series of experiments varying the Methanol:Water ratio were carried out to determine the optimum system for the 2.5wt%Au-2.5%Pd/TiO$_2$ calcined 400°C catalyst, with the other reaction parameters as standard. The results are illustrated in figure 3.4, and show that a methanol : water ratio of 80vol%:20vol% (as opposed to 65vol%35vol% methanol : water) was optimum for this catalyst.

It was interesting to note that the catalyst exhibited high activity in 100% water, which would be of interest if the reaction were to be scaled up to an industrial

level. A problem that can be encountered when using a 3-phase reactor set up is mass transfer limited at the catalyst : gas interface.
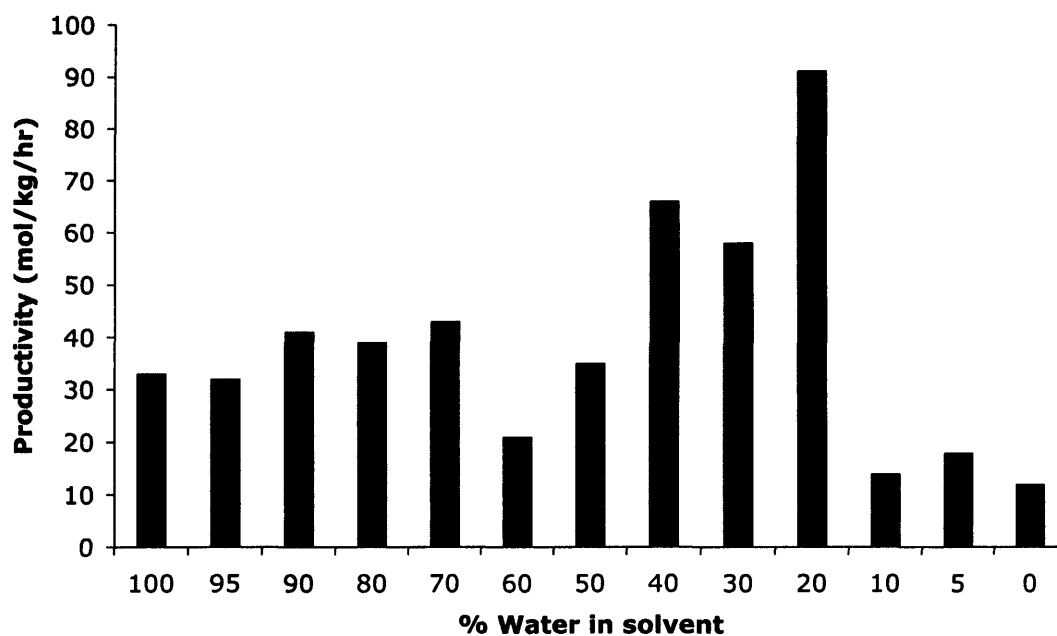
Figure 3.4 Influence of solvent composition on activity for 2.5wt%Au-2.5wt%Pd/TiO$_2$ catalyst calcined 400°C 3hours in air.

Experiments were conducted to ascertain whether, under standard reaction conditions, the yield of the hydrogen peroxide in water was independent of the catalyst mass, i.e. whether the reaction was diffusion limited in water. These results, shown in figure 3.5, clearly illustrate that the reaction is not diffusion limited in water.
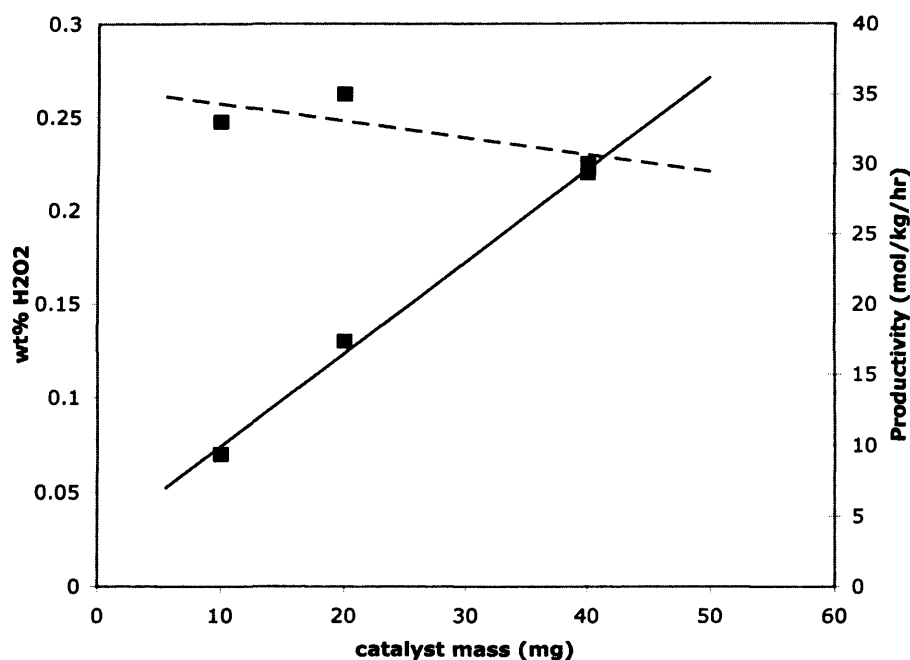
Figure 3.5 Effect of catalyst mass on hydrogen peroxide formation (●) and concentration (■) for 2.5wt%Au-2.5wt%Pd/TiO₂ catalyst calcined at 400°C for 3 hours in air. Reaction performed in pure water, all other conditions as standard (detailed in chapter 2)

3.3.5   Catalyst stability

Due to the nature of the impregnation preparation (deposition of Au and Pd cations), a series of experiments were conducted to determine the stability of the catalysts under standard reaction conditions. One of the key factors that must be considered for heterogeneous catalysts operating in three phase systems is the possibility that active components can leach into the reaction mixture, thereby leading to catalyst deactivation or, in the worst case, leading to the formation of an active homogeneous catalyst. In order to demonstrate that the TiO₂ supported gold/palladium catalysts function as wholly heterogeneous catalysts, an experiment was carried out using a supported gold-palladium catalyst (calcined at 400 °C) at 2°C

and the yield of H_2O_2 was determined. Following this reaction, the catalyst was removed by careful filtration and the solution was used for a second experiment using O_2/H_2. No further H_2O_2 was formed and this confirms that the formation of hydrogen peroxide involves gold or palladium acting as a wholly heterogeneous catalyst.

Table 3.5 Leaching of gold and palladium in 2.5wt%Au-2.5wt%Pd/TiO$_2$ after reaction

Pre-treatment	Use	Loss of Au (%)	Loss of Pd (%)
Air, 25°C	1	80	90
	2	92	95
Air, 200°C, 3 h	1	11	0
	2	13	0
Air, 400°C, 3 h	1	0	0
	2	0	0

(10mg catalyst, reaction conditions outlined in table 3.1

Metal loss calculated as metal in used catalyst/metal in fresh catalyst x 100%)

In contrast, the uncalcined Au-Pd/TiO2 catalysts were particularly unstable and could not be re-used effectively. Atomic absorption analysis revealed that almost all the Au and Pd was lost during the initial usage. Table 3.5 shows the loss of palladium and gold by leaching after catalytic testing for the following 2.5% Au/2.5% Pd/TiO2 catalysts: uncalcined, calcined at 200°C and calcined at 400°C. The catalyst calcined at 400 oC did not leach either Au or Pd within detection limits. However, the catalysts which were uncalcined and calcined at 200oC lost both gold and palladium after reaction and showed consequent de-activation in subsequent re-use test (figure 3.6) It is interesting to note that the uncalcined catalyst maintains a

higher productivity after 3 uses (where > 90% of the metals have leached) than the stable catalyst calcined at 400°C.
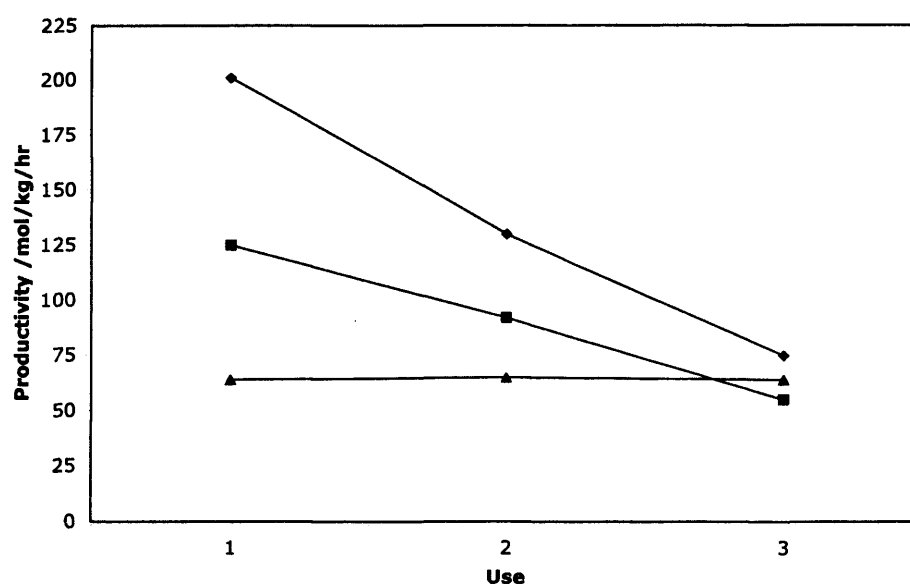
Figure 3.6 The effect of number of uses on the productivity of H_2O_2 formation for a series of 2.5wt%Au-2.5wt%Pd/TiO₂ catalysts uncalcined (◆), calcined air 200°C (■) and calcined air 400°C (▲) Blanks were performed after each use to ensure no residual activity in the autoclave.

3.4   Spectroscopic analysis

A number of different spectroscopic techniques were employed to attempt to elucidate the nature of the supported Au-Pd catalysts. The catalysts were studied using a number of surface sensitive techniques, namely by X-ray photoelectron spectroscopy (XPS) and scanning transmission electron microscopy (STEM). The catalysts all had a total BET surface area in the range of 35-45m^{2}g^{-1} which was not considered an important factor with respect to activity.

3.4.1   X-Ray Photoelectron spectroscopy (XPS)

X-ray photoelectron spectroscopy (XPS) was conducted as detailed I previously in chapter 2

3.4.1.1 XPS analysis of 2.5wt%Au-2.5wt5Pd/TiO$_2$ heat treated catalysts.

Figure 3.5 shows the combined Au(4d) and Pd(3d) spectra for a 2.5 wt% Au-2.5 wt% Pd/TiO$_2$ catalyst after different heat treatments. For the uncalcined sample, which exhibits the highest rate of H$_2$O$_2$ production that we have observed to date for a titania-supported catalyst, there are clear spectral contributions from both Au and Pd leading to severe overlap of peaks.
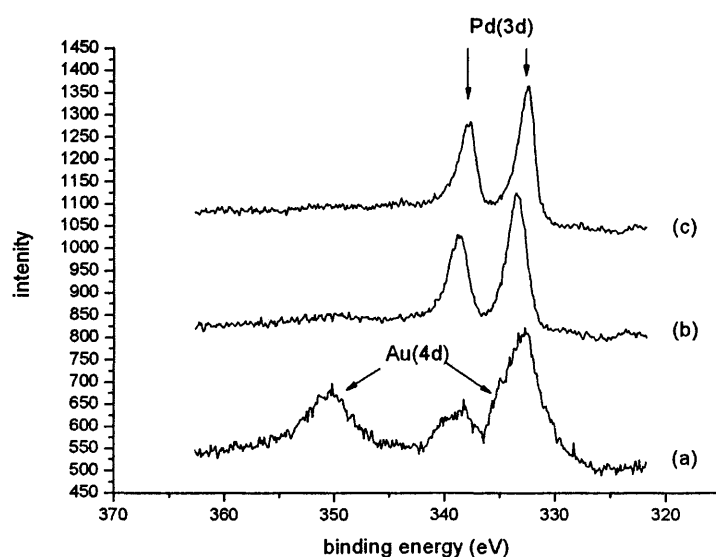
Figure 3.7 Au(4d) and Pd(3d) spectra for a 2.5 wt% Au-2.5 wt% Pd/TiO$_2$ catalyst after different heat treatments (a) uncalcined, (b) calcined at 200 °C in air, (c) calcined at 400 °C in air and 500 °C in hydrogen

After heat treatment at 200°C there is a dramatic decrease in the intensity of the Au(4d) peaks, and after calcination in air at 400°C followed by reduction in H$_2$ at 500°C, the intensity of the Au(4d$_{3/2}$) feature is below detection limits. In order to quantify the surface composition of the uncalcined catalyst the spectral envelope was deconstructed into its respective Pd(3d) and Au(4d) components. This was achieved

by subtracting out the Pd(3d) contribution, using a suitably scaled and shifted reference spectrum. Although the calcined and reduced sample provides such a standard in principle, it is clear from a visual inspection that the FWHM of the Pd($3d_{3/2}$) peak is much greater in the uncalcined spectrum; this may be in part due to the palladium being present as both Au-Pd alloy particles and pure Pd particles.

3.4.1.2 XPS analysis of uncalcined 2.5wt%Au-2.5wt%Pd/TiO₂ before and after reaction.

The XPS spectra of the uncalcined 2.5wt%Au-2.5wt%Pd/TiO₂ was taken after reaction in an attempt to clarify the conformational changes of the catalyst during the reaction. The spectra observed for the uncalcined sample after reaction (Fig. 3.8) is consistent with the substantial leaching of metal into solution observed in the catalytic studies, showing weak Pd features and no detectible gold intensity.
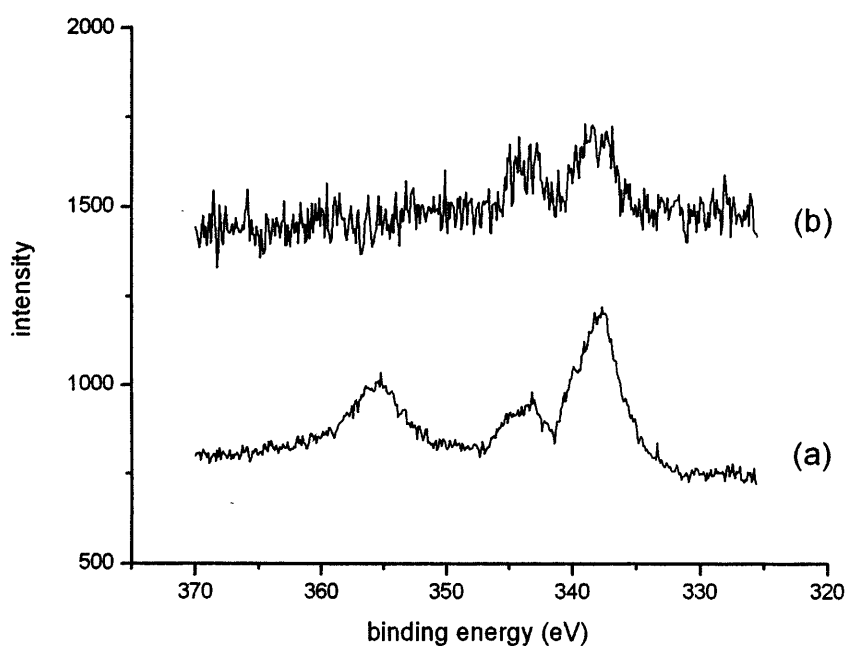
Figure 3.8 Au(4d) and Pd(3d) spectra for an uncalcined 2.5 wt% Au-2.5 wt% Pd/TiO₂ catalyst (a) before and (b) after reaction

3.4.2. Scanning Transmission electron microscopy (STEM) analysis

STEM was performed on the samples as detailed in chapter 2. XEDS and ADF imaging was performed as detailed in chapter 2.

3.4.2.1 STEM analysis of uncalcined 2.5wt%Au-2.5wt%Pd/TiO$_2$

Annular dark field (ADF)-STEM images of the uncalcined Au-Pd/TiO$_2$ (2.5% Au - 2.5% Pd) catalyst revealed a bi-modal metal particle size distribution. The smaller particles ranged from approximately sub 1 nm to 8 nm, with the majority of the particles existing at the lower end of this range. In contrast, the larger particles ranged from 40 to 70 nm in diameter, however, they were definitely the minority phase. STEM-XEDS mapping analysis revealed the co-existence of at least three types of particles as shown in Figure 3.9.
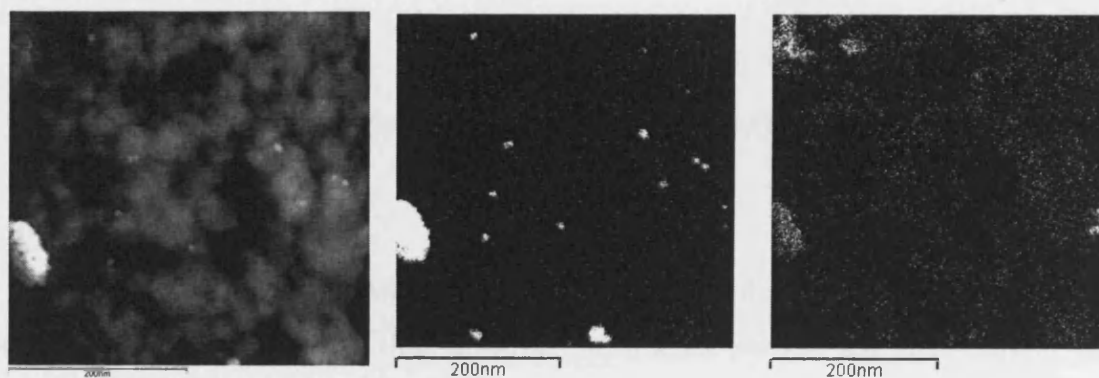
Figure 3.9   HAADF image (left) of 2.5wt%Au-2.5wt%Pd/TiO$_2$ uncalcined sample and corresponding XEDS maps of Au M$_2$ (centre) and Pd L$_1$ (right); note the presence of pure-Au, pure-Pd, and larger Au-Pd alloy particles

The majority of the smaller particles were pure-Au, whereas only a very small fraction were pure-Pd. In contrast, all of the larger particles were Au-Pd alloys as evidenced by the spatial coincidence of the gold and palladium x-ray maps. A minority of the smaller particles also contained both gold and palladium as shown in Figure 3.10. Also of note in this image is the presence of very small metal particles (< 1 nm) which were not identified by XEDS due to the extremely poor x-ray signal they emitted.
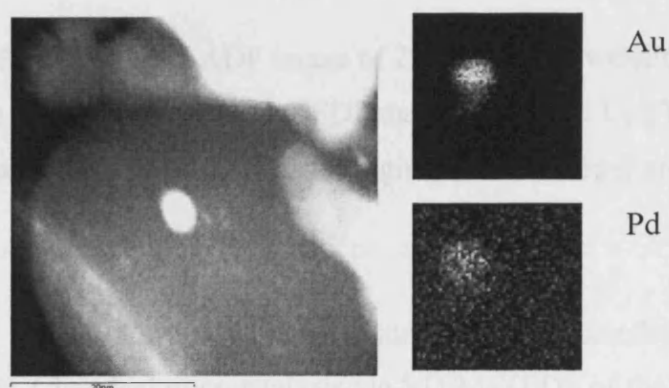
Figure 3.10 ADF STEM image showing small alloy particle in uncalcined 2.5wt%Au-2.5wt%Pd/TiO$_2$ sample (left); reduced raster Au M$_2$ map (top right), and Pd L$_1$ map (lower right)

3.4.2.2 STEM analysis of 2.5wt%Au-2.5wt%Pd/TiO$_2$ 400°C 3 hr air

For the calcined Au-Pd/TiO$_2$ sample, a similar bi-modal particle size distribution was found, this time however the smaller particle size distribution was slightly larger than that in the uncalcined sample (2 and 10 nm) while most of the larger particles fell between 35 and 80 nm in size.
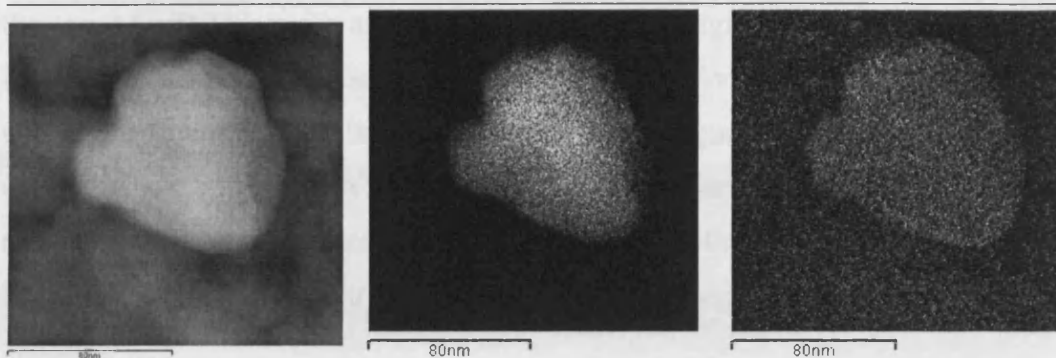
Figure 3.11   STEM-ADF image of 2.5wt%Au-2.5wt%Pd/TiO_2 showing large alloy particle (left), Au M_2 STEM-XEDS map (centre), Pd L_1 STEM-XEDS map (right); note that the Pd signal appears to originate from a larger area than that of the Au signal

In addition a few isolated particles exceeded 120 nm in diameter (see Table 5). Chemical microanalysis via STEM-XEDS of the calcined sample once again revealed that the larger particles all consisted of Au-Pd alloys (Figure 3.11). However, in marked contrast to the uncalcined catalyst, all of the smaller particles observed consisted entirely of pure-Pd (Figure 3.12).
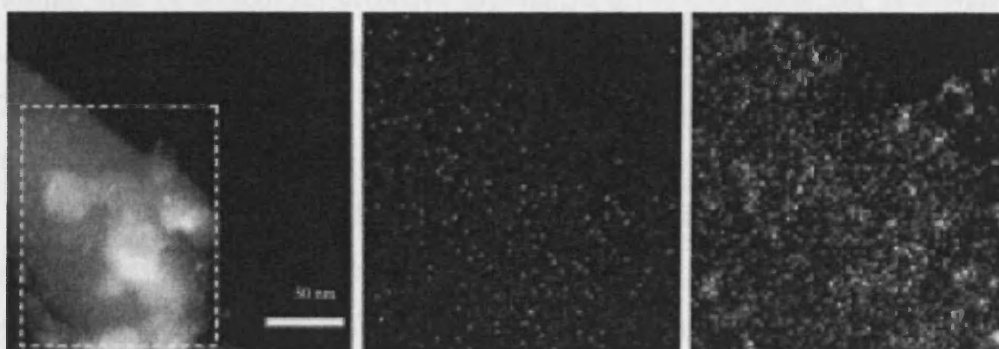
Figure 3.12   HAADF images showing small Pd particles in the calcined 2.5wt%Au - 2.5wt.%Pd/TiO_2 (left), reduced scan area Au M_2 map (centre), and Pd L_1 map (right); Note the lack of gold signal in these particles

No pure-Au particles or small alloy particles were observed at all in this calcined catalyst. Energy dispersive X-ray (XEDS) maps of the larger particles using

the Au M_2 (9.712 keV) and Pd L_α (2.838 keV) signals are spatially coincident indicating that the metal nano-particles in the field of view are in fact Au-Pd alloys. Closer inspection of the larger alloy particle in Figure 3.8 shows that a definite discrepancy exists between the spatial extent of the Au and Pd signals; i.e. the Pd x-ray signal always originates from a larger area than the corresponding gold signal. This suggests that there is a tendency for Pd surface segregation to occur in the alloy particles.

3.5   Discussion

3.5.1   Catalyst preparation and stability

Titania supported gold catalysts prepared by impregnation and deposition precipitation show distinct differences in activity for CO oxidation and H_2O_2 synthesis. The calcined 5%Au/TiO$_2$ catalyst prepared by impregnation was 20 times more active for H_2O_2 synthesis than the corresponding catalyst prepared by deposition precipitation, whereas the DP prepared catalysts were all active for CO oxidation, the impregnated catalysts were completely inactive. This inverse relationship can be attributed to the Au particle size on the catalyst. Deposition precipitation produces highly dispersed, nano-crystaline gold particles[9, 10], the optimum size of which, for effective low temperature CO oxidation, is 2-4nm[11, 12]. Catalysts prepared by impregnation tend to consist of less well-dispersed, large (>20nm) gold particles. The correlation between particle size and activity for H_2O_2 synthesis seems to favour larger particles.

It is known that heat treatment of supported gold catalysts causes sintering, due to the low melting point of gold (1337K) and the consequent mobility of gold at relatively low temperatures. Calcination of the DP catalyst causes a decrease in its activity for CO oxidation, which is consistent with an increase in particle size as the gold agglomerates on the TiO$_2$. The DP Au/TiO$_2$ catalysts perform better for H_2O_2 synthesis as the calcination temperature increases, indicating that the large particles formed during calcination are the active species on the support surface.

The Au-Pd catalysts prepared by impregnation are markedly more active for H_2O_2 synthesis than Au or Pd monometallic catalysts. These bimetallic catalysts form large "core-shell" particles on calcination, with an Au core surrounded by a Pd

shell, which is shown clearly by XPS (figure 3.7) and STEM (figure 3.11). The uncalcined catalysts show features from both Au and Pd, whereas calcining the catalyst at temperatures greater than 200°C results in the complete attenuation of the emission from the Au(4d) levels. Since AAS measurements show no loss of gold after calcination, it is reasonable to conclude that the metal particles have a core-shell structure, with the gold at the core covered by a Pd shell of sufficient thickness to attenuate completely the flux of electrons from the gold atoms. The uncalcined catalysts showed much higher catalytic activity, but are highly unstable under reaction conditions. It is interesting to note that proportionately, the loss of metals by leaching is much larger than the expected decrease in productivity for hydrogen peroxide formation as the used dried catalyst, despite having lost >90% Au and Pd is still highly active.

The Au-Pd catalyst dried at 25°C and used 3 times still has an activity comparable to the 400°C calcined Au-Pd catalyst, albeit with approximately 5% of the original metal loading remaining. The XPS spectrum of the uncalcined fresh catalyst (figure 3.6) shows clear Au and Pd contributions, where as after one use the Au contribution has disappeared entirely, with a decrease in the Pd signal. We know from AAS that the Au is still present after one use, so the high activity of the used uncalcined catalyst possibly could be attributed to the formation of core shell particles during the reaction, or the formation of some other reactive species during the reaction.

For the calcined catalyst, the XPS spectrum (figure 3.7) suggests that the photoelectron flux emitted from the gold atoms in the core is strongly attenuated due to inelastic scattering of the electrons during transport through the Pd shell, leading to a much reduced Au signal intensity compared with Pd. A similar enrichment has been observed[13] for bulk Pd-Au alloys heated in oxygen at temperatures greater than 300 °C, in which the surface layer is known to consist of PdO. Thermodynamically, this is a consequence of the exothermic heat of formation of PdO compared with the endothermic heat of formation of Au_2O_3. Interestingly, it was also found that hydrogen treatment at 350 °C resulted in the complete reduction of the oxide without re-equilibration of the surface composition to that of the bulk, as observed.

The formation of Au-Pd core-shell structures has been reported previously for ligand-stabilized bimetallic Au-Pd colloids[14], and in the preparation of bimetallic nano-particles by the sonochemical reduction of solutions containing gold and palladium ions[15]. Such core-shell particles were found to exhibit superior catalytic activity compared with Au-Pd alloy particles exhibiting the same overall Au:Pd ratio[15, 16]. Detailed [197]Au Mössbauer measurements have confirmed the presence of a pure Au core, and also identified a thin alloy region at the interface between the Au core and Pd Shell[15-17]. Inverted Pd core/Au shell particles may be prepared, but with difficulty[17] - even if Au is deposited on already-formed Pd particles, Au core/Pd shell structures are formed[18]. Interestingly, the core-shell particles reported in this study are stable at temperatures up to at least 500 °C, in contrast to core-shell nanoparticles prepared ultrasonically in a porous silica support, where transformation to a random alloy was observed at 300 °C[19].

In comparing the calcined and uncalcined catalysts, the most striking difference is the composition of the smaller particles in each sample. While both were found to contain small palladium particles, only the uncalcined sample exhibited any pure gold particles. Indeed, pure gold particles were not observed in the previous studies of the alumina supported catalysts.[1,2] This observation suggests that the chemical composition of the metal particles in these catalysts is strongly influenced by the heat treatment process used. It is also interesting to note the presence of considerably larger metal particles in this uncalcined sample (see Figure 3.9), suggesting that they are either a direct by-product of the impregnation synthesis process or that they form over time even in the absence of an elevated temperature calcination process.

Upon heat treatment, the smaller pure-Au particles sinter and combine with palladium to form the large alloy particles discussed previously. The origin of the large population of small, pure-Pd particles after this heat treatment is still undetermined. One possible explanation is that there is a significant concentration of palladium in the uncalcined sample that is atomically dispersed and was not detected by the STEM investigation and which aggregates to larger particles upon heat treatment. Another possibility is that the small palladium particles pre-existed in the

uncalcined catalyst but did not bind well to the titania particles and was leached off during wet-preparation of the STEM sample into the methanol used.

It is a well-established that as the radius of metal particles is reduced to approximately 10 nm, the melting point of that metal is lowered significantly below the value exhibited by the bulk metal. Using the equation developed by Buffat et al[20], a plot can be made for the melting point of gold and palladium as a function of particle size, as shown in Figure 3.13. Clearly, the drying temperature (120°C) and the calcination temperature (400°C) are both a much higher fraction of the melting point of gold than of palladium in the region where the particle radius is less than 5 nm.
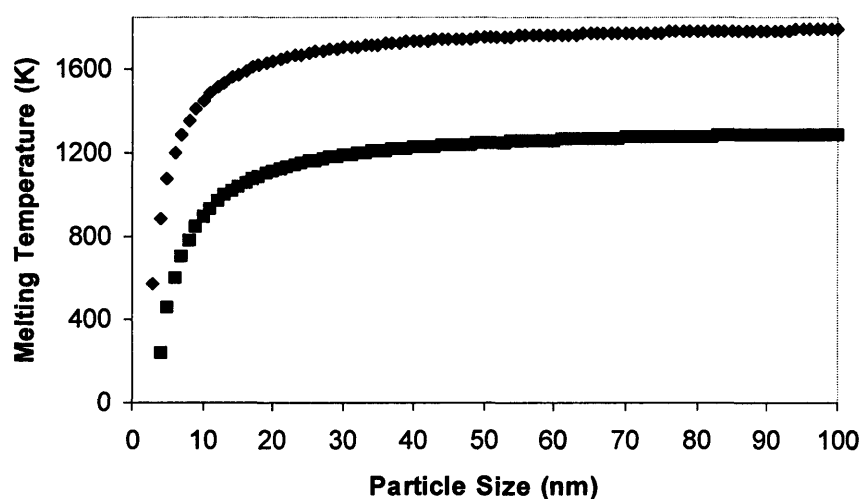
Figure 3.13 Melting point as a function of particle size for palladium and gold; note that in the 5 nm range the melting point of gold (■) is significantly lower than that of palladium (♦).

This observation may explain the presence of pure-Pd and lack of pure-Au particles in the calcined sample since the less refractory Au (T_m(bulk) = 1064 °C) would have a significantly higher atomic mobility than that of the Pd (T_m(bulk) = 1828 °C). The increased mobility of the gold relative to the palladium would result in it being incorporated into the larger particles (as observed), while the palladium would need significantly more time to sinter to this same degree. The presence of

gold nanoparticles in the 120°C dried sample and the possible retention of atomically dispersed palladium could also be explained by this strong difference in mobility between the Au and Pd nanoclusters at this drying temperature.

Finally, the heat treatment also produces the core-shell structure that was previously discussed, with a strong tendency for palladium surface segregation. Since gold and palladium exhibit a complete solid solution over the entire composition range, this effect is not expected. However, similar palladium segregation has been observed in bulk alloys when an elevated heat treatment in oxygen is performed. This is presumably brought about by preferential formation of Pd-O bonds at the alloy surface since in this temperature range palladium oxidizes more readily than gold[13]

It is not yet clear from our studies with the uncalcined materials where the origin of the catalytic activity lies. It could arise from a number of possibilities (a) active surface bound metallic particles which subsequently are dissolved and the solution species is inactive, (b) small colloidal particles are released into the solvent and these display high activity, and/or (c) the solution form of the leached metal is the active component. It has not proved possible to distinguish between these three cases, and indeed all three may be operative, since at the end of the experiment in the autoclave no gold or palladium remains in solution, hence the colloidal particles or soluble species are rapidly deposited onto the autoclave and stirrer. Numerous blank experiments have shown that this deposited form of metal is inactive, and no metal deposition is abserved. Lunsford[21, 22] has shown that colloidal Pd is very active for H_2O_2 synthesis, and indeed can play a role in many of the previous Pd catalysed reactions. Hence it is possible that the high activities observed with catalysts that are not calcined may be due to the generation of colloidal metallic particles which are both highly efficient catalysts and short lived. However, it is clear from the characterisation studies that the uncalcined samples are the most complex structurally.

3.5.2 Influence of reaction time

It can be seen from table 3.3 that increasing the time of reaction leads to an overall increase in the total yield to H_2O_2 as the conversion of H_2 approaches 100%, however the reaction is less selective with increasing time due to the preferential production of water. The initial activity of the catalyst ($114mol_{H2O2}/kg_{cat}h$) with high selectivity (93%) represents the highest rate based on catalyst mass observed thus far with any Au- or Pd-based catalyst for the direct synthesis of H_2O_2. The selectivity is notably higher than the values previously reported by Landon *et. al.* for Au/Al_2O_3 catalysts[1,2], and also for Pd catalysts. For example Choudhary *et al.* obtained[23, 24] selectivities to H_2O_2 of 85% and 72%, at H_2 conversions of 21% and 9% using Pd/Ga_2O_3 and Pd/H-ZSM-5 catalysts, respectively. Of course the optimal conditions will vary with other conditions such as temperature and pressure, and so it can be reasonably anticipated that at higher temperatures and reaction pressures much shorter reaction times will be preferred. This means that the direct synthesis method using diluted reactants, that avoid the potential for explosion hazards, will only produce relatively dilute solutions and hence the methodology may be better suited to *in-situ* utilisation in chemical syntheses in which the H_2O_2 is used as soon as it is formed. In this scenario, optimum use can be made of the very high initial rates of H_2O_2 formation displayed by the catalysts. Initial *in-situ* experiments using benzyl alcohol as a model substrate showed that 100% selectivity to benzaldehyde could be achieved at 50% conversion, in a 30 minute reaction at room temperature using 10mg of catalyst under vigorous stirring (1200rpm). The reaction did not proceed in either the absence of the catalyst or in the absence of hydrogen, suggesting the reaction proceeded using the hydrogen peroxide formed as the oxidant. The yield of benzaldehyde corresponds to the stoichiometric use of H_2O_2, and no residual H_2O_2 was present after reaction, determined by titration of the reaction medium immediately after reaction.

3.5.3 Influence of catalyst mass

The effect of increasing the amount of catalyst in the autoclave is shown in Fig. 3.2 for the 2.5% Au/2.5% Pd/TiO$_2$ calcined at 400 °C. It is apparent that the yield of H$_2$O$_2$ produced increases as the amount of catalyst is increased. However the rate of H$_2$O$_2$ synthesis is highest at lower catalyst masses, and although the rate is linear for catalyst masses up to 20 mg, under standard reaction conditions a catalyst mass of 10 mg gives a reasonable compromise between rate and overall yield of H$_2$O$_2$. It is worth noting however that catalyst masses of 20 mg can be used effectively and in cases where the rate is extremely low a catalyst mass of 50 mg, particularly for Au monometallic catalysts, can be employed. The results also indicated that the reaction in not mass transport limited in either a water only medium or a methanol : water system as H$_2$O$_2$ concentration increases with increasing catalytic mass.

3.5.4 Influence of solvent

There are three interesting features of the data presented in section 3.3.4. First, there is the sensitivity to the optimum methanol : water ratio, and in particular increasing the methanol concentration above the optimal value leads to a dramatic decrease in the rate of hydrogen peroxide synthesis. The second is that the total absence of water leads to very low rates (12mol/h-kg$_{cat}$) being observed. Substitution of acetone for methanol illustrates this even more, with no detectable formation of H$_2$O$_2$ in 8.5g acetone. Thirdly, the use of pure water still leads to an effective rate for the production of hydrogen peroxide. However, there are two possible causes for these effects, namely the reaction becomes mass transfer limited due to the change in the solvent mixture, and secondly, a related factor is that the solubility of hydrogen and oxygen will vary as a function of the composition of the solvent and this will therefore directly affect the rate of synthesis, even in the absence of diffusion limitations.

Whether the reaction was mass transport limited for watter only and the standard water-methanol solvent mixture was investigated by varying the amount of

catalyst and the results are shown in Figure 3.5. For the water only experiments, although the rate of hydrogen peroxide synthesis is lower than when methanol is present the concentration of hydrogen peroxide produced varies linearly with the catalyst mass between 10 – 40 mg. In addition, the rate of hydrogen peroxide production is reasonably constant as the catalyst mass is varied. The observations lead us to conclude that the reaction with this catalyst using water as solvent is not mass transport limited. For the standard solvent mixture the concentration of hydrogen peroxide is linearly dependent on the mass catalyst up to a mass of 20 mg (figure 3.2) . Above this the concentration of hydrogen peroxide is not greatly enhanced and the rate of production is decreased (Figure 3.5). Although the rate of hydrogen peroxide synthesis is enhanced by the addition of methanol to the water, the water only reaction mixture can utilise higher catalyst masses and consequently can still achieve enhanced rates of reaction. As the gases are more soluble in methanol[25] the rate with pure methanol should be higher than that of pure water, but this is not the case. This may indicate that water plays an essential role in the reaction mechanism, maybe through the provision of surface hydroxyls at the interface between the support and the alloy nano-crystals. Industrial application of the direct synthesis route is likely to favour the use of non-organic solvents. In particular, small-scale synthesis for medical uses will necessitate the use of water as a solvent.

3.6 Conclusions

Hydrogen peroxide synthesis over titania supported Au, Pd and Au-Pd catalyst was explored in a stirred autoclave reactor.

I) Au/TiO$_2$ catalysts prepared by impregnation (IMP) are more active for H$_2$O$_2$ synthesis than those prepared by deposition precipitation (DP). For CO oxidation, an opposite trend is observed. Large Au nano-crystals produced *via* IMP (or calcination of DP catalysts) appear to preferential for H$_2$O$_2$ synthesis, whereas smaller Au nano-crystals (DP) are the active species for the oxidation of CO.

II) Bimetallic Au-Pd/TiO$_2$ catalysts form a core-shell, with a Pd shell surrounding an Au core, on calcination, as seen by XPS and STEM analysis. These large (~80nm) are very active for the direct synthesis of H$_2$O$_2$, achieving higher selectivity to H$_2$O$_2$ than Pd only catalysts. Calcined Au-Pd/TiO$_2$ catalysts are very stable over 3 uses, whereas uncalcined catalysts, although more active, are not stable under standard reaction conditions.

III) The reaction is not mass transport limited when carried out in water or water : methanol solvent systems using the small scale stirred autoclave reactor.

IV) The high initial activity and selectivity of the calcined catalysts can be successfully utilised to oxidise benzyl alcohol to benzaldehyde with 100% selectivity.

3.7 References

[1]   P. Landon, P. J. Collier, A. F. Carley, D. Chadwick, A. J. Papworth, A. Burrows, C. J. Kiely, G. J. Hutchings, *Physical Chemistry Chemical Physics* **2003**, *5*, 1917.

[2]   P. Landon, P. J. Collier, A. J. Papworth, C. J. Kiely, G. J. Hutchings, *Chemical Communications (Cambridge, United Kingdom)* **2002**, 2058.

[3]   M. Haruta, M. Date, *Applied Catalysis, A: General* **2001**, *222*, 427.

[4]   M. Haruta, S. Tsubota, T. Kobayashi, H. Kageyama, M. J. Genet, B. Delmon, *Journal of Catalysis* **1993**, *144*, 175.

[5]   S. D. Lin, M. Bollinger, M. A. Vannice, *Catalysis Letters* **1993**, *17*, 245.

[6]   F. Moreau, C. Bond Geoffrey, O. Taylor Adrian, *Chemical communications (Cambridge, England)* **2004**, 1642.

[7]   F. Boccuzzi, A. Chiorino, M. Manzoli, D. Andreeva, T. Tabakova, *Journal of Catalysis* **1999**, *188*, 176.

[8]   D. C. Andreeva, V. D. Idakiev, T. T. Tabakova, R. Giovanoli, *Bulgarian Chemical Communications* **1998**, *30*, 59.

[9]   B. Schumacher, V. Plzak, M. Kinne, R. J. Behm, *Catalysis Letters* **2003**, *89*, 109.

[10]   T. Akita, M. Okumura, K. Tanaka, M. Haruta, *Journal of Catalysis* **2002**, *212*, 119.

[11]   F. Moreau, G. C. Bond, *Applied Catalysis, A: General* **2006**, *302*, 110.

[12]   F. Moreau, G. C. Bond, A. O. Taylor, *Journal of Catalysis* **2005**, *231*, 105.

[13]   L. Hilaire, P. Legare, Y. Holl, G. Maire, *Surface Science* **1981**, *103*, 125.

[14]   A. F. Lee, C. J. Baddeley, C. Hardacre, R. M. Ormerod, R. M. Lambert, G. Schmid, H. West, *Journal of Physical Chemistry* **1995**, *99*, 6096.

[15]   H. Takatani, H. Kago, Y. Kobayashi, F. Hori, R. Oshima, *Transactions of the Materials Research Society of Japan* **2003**, *28*, 871.

[16]   Y. Kobayashi, S. Kiao, M. Seto, H. Takatani, M. Nakanishi, R. Oshima, *Hyperfine Interactions* **2004**, *156/157*, 75.

[17]   H. H. Takatani, F; Nakaishi, M; Oshima, R, *Austarlia Journal of Chemistry* **2003**, *53*, 1025.

[18]   C. Kan, W. Cai, C. Li, L. Zhang, H. Hofmeister, *Journal of Physics D: Applied Physics* **2003**, *36*, 1609.

[19]   T. Nakagawa, H. Nitani, S. Tanabe, K. Okitsu, S. Seino, Y. Mizukoshi, T. A. Yamamoto, *Ultrasonics Sonochemistry* **2004**, *12*, 249.

[20]   P. A. Buffat, *Thin Solid Films* **1976**, *32*, 283.

[21]   D. P. Dissanayake, J. H. Lunsford, *Journal of Catalysis* **2002**, *206*, 173.

[22]   D. P. Dissanayake, J. H. Lunsford, *Journal of Catalysis* **2003**, *214*, 113.

[23]   V. R. Choudhary, A. G. Gaikwad, S. D. Sansare, *Catalysis Letters* **2002**, *83*, 235.

[24]   V. R. Choudhary, S. D. Sansare, A. G. Gaikwad, *Catalysis Letters* **2002**, *84*, 81.

[25]   A. I. Dalton, Jr., R. W. Skinner, (Air Products and Chemicals, Inc., USA). Application: US, **1982**, pp. 6 pp Cont.

Chapter Four

Chapter Four : Direct synthesis of H₂O₂ from H₂ and O₂ over supported Au, Pd and Au-Pd catalysts

4.1   Introduction

Following on from the work detailed in chapter 3 for Au-Pd catalysts supported on TiO₂ for H₂O₂ synthesis, a series of catalyst were prepared on other oxide supports, namely Fe₂O₃ (prepared by co-precipitation), Al₂O₃ and SiO₂. These catalysts were prepared by impregnation, and their activity for H₂O₂ synthesis evaluated. STEM and XPS characterisation techniques were employed to evaluate the nature of the active site, and to determine whether the catalysts form a core shell structure seen previously with TiO₂ supported catalysts.

4.2   Direct synthesis of H₂O₂ from H₂ and O₂ over alumina supported Au, Pd and Au-Pd catalysts

4.2.1   Effect of Au-Pd ratio on hydrogen peroxide synthesis

Au, Pd and Au-Pd catalysts supported on alumina were prepared using impregnation methods and these were evaluated, after the catalysts had been calcined at 400°C for 3 hours in static air, for the synthesis of H₂O₂ and the oxidation of CO. The results shown in Table 4.1 demonstrate that the catalysts are active for H₂O₂ synthesis but are totally inactive for CO oxidation, as demonstrated for TiO₂ supported catalysts discussed in chapter 3.

As noted previously, the pure Au catalysts generate H₂O₂ but at low rates. The addition of Pd to Au significantly enhances the catalytic performance for the synthesis of H₂O₂, and moreover it is interesting to note that there is an optimum Pd-Au composition (Pd : Au ~ 1 : 5) where the rate of H₂O₂ production is much higher than for the pure Pd catalyst, which in itself is significantly more active than pure gold.

Table 4.1 Effect of calcination and Au:Pd composition of Au-Pd/Al$_2$O$_3$ catalysts for H$_2$O$_2$ synthesis under standard reaction conditions using 50mg catalyst.

Catalyst	Calcination	Productivity (mol-H$_2$O$_2$/h-Kg$_{cat}$)	H$_2$O$_2$ (wt.%)	CO conversion (%)
5%Au/Al$_2$O$_3$	Air 400 °C	2.6	0.0026	<1
4.2%Au0.8%Pd/Al$_2$O$_3$	Air 400 °C	17	0.017	<1
2.5%Au2.5%Pd/Al$_2$O$_3$	Air 400 °C	15	0.015	<1
5%Pd/Al$_2$O$_3$	Air 400 °C	9	0.009	<1
5%Au/Al$_2$O$_3$	Air 400 °C+ H$_2$ 500 °C	1	0.001	<1
4.2%Au0.8%Pd/Al$_2$O$_3$	Air 400 °C+ H$_2$ 500 °C	21	0.021	<1
2.5%Au2.5%Pd/Al$_2$O$_3$	Air 400 °C+ H$_2$ 500 °C	9.3	0.093	<1
5%Pd/ Al$_2$O$_3$	Air 400 °C+ H$_2$ 500 °C	6	0.006	<1

(H$_2$O$_2$ synthesis : 10mg catalyst in 5.6g Methanol 2.9g water at 2°C for 30 mins, molar ratio H$_2$:O$_2$ 1:2 30 bar total pressure, CO oxidation : 50mg catalyst, 25°C, 22.5ml min^{-1})

All catalysts show very low activity for CO oxidation.

4.2.2 Effect of calcination conditions for H$_2$O$_2$ synthesis

A series of Au-Pd/Al$_2$O$_3$ catalysts were prepared using the impregnation method, calcined at 400 °C and then reduced in H$_2$ at 500 °C. This is similar to the method of catalyst preparation used by Landon *et. al*[1, 2] previously for Au-Pd/Al$_2$O$_3$ catalysts. The results (Figure 4.1) show that reduction following calcination increases the rate of H$_2$O$_2$ synthesis for the optimum Au-Pd composition but decreases the rate for all other compositions. A large number of formulations were investigated and the results confirm that a composition of 4.2 wt% Au–0.8 wt% Pd gives the highest catalytic performance.
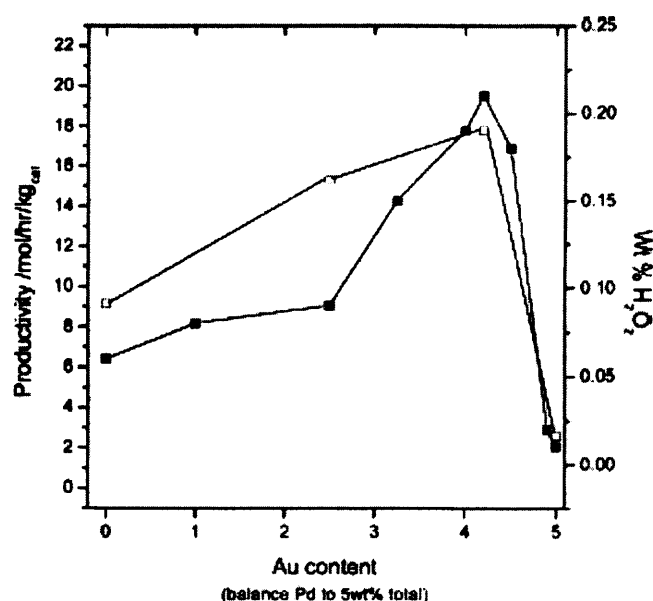
Figure 4.1 Effect of addition of Au to supported Pd/Al$_2$ O$_3$ catalysts for the synthesis of hydrogen peroxide. Catalysts (50mg) calcined at 400 °C in air (□) or calcined in air at 400 °C and reduced at 500 °C with hydrogen (■).

4.2.3 Catalyst stability

The effect of treating the alumina catalysts at lower temperatures prior to use was investigated, and this can lead to improved catalytic performance (as seen in the case of titania supported catalysts in chapter 3). However, a key consideration for heterogeneous catalysts operating in three phase systems is whether active components leach into the reaction mixture; this may lead to catalyst deactivation or, in the most extreme case, may lead to the formation of an active homogeneous catalyst. To determine whether the supported gold/palladium

catalysts functioned as wholly heterogeneous catalysts, an experiment was carried out using a 2.5 wt% Au-2.5 wt% Pd/Al$_2$O$_3$ dried catalyst and a catalyst calcined at 400 °C (Table 4.2). The yield of H$_2$O$_2$ was determined after one use, the catalyst retrieved and analysed by AAS to determine metal content. Following this reaction, the catalyst was removed by careful filtration and the solution was used for a second experiment using O$_2$/H$_2$. No further H$_2$O$_2$ was generated for either the dried or calcined catalyst and this confirms that the formation of hydrogen peroxide involves gold acting as a wholly heterogeneous catalyst. However, the activity of the dried catalyst was much lower on a second use, corresponding to a loss >80% of the total Au and Pd. The catalyst calcined at 400°C was stable, and maintained activity after 2 uses.

Table 4.2 Leaching of gold and palladium in 2.5%Au2.5%/Pd Al$_2$O$_3$ catalysts after reaction. Influence of the calcination temperature

Pre-treatment	Run	Loss of Au (%)[a]	Loss of Pd (%)[a]	Productivity (mol/h-kg$_{cat}$)
air, 25 °C,	1	75	79	65
	2	80	85	41
air, 400°C, 3 h.	1	0	0	15
	2	0	0	15

[a] (gold or palladium present in the fresh catalyst - gold or palladium after run 1 or 2) / (gold or palladium present in the fresh catalyst) x 100. Reaction carried out under standard reaction conditions as detailed in table 4.1).

4.2.4 Effect of catalyst aging

In order to study the effect of storage on catalyst activity (since typically, catalyst performance declines with storage for many catalysts) a sample of the most active 2.5 wt % Au-2.5 wt % Pd/Al$_2$O$_3$ catalyst (previously calcined at 400 °C) was stored in a sealed container in the dark for 12 months at ambient conditions. Re-

evaluation of the catalytic performance of this catalyst showed that under the standard reaction conditions, the activity of the sample had increased from 15 mol of H_2O_2/h/kgcat (Table 4.1) to 52 mol of H_2O_2/h/kgcat, representing a dramatic increase in productivity, and this is similar to the activity observed in chapter 3 for TiO_2 supported catalysts.

4.2.3 Catalyst Characterisation

To determine the nature of the alumina supported Au:Pd catalysts a detailed investigation of freshly prepared catalysts was carried out using electron microscopy and X-ray photoelectron spectroscopy. In previous studies the microstructure of the calcined and reduced samples was explored and demonstrated that the addition of Pd to Au produces Au-Pd alloys over the whole range of particle sizes observed.[1,2]

4.2.3.1 XPS analysis

The Au(4d)-Pd(3d) XPS spectra for the two most active Au-Pd/Al_2O_3 catalysts (with compositions of 4.2 wt% Au-0.8 wt% Pd and 2.5 wt% Au-2.5 wt% Pd) are shown in Figure 4.3 for the uncalcined, and in Figure 4.4 for the calcined (400 °C) samples.

Because of the overlap between the $Au(4d_{5/2})$ and Pd(3d) signals, in order to estimate the Au:Pd molar ratios we must first calculate the intensity of the former using the $Au(4d_{3/2})$ peak intensity and the known intensity ratio of the spin-orbit components. This is then subtracted from the measured Pd(3d) peak intensity and the Pd(3d)/$Au(4d_{5/2})$ ratio corrected using the sensitivity factors of Wagner[3] to obtain the surface Pd:Au molar ratio.
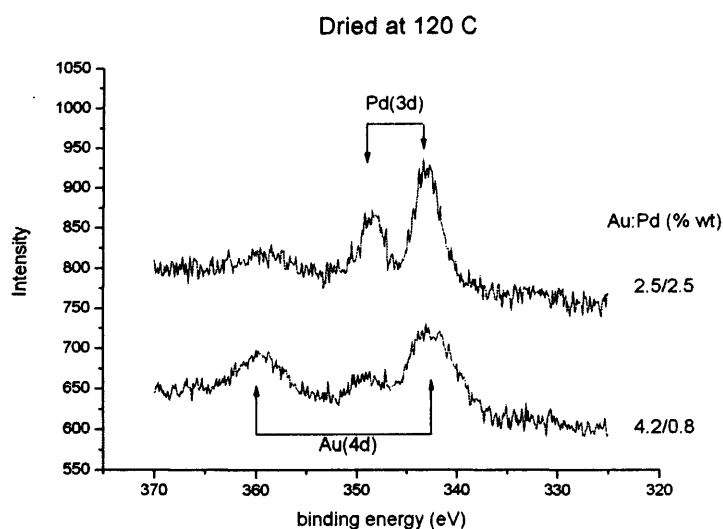
Dried at 120 C

Figure 4.3 Au(4d) and Pd(3d) spectra for two Au-Pd/Al$_2$O$_3$ catalysts dried at 120°C in air
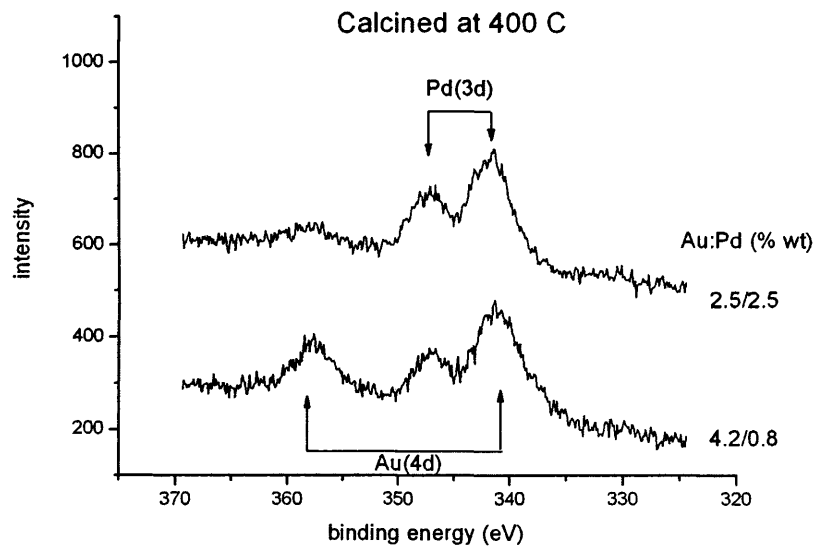
Calcined at 400 C

Figure 4.4 Au(4d) and Pd(3d) spectra for two Au-Pd/Al$_2$O$_3$ catalysts calcined at 400°C in air

For both samples the uncalcined catalysts exhibit a Pd:Au ratio lower than that expected from the known composition (assuming a random solid solution) but

calcination in air at 400 °C (figure 4.4) leads to a surface enrichment in Pd (Table 4.3).

Table 4.3. Comparison of measured (XPS) and expected Pd:Au ratios for two Au-Pd/Al$_2$O$_3$ catalysts

Composition	Treatment	Pd:Au molar ratio	
		Measured	Theoretically expected (for random solid solution)
4.2% Au-0.8% Pd	Dried 120 °C	0.23	0.35
	Calcined 400 °C	0.50	0.35
2.5% Au-2.5% Pd	Dried 120 °C	1.65	1.86
	Calcined 400 °C	3.06	1.86

4.2.3.2 STEM analysis of fresh catalysts

STEM and XEDS results for the fresh calcined 2.5 wt % Au-2.5 wt % Pd/Al$_2$O$_3$ catalyst reported previously[1] showed that this sample is comprised of well-dispersed fcc metal particles with a size range of between 2 and 10 nm with the majority being at the lower end of the size range. Detailed STEM and EDS analysis showed that the particles all were comprised of both Au and Pd and that the ratio of Au/Pd was *ca* 1:1 with a slight enrichment of Pd in the larger particles. Very few particles over 10 nm in diameter were observed in the fresh catalyst

4.2.3.3 STEM analysis of aged catalysts

The aged 2.5 wt% Au-2.5 wt% Pd/Al$_2$O$_3$ catalyst previously calcined at 400°C was examined by annular dark field STEM imaging to characterize the size and composition of the metallic particles (Figure 4.5).
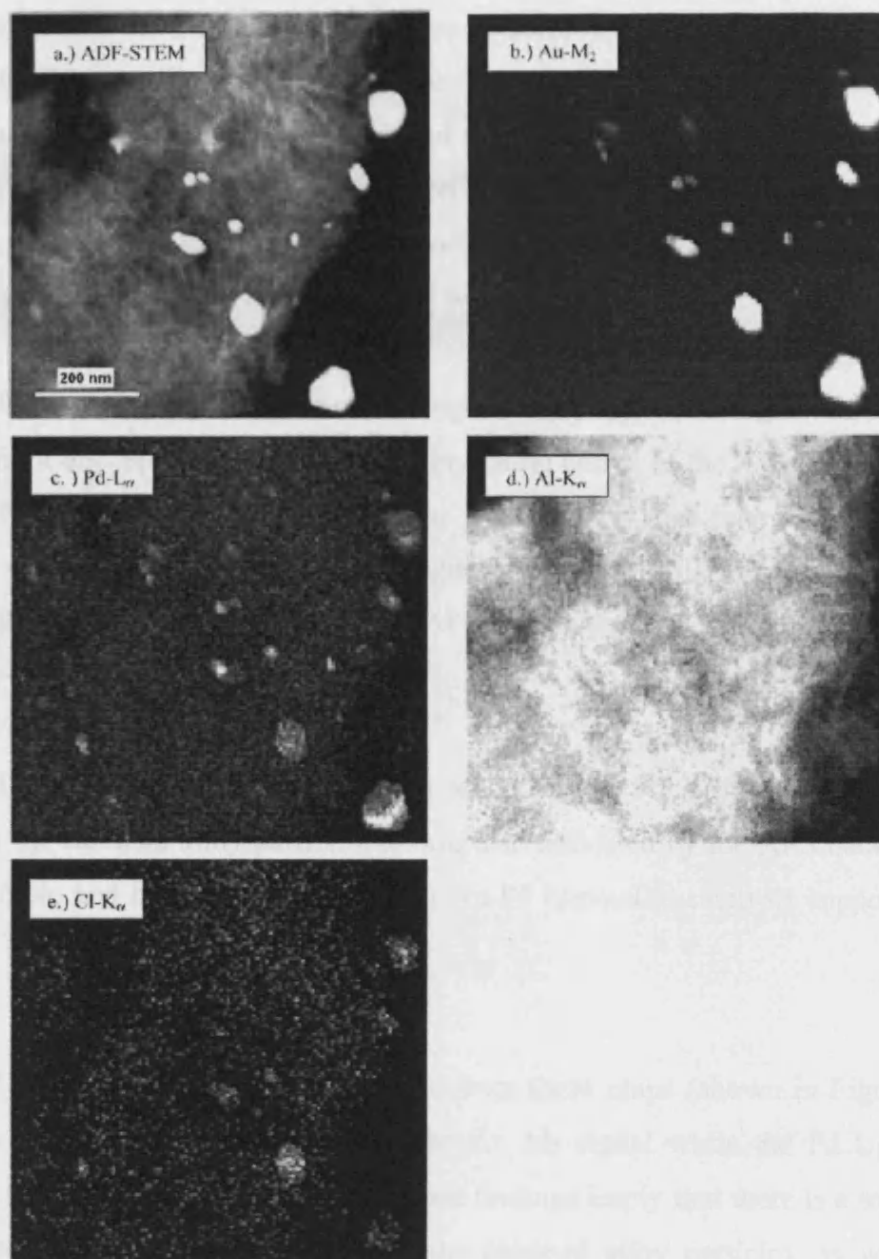
Figure 4.5. Montage of STEM data from the calcined 2.5 wt % Au-2.5 wt % Pd/Al$_2$O$_3$ sample. (a) ADF image and corresponding XEDS maps using (b) Au M$_2$, (c) Pd L$_\alpha$, (d) Al K$_\alpha$, and (e) Cl K$_\alpha$ signals.

It was found (Figure 4.5a) that the sample exhibited a bimodal size distribution. The smallest particles once again fell into the 3-10 nm size range (mean diameter = 3.6 nm), but also present were some considerably larger particles that ranged in size from 35 to 50 nm (mean diameter = 38 nm). STEM-XEDS

analyses of this Au-Pd catalyst were also performed, and typical chemical maps shown in Figure 4.5b,c show the existence of a Au-Pd alloy as well as occasional very small Pd-only particles. It was found that nearly all of the particles tended to be Au-Pd alloys and that the composition of the particles was size-dependent. In general, the smaller the particle, the more Pd-rich and Au-deficient the particle becomes in contrast to the larger particles which are Au rich.

Further inspection of one of the larger alloy particles in Figure 4.5 suggests that a slight discrepancy exists between the spatial extent of the Au and Pd signals; *i.e.* the Pd X-ray signal seems to originate from a larger area than the gold signal. This is most clearly observed in the digitally colored RGB image (Figure 4.6), which shows a predominance of the Pd (blue) signal at the perimeter of the particle.

These data imply that there is a tendency for Pd surface segregation to occur in the calcined alloy particles, as was also indicated by the XPS data for the fresh sample and has also been found for Au-Pd bimetallic catalysts supported on TiO_2.

Line scans across a single particle from these maps (shown in Figure 4.7) reveal a Gaussian type distribution in the Au M_2 signal while the Pd L_1 signal exhibits a flatter, top-hat distribution. These findings imply that there is a tendency for Pd surface segregation to occur in the calcined alloy particles, as was also indicated by the XPS data.

The data from XPS and STEM indicate the presence of a core-shell structure, with an Au core surrounding a Pd shell, as seen with the TiO_2 supported Au-Pd catalysts discussed in chapter 3.
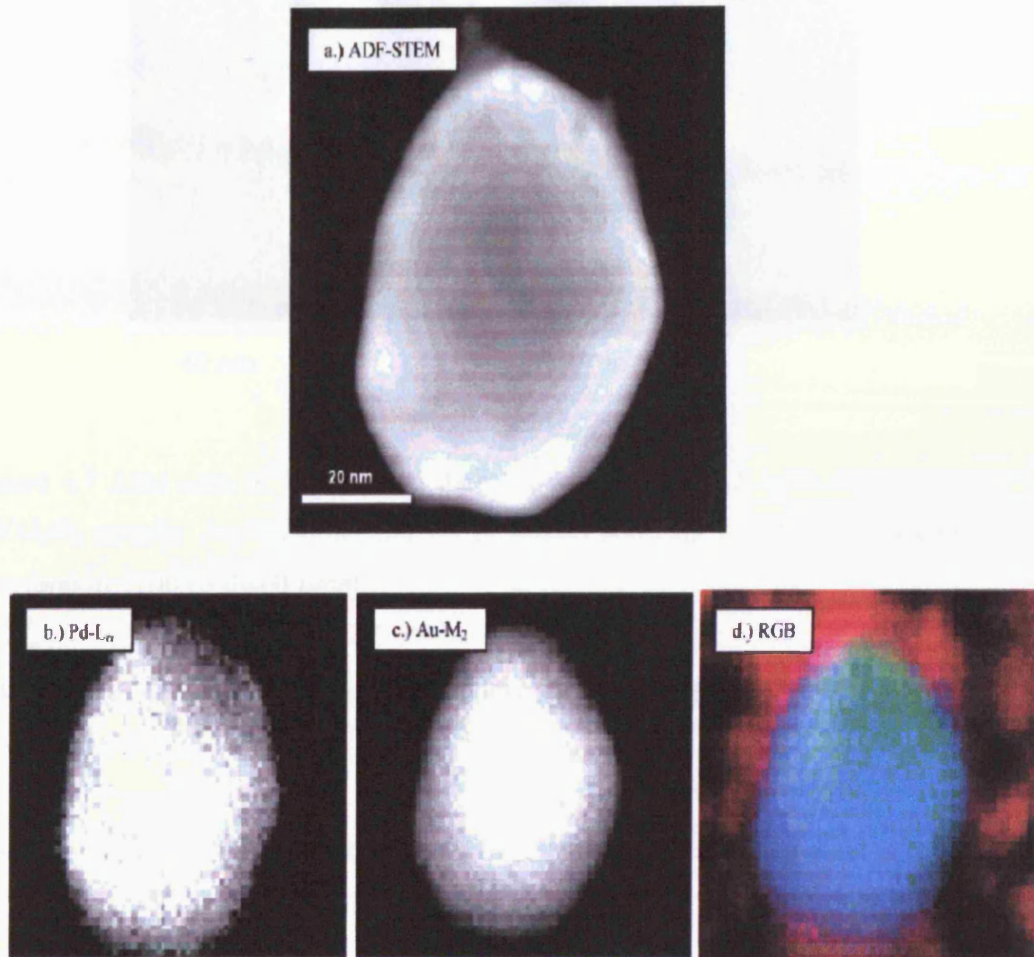
Figure 4.6. Montage of STEM data from a 25 nm particle in the calcined 2.5 wt % Au-2.5 wt % Pd/Al$_2$O$_3$ sample. (a) ADF image with corresponding XEDS maps of (b) Pd L$_\alpha$, (c) Au M$_2$, and (d) reconstructed RGB (red = Al, = green = Au, and Pd = blue) image showing preferential surface enrichment of Pd.
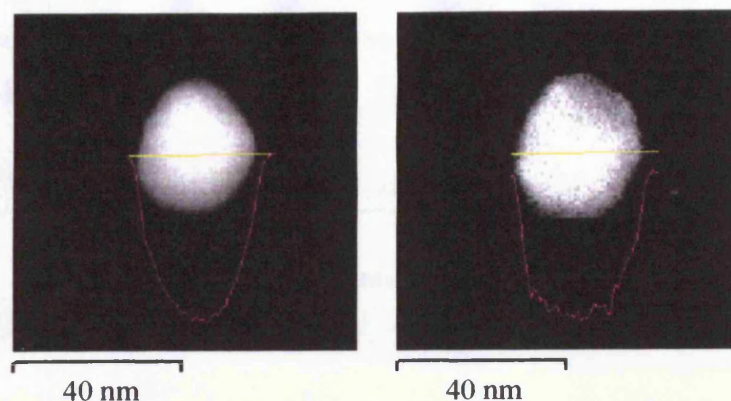
Figure 4.7 Line scan of XEDS map data for the calcined 2.5 wt% Au-2.5 wt% Pd/Al$_2$O$_3$ sample; Au M$_2$ (left) and Pd L$_1$ (right) showing a difference in count distribution, [200 μs dwell time].

4.3 Direct synthesis of H$_2$O$_2$ from H$_2$ and O$_2$ over iron oxide supported Au, Pd and Au-Pd catalysts

4.3.1 Effect of preparation methods on H$_2$O$_2$ synthesis and CO oxidation

Au, Pd and Au-Pd catalysts prepared using impregnation and co-precipitation methods were evaluated for the synthesis of H$_2$O$_2$ and the oxidation of CO using standard reaction conditions. The results shown in Table 4.4 demonstrate that co-precipitation is the preferred method of preparation of active catalysts for CO oxidation, whereas the best catalysts for H$_2$O$_2$ synthesis are prepared by impregnation. There appears to be an inverse correlation since catalysts that are active for one reaction are inactive for the other and *vice versa*. This was also seen in chapter 3 for TiO$_2$ supported catalysts prepared by impregnation and deposition precipitation. The co-precipitated gold catalysts all give rates of H$_2$O$_2$ synthesis that are an order of magnitude less than the Au catalysts made by impregnation and the non-calcined Au/Fe$_2$O$_3$ catalyst prepared by co-precipitation give an even poorer performance.

Table 4.4 Catalytic performance of a variety of Au, Au-Pd and Pd catalysts supported on Fe_2O_3

Catalyst	Preparation method	Pre-treatment	Productivity mol-H_2O_2/h-kg_{cat}	H_2O_2 Production Wt.%	CO conversion %
5%Au/Fe_2O_3	co-precipitation	air 25 °C	0.126	0.001	100
5%Au/Fe_2O_3	co-precipitation	air, 400 °C	0.207	0.002	91
5%Au/Fe_2O_3	co-precipitation	air, 600 °C	0.366	0.004	0
5%Au/Fe_2O_3	impregnation	air, 400 °C	0.54	0.005	<1
2.5%Au-2.5%Pd/Fe_2O_3	impregnation	air, 400 °C	16	0.161	<1
5%Pd/Fe_2O_3	impregnation	air, 400 °C	3.6	0.036	<1

For the catalysts calcined at 400 °C made by impregnation, the pure Au catalysts all generate H_2O_2 but at low rates. The addition of Pd to Au significantly enhances the catalyst performance for the synthesis of H_2O_2 and the effect is very similar to previous studies with alumina and TiO_2 as supports. The 2.5%Au-2.5%Pd/Fe_2O_3 catalyst showed 22% selectivity to H_2O_2, with a H_2 conversion of 71%, at 2°C.

4.3.2   STEM-XEDS and HREM analysis of Au-Pd/Fe_2O_3 samples

STEM-XEDS mapping and ADF imaging studies were carried out on the 2.5wt%Au-2.5wt%Pd/Fe_2O_3 catalysts. These samples were also found to exhibit a bi-modal size distribution of metal particles similar to that found in the alumina-

supported catalysts.[1,2] The smaller particles ranged between 4 and 10 nm whereas the larger particles were between 30 and 70 nm in size (see Table 4.6). However, the pure-gold and pure-palladium only catalysts tended to give just larger metallic particles (Table 4.6).

Table 4.6 – Particle sizes for the supported $Au-Pd/Fe_2O_3$ catalysts[a]

Catalyst	Small Metal Particle Size (nm)	Large Metal Particle Size (nm)
5% Au/ Fe_2O_3	-	48
2.5%Au-2.5%Pd / Fe_2O_3	4.6	32
5% Pd/ Fe_2O_3	-	53
2.5%Au-2.5%Pd / Al_2O_3	3.6	38

[a] - Averaged over more than twenty particle size measurements

Initial STEM-XEDS mapping and ADF imaging experiments indicated that the palladium signal appeared to be originating from a slightly larger area than the gold signal, suggesting that a palladium rich shell surrounds a gold rich core in these alloy particles (Figure 4.7). The line scans (figure 4.6) across two of the alloy particles in the XEDS maps show a clear difference in Au and Pd count distribution. The gold signal follows a Gaussian distribution with a maximum at the particle centre, while the palladium signal shows a more "top-hat" type of distribution where the counts appear more uniform across the particle interior but with slight peaks near the particle perimeter. This observation seems to suggest segregation of palladium to the surface, as also observed in the earlier XPS study of the $Au-Pd/Al_2O_3$ catalysts.
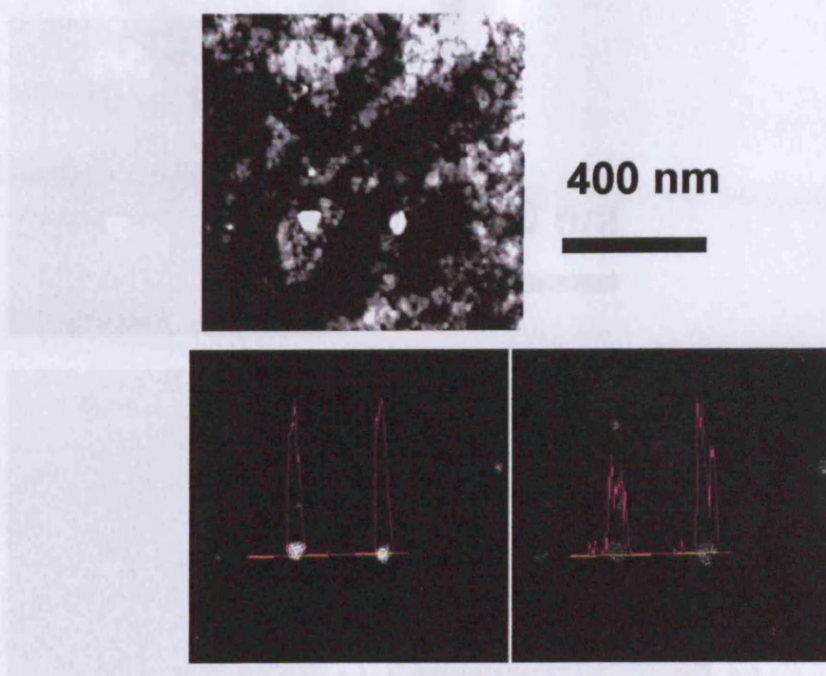
Figure 4.6 HAADF image (top) and corresponding XEDS maps of Au (lower left) and Pd (lower right) from the 2.5%Au-2.5%Pd/Fe$_2$O$_3$ sample. Line scans across two particles show a difference in x–ray signal spatial distribution between the Au and Pd signals. [100 µs Dwell Time]

A short electron probe dwell time of 100 µs was deliberately used to acquire the XEDS maps in order to minimize the effects of beam damage in the specimen. However, on the downside, this short dwell time produced only 6-10 palladium x-ray counts per pixel and around 40 Au X-ray counts per pixel, due to the very different ionization and electron scattering cross-sections of these two elements. This low number of Pd counts could theoretically introduce significant statistical inaccuracies into the method.
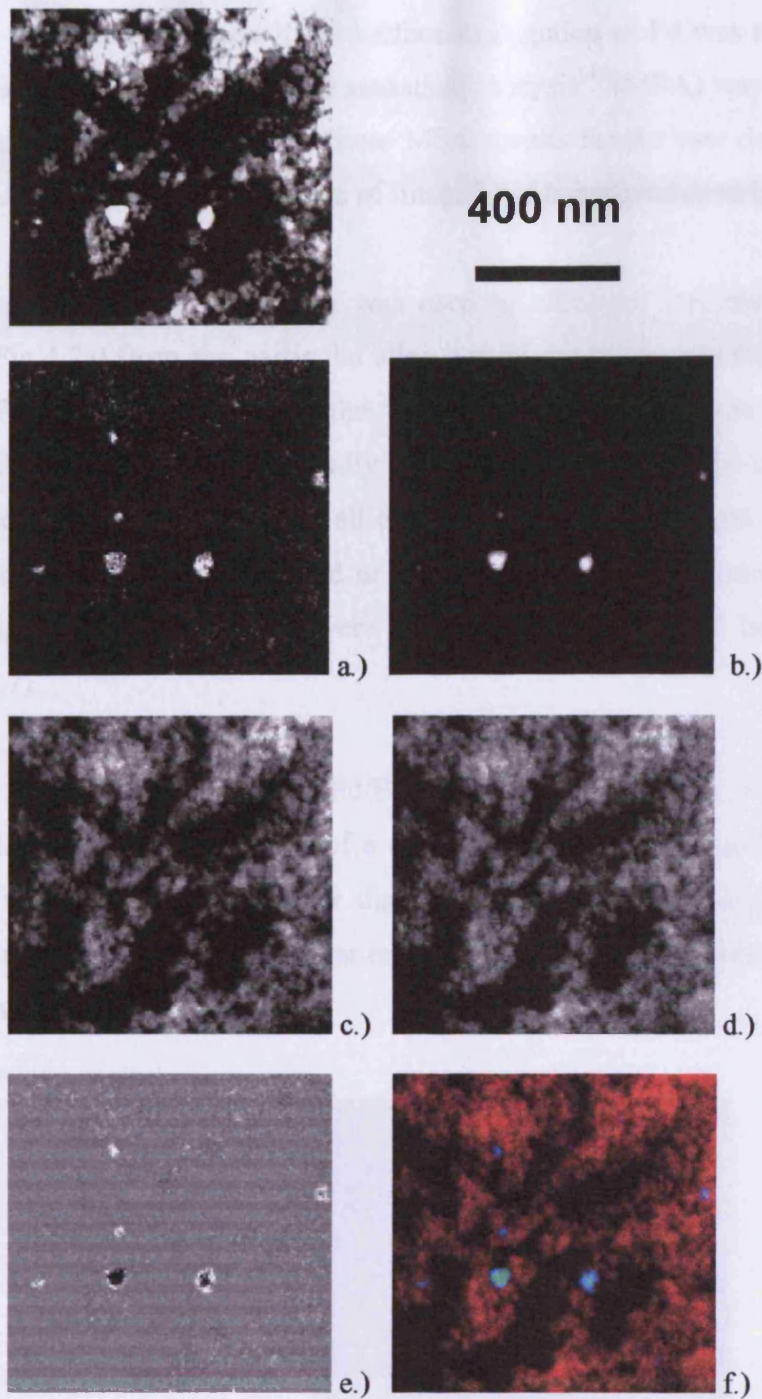
Figure 4.7 HAADF image (top) and MSA reconstructed XEDS maps of Pd (a), Au
(b), Fe (c), O (d), fully isolated Pd signal (e), and reconstructed RGB image of
filtered data (f, red = oxygen, green = gold, and blue = palladium) in the 2.5%Au-
2.5%Pd/Fe$_2$O$_3$ sample, [100 µs Dwell Time]

To investigate if the surface segregation of Pd was truly occurring in these nanoparticles, multi-variate statistical analysis[4] (MSA) was performed on the data set shown in Figure 4.6. These MSA results for the raw data presented in Figure 4.6 are given in the montage of images and maps presented in Figure 4.7.

Clearly, after MSA was used to eliminate statistical noise the Pd-signal (Fig.4.7a) from any particular alloy occupies a larger area than that of the Au signal (Fig.4.7b). In contrast, the MSA filtered maps of the Fe (Fig.4.7c) and O (Fig.4.7d) signals are spatially coincident. MSA was also used to fully isolate the Pd-signal (Fig. 4.7e) from all of the other components and it is clearly shown that Pd is strongly concentrated at the perimeter of the particles. Finally, the isolated signals for each element were used to construct an RGB image (as shown in Fig. 4.7).

The 2.5%Au-2.5%Pd/Fe$_2$O$_3$ supported catalysts were also examined by HREM. A lattice image of a single 40 nm diameter Au-Pd particle is shown in Figure 4.8, and it appears that there is a slight but abrupt change in contrast (indicated by the arrow) that takes place at a radius of approximately 15 nm from the centre of the particle.
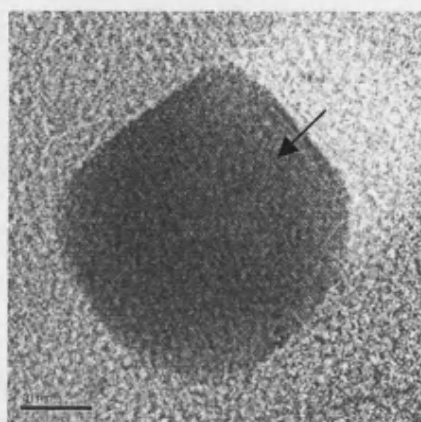

Figure 4.8 HRTEM image from the Au-Pd/Fe$_2$O$_3$ catalyst sample showing a single Au-Pd particle having a core-shell structure [space bar 10 nm].

4.4 Direct synthesis of H_2O_2 from H_2 and O_2 over silica supported Au, Pd and Au-Pd catalysts

Au, Pd and Au-Pd catalysts supported on silica were prepared using impregnation and these were evaluated for the synthesis of H_2O_2 after the catalysts had been calcined at 400°C.

Table 4.7 Activity of silica supported Au, Pd and Au-Pd catalysts in comparison to previously studied oxide supported catalysts.

Catalyst	Productivity (mol-H_2O_2/h/Kg_{cat})	H_2O_2 Wt.%
5%Au/SiO$_2$	1.0	0.001
2.5%Au/2.5%Pd/SiO$_2$	80	0.08
5%Pd/SiO$_2$	160	0.16
5%Au/TiO$_2$	7	0.007
2.5%Au/2.5%Pd/TiO$_2$	64	0.064
5%Pd/TiO$_2$	32	0.032
5%Au/Fe$_2$O$_3$	0.54	0.026
2.5%Au/2.5%Pd/Fe$_2$O$_3$	16	0.0163
5%Pd/Fe$_2$O$_3$	3.6	0.0036
5%Au/Al$_2$O$_3$	2.6	0.0026
2.5%Au/2.5%Pd/Al$_2$O$_3$	15.3	0.015
5%Pd/Al$_2$O$_3$	9.1	0.0091

All catalysts prepared by impregnation, calcined 400°C and tested as outlined in table 4.1

The results shown in Table 4.7 demonstrate that, unlike Al_2O_3, TiO_2 and Fe_2O_3 supported catalysts the 5%Pd catalyst is more active than the 2.5%Au-2.5% bimetallic catalyst. It is also interesting to note that the silica supported Au-Pd and Pd catalysts give a significantly higher rate for the synthesis of hydrogen peroxide when compared with the titania, alumina or iron oxide supported catalysts.

4.4.1 Effect of Pd content on silica supported Au-Pd catalysts active for H_2O_2 synthesis

In order to determine whether the activity of the Au-Pd silica supported catalysts scales with Pd content, a series of mono metallic Pd and the analogue bimetallic Au-Pd catalysts were prepared by impregnation, calcined and tested for H_2O_2 synthesis. The results are shown in figure 4.9.
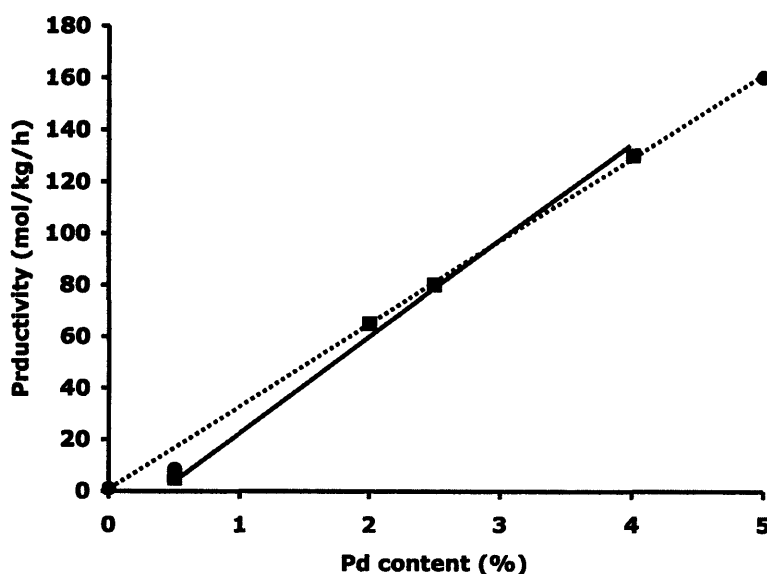

Figure 4.9 Silica supported Pd (●, ...) and Au-Pd (■, —5wt% total) catalysts for H_2O_2 synthesis

From figure 4.9 it is clear that the activity of the bimetallic Au-Pd catalysts scales with Pd content, and the addition of Au to the catalysts to give 5wt% total

metal loading does not induce the synergistic effect seen with other oxide supported catalysts.

4.4.2 Generality of the lack of synergy in silica supported Au-Pd catalysts

In order to determine whether the activity of all silica supported Au-Pd catalysts prepared by impregnation is determined by Pd content, a series of Au-Pd and Pd catalysts supported on 2 different silica supports (JM) were prepared and evaluated for H_2O_2 synthesis. The results, illustrated in figure 4.10, show that using 3 different silica supports, in all cases Pd catalysts were more active for H_2O_2 synthesis than the Au-Pd catalysts.
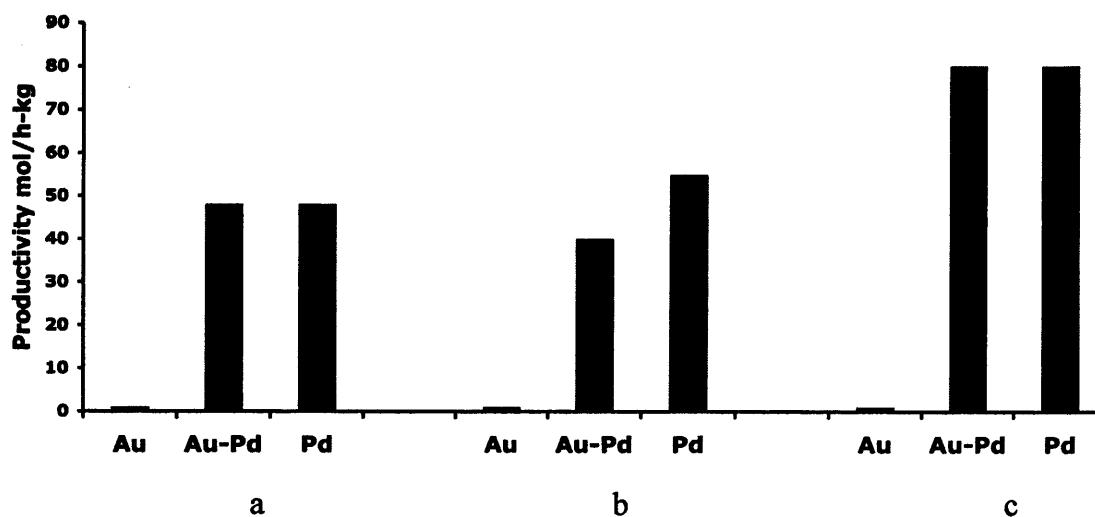

Figure 4.10 Calcined (400°C) Au, Au-Pd and Pd (5wt% total) catalysts supported on SiO_2 (a, b Johnson Matthey, c Grace) for H_2O_2 synthesis under standard reaction conditions.

4.4.3 Catalyst stability

As detailed in chapter 3 dried impregnated Au-Pd catalysts are extremely active for H_2O_2 synthesis, although unless subject to calcination above 400°C they are extremely unstable and lose activity on reuse. A series of experiments were conducted to determine whether the supported SiO_2 catalysts are subject to the same deactivation. The results, shown (figure 4.11) show that although the catalyst dried at 95°C are extremely active for H_2O_2 synthesis the activity drops from 120mol/h-kg$_{cat}$to 30mol/h-kg$_{cat}$on a second use.
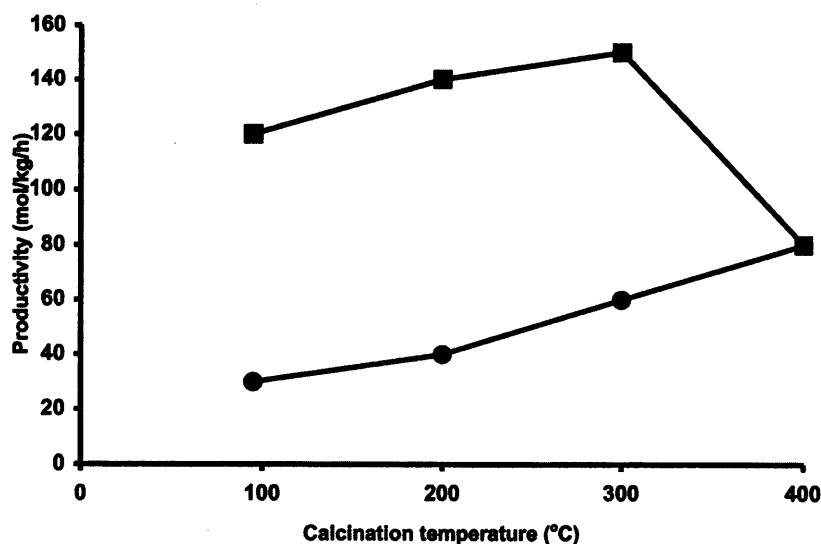
Figure 4.11 Effect of calcination temperature on activity of 2.5wt%Au-2.5wt%Pd/SiO$_2$ (grace) catalyst for H_2O_2 synthesis, first use (■) and re-use (●)

However, unlike the TiO_2 supported catalysts the activity of the 95°C dried catalyst increases on calcination in static air to 160mol/h-kg$_{cat}$for a catalyst calcined at 300°C. This catalyst is still subject to deactivation. Calcination at 400°C produces a stable catalyst that has an activity of 80mol/h-kg$_{cat}$

4.4.3 Catalyst Characterisation

4.4.3.1 XPS analysis

Figure 4.12 shows the combined Au(4d) and Pd(3d) spectra for a 2.5 wt% Au-2.5 wt% Pd/SiO$_2$ catalyst after different heat treatments. For the uncalcined sample, there are clear spectral contributions from both Au and Pd leading to severe overlap of peaks.
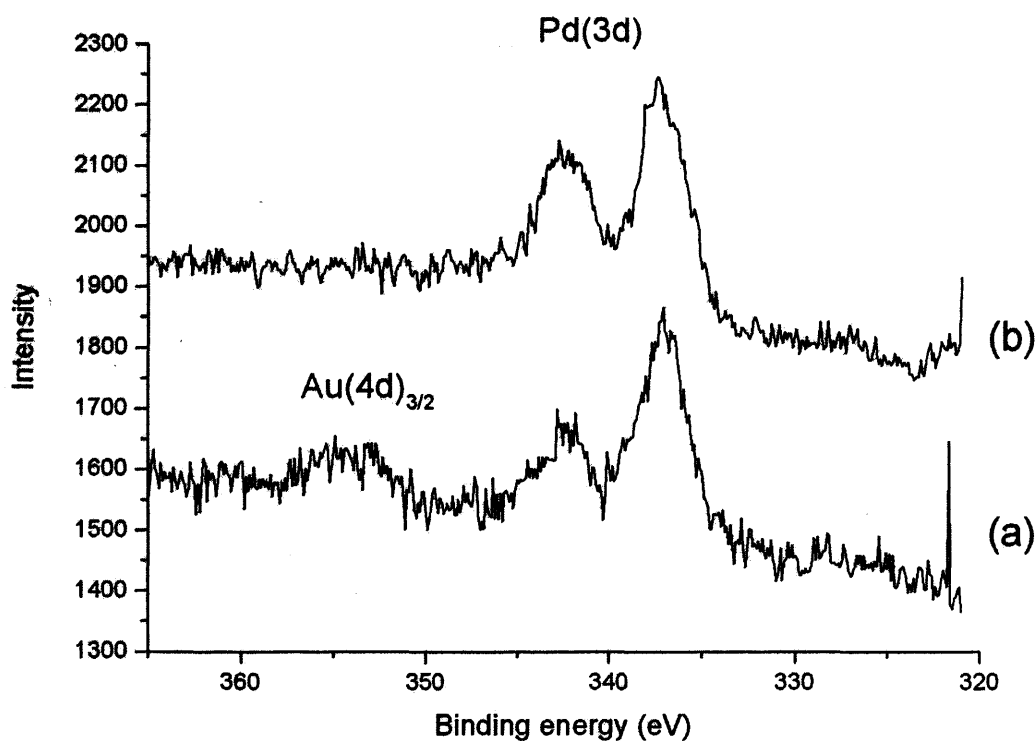
Figure 4.12 Au(4d) and Pd(3d) spectra for a 2.5 wt% Au-2.5 wt% Pd/SiO$_2$ catalyst after different heat treatments (a) uncalcined, (b) calcined at 400 °C in air

After calcination in air at 400°C , the intensity of the Au(4d$_{3/2}$) feature is below detection limits whereas it is quite clear in the dried sample.

4.4.3.2 STEM analysis

STEM-XEDS mapping and ADF imaging studies were carried out on a typical 2.5wt%Au-2.5wt%Pd/SiO$_2$ (figures 4.13, 4.14). Large gold-rich particles (10nm) are observed on the silica map (4.13c) whereas the Pd particles are much

smaller and highly dispersed (4.13d). The co-incidence of these particles suggest a homogenous alloy, however this cannot bee confirmed due to the size of the particles.
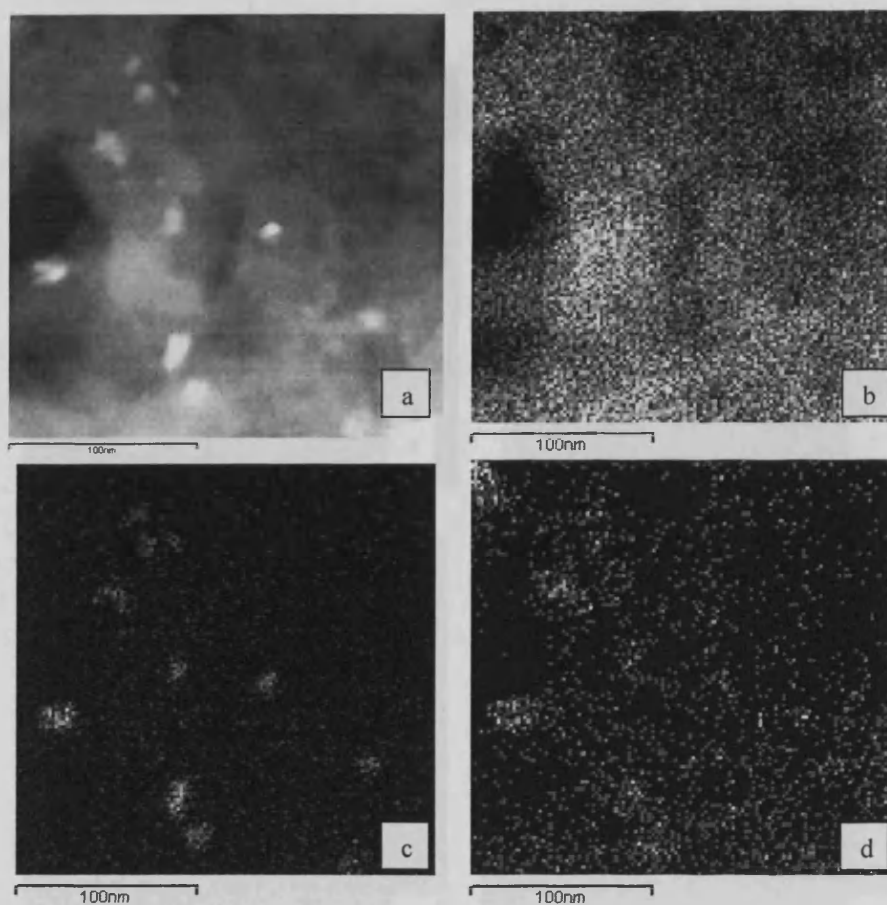
Figure 4.13. Montage of STEM data from the calcined 2.5 wt % Au-2.5 wt % Pd/SiO$_2$ sample. (a) ADF image and corresponding XEDS maps using (b), Si K$_\alpha$ (c) Au M$_2$. (d) Pd L$_\alpha$

Figure 4.14 shows that carbonaceous impurities exist within the silica and whilst they are few they co-incide with large (20nm) Pd rich particles. In this case the gold particles exist in highly dispersed, small nano-crystals.

Figure 4.14 Montage of STEM data from the calcined 2.5 wt % Au-2.5 wt %

Pd/SiO$_2$ sample. (a) ADF image and corresponding XEDS maps using (b), Si K$_\alpha$ (c) Au M$_2$, (d) Pd L$_\alpha$ and (e) C K$_\alpha$
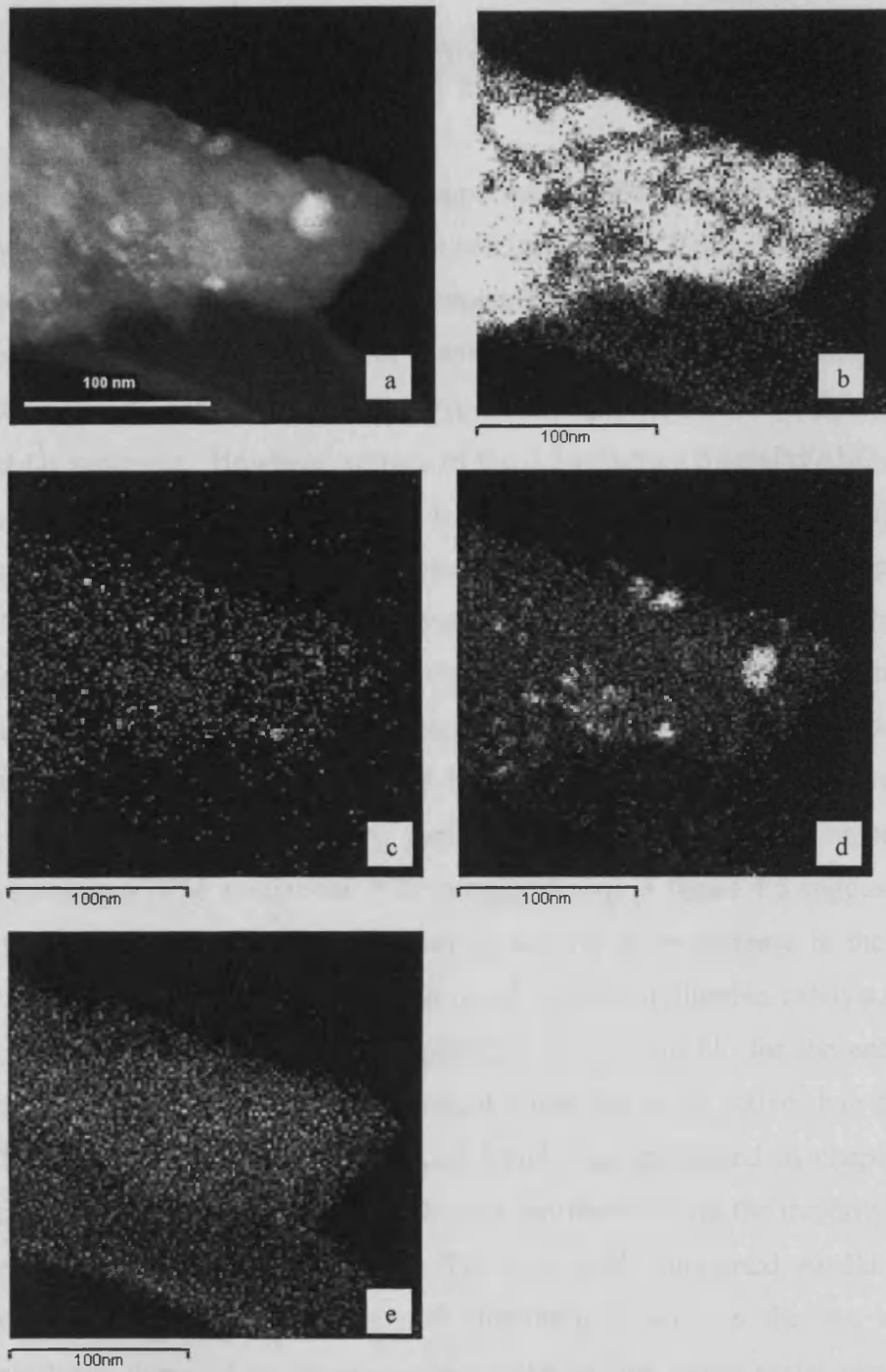
4.5   Discussion

4.5.1   Catalyst preparation, activity and stability

The Fe$_2$O$_3$ and Al$_2$O$_3$ supported Au-Pd catalyst both exhibit higher activities for H$_2$O$_2$ synthesis, when calcined at 400°C for 3 hours in air, than the corresponding Pd analogue. This synergistic effect of the addition of Pd to an Au catalyst was seen previously in chapter 3 for TiO$_2$ supported catalysts, and of all the catalysts the TiO$_2$ supported Au-Pd catalyst showed the highest activity for H$_2$O$_2$ synthesis. However, storage of the 2.5wt%Au-2.5wt%Pd/Al$_2$O$_3$ catalyst in a sealed container for 12 months led to a 3 fold increase in activity for H$_2$O$_2$ synthesis compared to the fresh catalyst, exhibiting an activity comparable to the 2.5wt%Au-2.5wt%Pd/TiO$_2$ catalyst. It has been reported elsewhere that the impregnation process does not produce a very strong bond between metal particles and the oxide support[5]. If the atomic mobilities of the gold and palladium were sufficient, then the atoms would be able to agglomerate and grow over time, producing ever larger Au-Pd particles. This hypothesis is supported by the extensive STEM studies-the ADF images shown in figure 4.5 suggest that a time-dependent growth process is occurring leading to an increase in the particle size distribution when compared to the freshly prepared alumina catalyst. This would suggest that these larger Au-Pd particles are responsible for the enhancement in catalytic activity, and particles around 35nm are more active than those <10nm. This is in agreement with the Au-Pd/TiO$_2$ data presented in chapter 3-in these catalysts there is a bimodal particle size distribution with the majority of the larger particles in the 35-80nm range. The iron oxide supported Au-Pd catalyst also exhibited a bimodal particle size distribution, whereas the Au and Pd only catalysts, prepared by impregnation consist of just larger metal particles. When considering the data for CO oxidation, and comparing preparation methods, it is clear that the methods which produce smaller gold particles (co-precipitation for

iron oxide catalyst, deposition precipitation for alumina supported catalyst) are preferred to impregnation methods which produce larger gold particles. It is possible to comment further on the role of Au particle size in relation to the activation of CO and H_2 with respect to oxidation. In this study the Au/Fe_2O_3 sample prepared by impregnation is shown to exhibit relatively large nanoparticles only, (*ca.*48 nm in diameter). This catalyst gives a rate of hydrogen peroxide formation of 0.54 mol-H_2O_2/h-Kg_{cat}. The microstructure of the 5 % Au/Fe_2O_3 catalysts prepared by co-precipitation has been examined in detail previously for studies of CO oxidation[6, 7]. Examination of samples dried at 25 °C did not reveal the presence of Au particles and such samples gave a much lower rate of hydrogen peroxide formation of 0.13 mol-H_2O_2/h-Kg_{cat}. The Au/Fe_2O_3 samples calcined at 400 °C exhibited a fairly uniform particle size of *ca.* 5 nm of cuboctahedral Au nanocrystals and this catalyst exhibited an intermediate rate of hydrogen peroxide formation of 0.21 mol-H_2O_2/h-kg_{cat}. Hence the rate of hydrogen peroxide formation increases with increasing Au particle size. The rate of CO oxidation, as expected, shows the reverse trend. Hence we conclude that the active sites for the activation of H_2 are significantly different from those active for CO oxidation and are associated with relatively large particles.

Studies into the stability of the catalysts for H_2O_2 synthesis at different calcination temperatures illustrate that, as with TiO_2 catalysts, the activity of the dried catalysts is much higher than that of the calcined catalyst, although the dried catalyst lost almost all of the total metal content after 1 use. It should be noted that proportionately, the loss of metals by leaching is much larger than the decrease in productivity for hydrogen peroxide formation. This is most likely due to the nature of the impregnation preparation, the dried sample will contain Au^{3+} and Pd^{2+} from the precursors, and drying in static air will not reduce the metals to the metallic oxidation state, and hence will not have formed a strong support-metal interaction on the surface. Emersion of this dried catalyst into the reaction medium will lead to dissolution of the metals in to the reaction solution. AAS of the corresponding medium does not indicate the presence of Au or Pd in the solution, so the most likely end point for the metals is plating on the metal stirrer bar. However, blank experiments with the stirrer after metals have leached from the catalysts are indeed blank, so the stirrer plating does not lead to the formation of an active catalyst.

Experiments conducted with varying Au-Pd ratios supported on Al$_2$O$_3$ indicated that a calcined 4wt%Au-1wt% Pd catalyst was most active for H$_2$O$_2$ synthesis, in comparison to the 2.5wt%Au-2.5wt%Pd standard catalyst. In order to investigate whether this was a general effect a 4wt%Au-1wt% Pd/TiO$_2$ catalyst was prepared, calcined and evaluated for H$_2$O$_2$ synthesis. This catalyst had an activity of 28mol/h-kg$_{cat}$, compared to 64mol/h-kg$_{cat}$for the standard 2.5wt%Au-2.5wt%Pd catalyst. This result indicates that the optimum composition of Au-Pd catalysts varies significantly depending on the support, and that each catalyst has to be dealt with on an individual basis.

4.5.2 Nature of the active site – "core-shell" formation

From the STEM images of the Au-Pd catalysts supported on Al$_2$O$_3$ and Fe$_2$O$_3$, the composition of the bimetallic particles was concluded to be of a "core-shell" nature, consisting of a gold-rich core surrounded by a palladium-rich shell.

The formation of such Au-Pd core-shell structures has been reported previously for ligand-stabilized bimetallic Au-Pd colloids[8], and in the preparation of bimetallic nano-particles by the sonochemical reduction of solutions containing gold and palladium ions[3] These core-shell particles exhibited superior catalytic activity compared with Au-Pd alloy particles which had the same overall Au:Pd atom ratio[3]. Detailed ^{197}Au Mössbauer studies confirmed the presence of a pure Au core, and there was also evidence for a thin alloy region at the interface between the Au core and Pd shell[3]. Our observations are consistent with these previous studies, and that the stable Au-Pd/Al$_2$O$_3$ catalysts prepared by calcination at 400 °C comprise of Au-Pd alloys in which the surface of the nano-particles is Pd rich. In this way it appears that Au is electronically promoting Pd for the direct oxidation reaction and this leads to the enhanced activity and selectivity observed with our supported Au-Pd alloyed catalyst. Additional evidence for this type of core-shell structure was found when the 2.5%Au-2.5%Pd/Fe$_2$O$_3$ supported catalysts were examined by HREM. Figure 4.8 indicates a typical Au-Pd particle, and the arrow indicated a change of intensity in the micrograph. This abrupt intensity variation could be indicative of a change in composition between the interior and perimeter, since any contrast change caused by projected thickness

variations in a spherical particle would be more gradual. The formation of a Pd rich shell surrounding an Au rich core could give rise to such a change in mass contrast, since Pd is 33 amu lighter than Au. Such surface enrichment has been observed for bulk Pd-Au alloys heated in oxygen at temperatures greater than 300°C,[9] where the surface layer was shown to consist of PdO. Interestingly, it was also found that subsequent hydrogen treatment at 350°C led to complete reduction of the oxide without re-equilibration of the surface metal composition. In contrast, the unreacted bulk alloys exhibited a surface composition identical with that of the interior.

Similar core-shell structures have also been found in Au-Ag nanoparticles.[4] In common with the Au-Pd phase diagram, the Au-Ag phase diagram predicts that a complete homogeneous solid solution should form, whereas in reality a definite surface Ag segregation effect has been experimentally observed. Hence this provides further circumstantial support for the unexpected conclusion that the Au-Pd particles in our active catalysts also comprise a core-shell structure.

4.5.3 Silica supported Au-Pd catalysts for H_2O_2 synthesis

The SiO_2 supported catalyst did not follow the trend of the TiO_2, Al_2O_3 and Fe_2O_3 oxides in that the bimetallic Au-Pd catalysts were not more active than Pd only catalysts for H_2O_2 synthesis, and the activity of the catalyst scaled directly with Pd content. The STEM images for the calcined 2.5wt%Au-2.5wt%Pd/SiO_2 catalysts show a much more complex system that that observed for the Au-Pd TiO_2, Fe_2O_3 and Al_2O_3 supported catalysts.

The dried Au-Pd/SiO_2 catalyst shows strong Au and Pd contributions in the XPS spectrum shown in figure 4.12. However, for the calcined Au-Pd/SiO_2 catalyst, the XPS spectrum (figure 4.12b) suggests that the photoelectron flux emitted from the gold atoms in the core is strongly attenuated due to inelastic scattering of the electrons during transport through the Pd shell, leading to a much reduced Au signal intensity compared with Pd. This core-shell model is consistent with the other oxide supported catalysts studied thus far.

However, the STEM analysis does not fit exactly with this model. It is clear that large particles are present on the silica catalysts, however the location Pd and Au on the silica is very different. There seems to be two different morphologies present. There are 'classic' metal particles, where Au exists on the bare silica, and the Pd exists on the carbon. The carbonaceous areas appear to contain many very small particles that are mostly Pd. These are the areas that appear 'speckly' in the images. Also, in contrast to all the other samples studied thus far, these samples have a small number of particles which appear to contain only Au. This apparent segregation of the Au and Pd could account for the activity of the Au-Pd/SiO$_2$ samples scaling with Pd content. It is well documented that supported Au catalysts are relatively inactive for H$_2$O$_2$ synthesis[10], whereas supported Pd catalysts are extremely active for H$_2$O$_2$ synthesis[11]. The large number of Pd only particles existing within the Au-Pd/SiO$_2$ samples could result in a catalyst displaying activity similar to the Pd only catalysts. However, no particles were large enough to study for the core-shell structure, so this cannot be ruled out. The sintering of the gold only particles on calcination could be responsible for the loss of the Au contribution in the XPS spectra shown in figure 4.12.

4.6   Conclusions

I. Au-Pd catalysts supported on Al$_2$O$_3$ and Fe$_2$O$_3$ are more active for H$_2$O$_2$ synthesis than the corresponding Pd only catalysts.

II. For SiO$_2$ supported catalysts, there is no synergy for Au-Pd catalysts, and the activity of the catalyst scales directly with Pd content.

III. The most active Au-Pd catalyst supported on Al$_2$O$_3$ was found to be 4wt%Au-1wt%Pd, whereas for TiO$_2$ supported catalysts 2.5wt%Au-2.5wt%Pd was found to be the optimum metal composition.

IV. Uncalcined (dried) catalysts are more active for H_2O_2 synthesis than calcined materials but are highly unstable and lose >90% metal content after 1 use.

V. The leached components from the uncalcined catalysts do not act as a homogenous catalyst

VI. Large (>30mn) Au-Pd particles are very active for H_2O_2 synthesis, as shown by storing 2.5wt%Au-2.5wt%Pd/Al_2O_3 catalysts for 12 months. Particle agglomeration occurs leading to a more active catalyst.

VII. Small Au particles supported on alumina and iron oxide are more active for CO oxidation than large ones, the opposite of which is true for H_2O_2 synthesis.

VIII. Au-Pd particles on alumina and iron oxide form core-shell particles on calcination, consisting of a Pd shell surrounding an Au core.

IX. Au and Pd particles supported on silica display a very complex structure. Carbon impurities contained in the silica promote the formation of large, Pd rich particles, whereas larger Au particles form on the silica. Highly dispersed Pd particles exist on the bare silica.

X. 5%Pd/SiO_2 is the most active, stable catalyst for H_2O_2 synthesis evaluated thus far.

4.7   References

[1]   P. Landon, P. J. Collier, A. F. Carley, D. Chadwick, A. J. Papworth, A. Burrows, C. J. Kiely, G. J. Hutchings, *Physical Chemistry Chemical Physics* 2003, *5*, 1917.

[2]   P. Landon, P. J. Collier, A. J. Papworth, C. J. Kiely, G. J. Hutchings, *Chemical Communications (Cambridge, United Kingdom)* 2002, 2058.

[3]   C. D. Wagner, L. E. Davis, M. V. Zeller, J. A. Taylor, R. M. Raymond, L. H. Gale, *Surf. Interface Anal.* 1981, *3*, 211.

[4]   N. Bonnet, *Journal of Microscopy (Oxford)* 1998, *190*, 2.

[5]   C. P. J. Poole, F. J. Owens, 2003.

[6]   R. M. Finch, N. A. Hodge, G. J. Hutchings, A. Meagher, Q. A. Pankhurst, M. R. H. Siddiqui, F. E. Wagner, R. Whyman, *Physical Chemistry Chemical Physics* 1999, *1*, 485.

[7]   N. A. Hodge, C. J. Kiely, R. Whyman, M. R. H. Siddiqui, G. J. Hutchings, Q. A. Pankhurst, F. E. Wagner, R. R. Rajaram, S. E. Golunski, *Catalysis Today* 2002, *72*, 133.

[8]   R. A. Sheldon, I. W. C. E. Arends, G.-J. ten Brink, A. Dijksman, *Accounts of Chemical Research* 2002, *35*, 774.

[9]   L. Hilaire, P. Legare, Y. Holl, G. Maire, *Surface Science* 1981, *103*, 125.

[10]   M. Okumura, Y. Kitagawa, K. Yamagcuhi, T. Akita, S. Tsubota, M. Haruta, *Chemistry Letters* 2003, *32*, 822.

[11]   J. H. Lunsford, *Journal of Catalysis* 2003, *216*, 455.

Chapter Five

Chapter Five : Direct synthesis of H_2O_2 from H_2 and O_2 over acid pre-treated Au, Pd and Au-Pd catalysts

5.1   Introduction

The decomposition (H_2O_2 → H_2O + ½ O_2) of hydrogen peroxide by the catalysts active for its formation is a major problem in the direct route for hydrogen peroxide synthesis. Another major problem in the direct synthesis route is the hydrogenation of hydrogen peroxide (H_2O_2 + H_2 → $2H_2O$).

Numerous groups[1-3] studying the direct route attempt to overcome the problem of the subsequent reaction for H_2O_2 after formation by using stabilisers, typically mineral acids and halides, in the reaction medium. The Solvay process[4] details the use of 1.6M H_3PO_4 and 0.0006M NaBr as stabilisers, as the decomposition reaction is less facile in acidic medium and halide ions are known to poison sites responsible for H_2O_2 decomposition. The Pd/BaSO$_4$ catalyst used can achieve selectivites up to 98%, one of the highest selectivities reported.

Degussa-Headwaters recently announced details of a plant utilising hydrogen peroxide produced *in situ* for the synthesis of propylene oxide[5]. Indeed, there is significant interest industrially for this process, indicated by recent patent literature filed by Degussa[6, 7]. However, the presence of stabilisers in the reaction medium for these processes poses problems for removal and refining of product after reaction. Moreover, the presence of dilute acids in stainless steel reactors would also pose problems on a large scale.

The work previously undertaken studying TiO_2[8], Al_2O_3[9] and Fe_2O_3[9] supported catalysts showed that high selectivity to H_2O_2 can be achieved in the absence of these stabilisers at low reaction temperatures (2 °C) using 10 mg of catalyst. In all cases the bimetallic Au-Pd catalyst was more selective for the direct synthesis of hydrogen peroxide than mono-metallic Pd. A series of experiments were carried out using various pre-treatments of the support prior to impregnation of Au and or Pd, to determine whether the selectivity of the catalysts could be improved.

5.2 Evaluation of Au, Pd and Au-Pd/Carbon catalysts for H$_2$O$_2$ synthesis under standard reaction conditions

5.2.1 Acid pre-treated Waterlink Sutcliffe carbon supported Au, Pd and Au-Pd catalysts for H$_2$O$_2$ synthesis

A series of Au, Pd and Au-Pd catalysts were prepared by impregnation of a Waterlink Sutcliffe Carbons Activated Carbon Grade: 207A, Mesh: 12x20 carbon as provided, calcined at 400°C for 3 hours in static air, and tested for H$_2$O$_2$ synthesis under standard reaction conditions as detailed in section 2, namely 10mg catalyst in 5.6g Methanol 2.9g water at 2°C for 30 mins, molar ratio H$_2$:O$_2$ 1:2. The results are shown in figure 5.1.
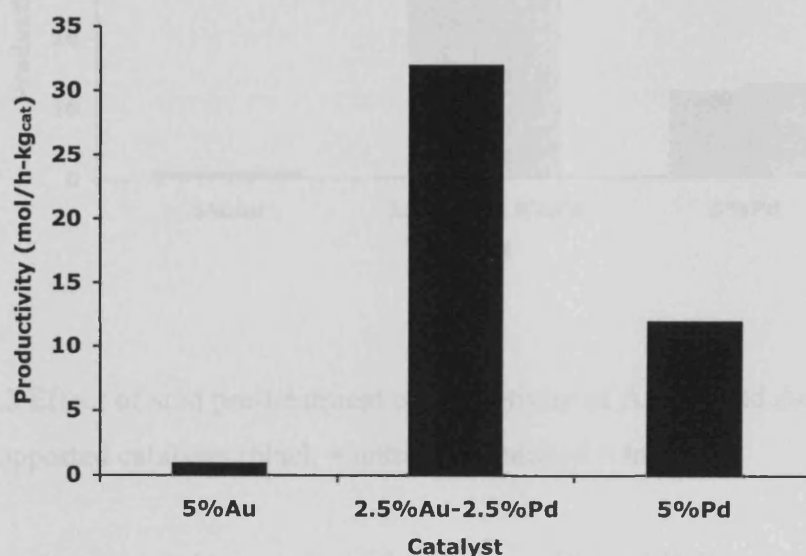

Figure 5.1 Activity of Au, Pd and Au-Pd activated carbon supported catalysts for H$_2$O$_2$ synthesis

As seen previously, the bimetallic Au-Pd catalysts were more active than either the Pd or Au monometallic catalysts, although the activity was lower than we have seen with TiO$_2$ supported catalysts. As is standard when using activated carbon as a support, the carbon was then subjected to an acid wash in order to remove any

metals or impurities that could be responsible for the decomposition reaction. The carbon was slurried in 10% HNO_3 for 3 hours, washed and dried prior to impregnation of the Au and/or Pd, followed by calcination at 400°C. The results for these catalysts are shown in figure 5.2. It is clear that although the acid pre-treatment does not affect the relative activity of the Au or Pd mono-metallic catalysts, it results in a 100% increase in activity for the bimetallic Au-Pd catalyst.
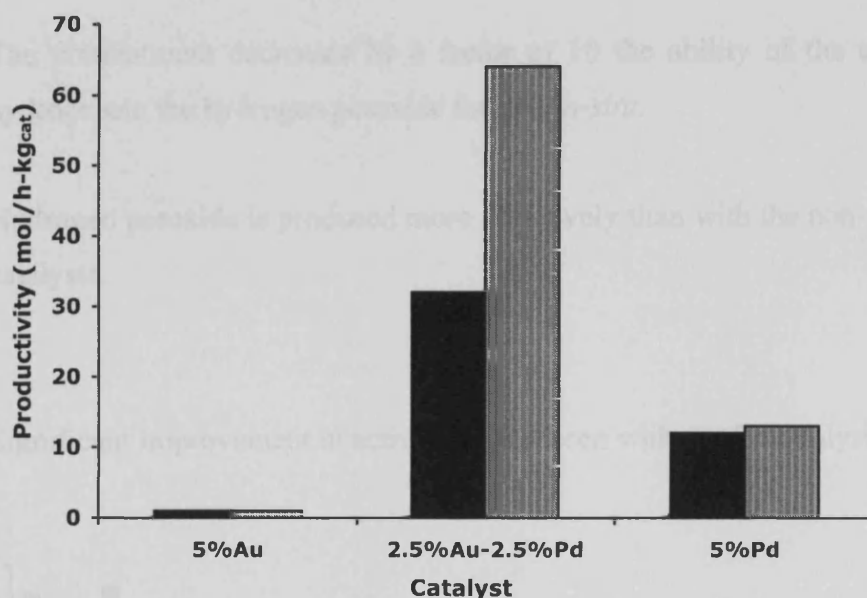

Figure 5.2 Effect of acid pre-treatment on the activity of Au, Pd and Au-Pd activated carbon supported catalysts (black = untreated, hatched = treated)

This observation led to a study of the decomposition of H_2O_2 over the catalyst, to see whether the washing may have removed an impurity active for decomposition. In the absence of hydrogen in the gas stream there was no decrease in H_2O_2 concentration in 30 minutes (full reaction conditions are listed in chapter 2). The experiments were repeated with 420psi 5%H_2/CO_2 present, and the results summarized in table 5.1. These results illustrate the following:

i.   Catalyst improvement is seen using a variety of acid concentrations, and only a small concentration of acid (2%) is required to bring about the improvement in the catalyst (figure 5.3).

ii.   Washing with water does not lead to an improvement in catalysis (*i.e.* an impurity is not being removed by washing).

iii.   The pretreatment decreases by a factor of 10 the ability of the catalyst to hydrogenate the hydrogen peroxide formed *in-situ*.

iv.   Hydrogen peroxide is produced more selectively than with the non-pretreated catalysts.

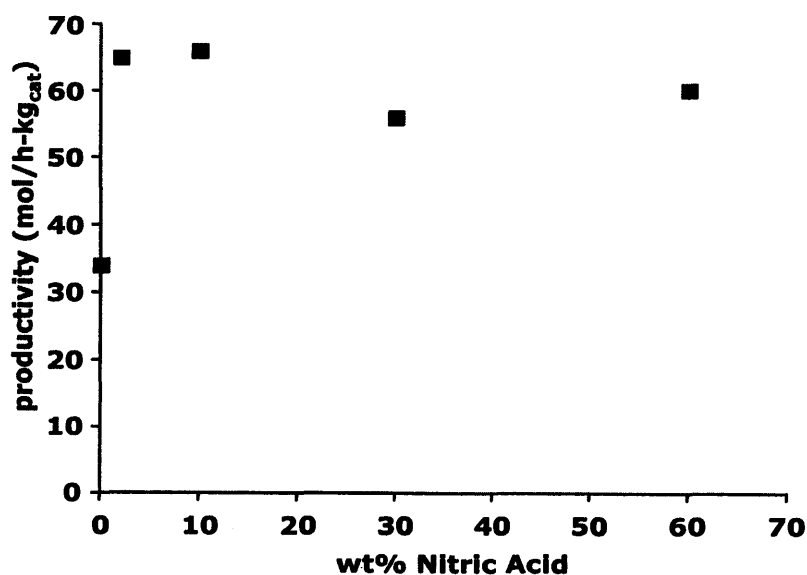v.   Significant improvement in activity is only seen with Au-Pd catalysts.

Figure 5.3 Effect of concentration of HNO_3 pre-treatment on the rate of H_2O_2 synthesis under standard reaction conditions (catalyst calcined 400°C 3hours in air)

Table 5.1 Selectivity, conversion and hydrogenation over Au, Pd and Au-Pd pre-treated catalysts

Catalyst	Pre-treatment	Productivity (mol/h-kg$_{cat}$)	H$_2$ conversion (%)	Selectivity (%)	Hydrogenation (%)
2.5wt%Au 2.5wt%Pd	None	34	28	24	19.4
2.5wt%Au 2.5wt%Pd	Water	35	28	24	20
2.5wt% Au 2.5% Pd	2% HNO$_3$	65	19	98	1
5%Au	None	0.7	~0	-	<0.5
5%Au	10%HNO$_3$	0.5	~0	-	<0.5
5%Pd	None	12	17	14	4
5%Pd	10%HNO$_3$	12	17	14	4.1
2.5wt%Au 2.5wt%Pd	10%HNO$_3$	66	20	98	1.4
2.5wt%Au 2.5wt%Pd	30% HNO$_3$	56	18	97	1.6
2.5wt%Au 2.5wt%Pd	60%HNO$_3$	60	19	98	1.7

(All catalysts calcined 400°C air. H$_2$O$_2$ synthesis reaction conditions : 10mg catalyst in 5.6g Methanol 2.9g water at 2°C for 30 min, molar ratio H$_2$:O$_2$ 1:2)

5.2.2 Acid pre-treated Carbon (Aldrich G60)-supported Au, Pd and Au-Pd catalysts for H_2O_2 synthesis

To investigate whether the acid pre-treatment was effective for other carbon supports a range of catalysts were prepared on a commercially available Aldrich G60 carbon which had been subjected to an acid wash, a water wash and also tested as provided. These results (Table 5.2) clearly illustrate again the benefits of pre-treating the support prior to impregnation, leading to a 50% increase in the productivity of the Au-Pd catalysts. To study whether this improvement in catalysis was a general acidic effect the G60 carbon was washed with a variety of acids and also a base (Table 5.2). Pre-treatment with HCl and H_3PO_4 leads to a slight improvement in the rate of H_2O_2 synthesis but the selectivity of these catalysts is lower than the HNO_3 pretreated catalyst and even the non-treated catalyst. Pre-treating the support in a basic solution is detrimental both to the activity of the catalyst and the selectivity to H_2O_2. Doping NO_3^-, K^+ and Na^+ onto the support prior impregnation (*via* washing with appropriate metal salts) with Au and or Pd had a negligible effect on catalyst activity, demonstrating that it is the acid treatment which is important. Addition of 1N HNO_3 during the impregnation step had no effect on the catalyst activity. Addition of 1N (1 wrt [H^+]) HCl was extremely detrimental to the catalyst activity.

Table 5.2 Activity and selectivity for G60 supported catalysts with various pre-treatments at 2°C

Catalyst	Pre-treatment	Selelctivity (H_2)	Productivity (mol/hg$_{cat}$/hr)
5%Pd/G60 Carbon	None	42	50
2.5%Au-2.5%Pd/G60 Carbon	Water	80	112
5%Pd/G60 Carbon	Water	42	50
2.5%Au-2.5%Pd/G60 Carbon	2%HNO$_3$	>98	160
5%Pd/G60 Carbon	2%HNO$_3$	42	52
2.5%Au-2.5%Pd/G60 Carbon	2%H$_3$PO$_4$	30	120
2.5%Au-2.5%Pd/G60 Carbon	2%HCl	15	130
2.5%Au-2.5%Pd/G60 Carbon	2%NH$_4$OH	24	70
2.5%Au-2.5%Pd/G60 Carbon	2% NH$_4$NO$_3$	80	100
2.5%Au-2.5%Pd/G60 Carbon	1N HCl [1]	5	20
2.5%Au-2.5%Pd/G60 Carbon	1N HNO$_3$ [1]	35	98
2.5%Au-2.5%Pd/G60 Carbon	2%NaNO$_3$	80	122
2.5%Au-2.5%Pd/G60 Carbon	2%KNO$_3$	80	120

(reaction conditions as detailed for table 5.2)

[1] 1N HNO$_3$/HCl added during the impregnation step

5.2.3 Effect of acid pre-treatment on oxide supports.

The effect of support pre-treatment was further extended to oxide supports, namely TiO_2 and SiO_2, to see if the effect was a general one. Acid pre-treatment of P25 TiO_2 with 2%HNO_3 again led to an increase in activity for the 2.5wt%Au-2.5wt%Pd catalyst, which was not observed for the Pd only catalyst (Table 5.3) There was also a significant increase in the selectivity of the Au-Pd bimetallic catalyst.

Table 5.3 Effect of acid pre-treatment on the performance of titania supported Au, Pd and Au-Pd catalysts

Catalyst	Pre-treatment	Selectivity (%)	Productivity (mol/h-kg$_{cat}$)
5%Au/TiO$_2$ (P25)	None	Nd	7
2.5%Au-2.5%Pd/TiO$_2$ (P25)	None	70	64
5%Pd/TiO$_2$ (P25)	None	21	30
5%Au/TiO$_2$ (P25)	Water	Nd	7
2.5%Au-2.5%Pd/TiO$_2$ (P25)	Water	70	64
5%Pd/TiO$_2$ (P25)	Water	21	31
5%Au/TiO$_2$ (P25)	2%HNO$_3$	Nd	8
2.5%Au-2.5%Pd/TiO$_2$ (P25)	2%HNO$_3$	95	80
5%Pd/TiO$_2$ (P25)	2%HNO$_3$	22	33

(Reaction conditions as table 5.2, catalysts calcined 400°C air. Nd=not determined)

Previous work (as detailed in chapter 4) using silica supported catalysts showed that the synergistic effect of Au addition to a Pd catalyst was not observed with these catalysts, and that the activity of Au-Pd catalysts scaled with Pd content in 3 different cases (chapter 4 figure 4.10). Acid pre-treatment of the SiO_2 prior to the impregnation of Au and Pd was carried out and the catalysts were again evaluated for H_2O_2 synthesis. Table 5.4 shows the effect of acid pre-treatment on the Au-Pd catalyst for 3 different types of silica. Surprisingly, considering the lack of synergy observed for the untreated support, in all cases the pre-treated Au-Pd catalyst showed higher activity for H_2O_2 synthesis than the pre-treated Pd only catalyst (figure 5.4).

Table 5.4 Effect of acid pre-treatment on silica supported Au-Pd catalysts

Catalyst	Pre-treatment	Selectivity (%)	Productivity (mol/h-kg_{cat})
2.5%Au-2.5%Pd/SiO$_2$[1]	None	80	108
2.5%Au-2.5%Pd/SiO$_2$[1]	Water	80	108
2.5%Au-2.5%Pd/SiO$_2$[1]	2%HNO$_3$	73	185
2.5%Au-2.5%Pd/SiO$_2$[2]	None	80	48
2.5%Au-2.5%Pd/SiO$_2$[2]	Water	80	48
2.5%Au-2.5%Pd/SiO$_2$[2]	2%HNO$_3$	78	138
2.5%Au-2.5%Pd/SiO$_2$[3]	None	42	40
2.5%Au-2.5%Pd/SiO$_2$[3]	Water	42	41
2.5%Au-2.5%Pd/SiO$_2$[3]	2%HNO$_3$	68	140

(reaction conditions as table 5.2)

[1] Grace, [2] Johnson Matthey, [3] Johnson Matthey more details in chapter 2)
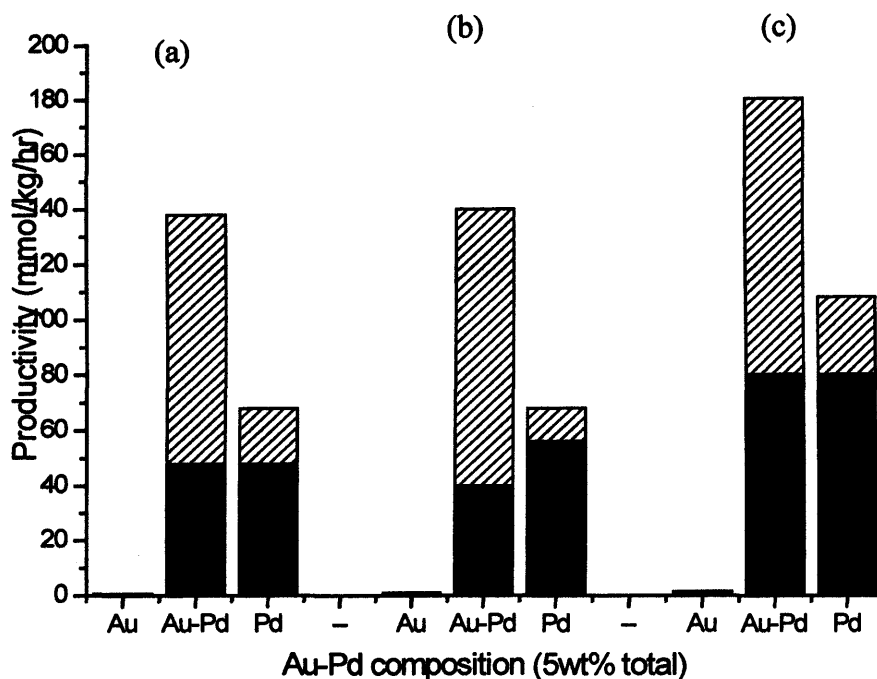
Figure 5.4 Effect of acid washing of support for silica supported catalysts (a, b Johnson Matthey; c Grace see experimental for further details

Black bars indicate catalyst activity prior to support pre-treatment, dashed bars show activity after 2%HNO$_3$ support pre-treatment.

In contrast to the TiO$_2$ and activated carbon supported catalysts, the acid-pre-treatment of the support seems to be effective for the monometallic Pd catalysts, although the effect of acid pre-treatment for the Au-Pd bimetallic catalyst is much higher, with an unexpected synergistic effect seen for the Au-Pd catalyst which was not observed for the untreated supported catalysts.

5.3   Further investigation into the origins of the beneficial effect of support acid pre-treatment

5.3.1 Catalyst stability

A series of experiments were undertaken to study the nature of the catalyst, and to see whether the beneficial effect of acid pre-treatment persisted with use. Catalyst stability has already been shown in chapters 3 and 4 to be a problem for uncalcined Au-Pd catalysts supported on TiO_2 and Al_2O_3 where Au and Pd leached into the reaction medium.

To evaluate the long-term stability of the calcined pre-treated catalysts, a series of reuse experiments were undertaken for the 2.5wt%Au-2.5wt%Pd catalysts supported on the G60 carbon and on TiO_2 (P25). The results of these re-use experiments (figures 5.6 and 5.7) clearly demonstrate that the catalysts do not lose any activity after 3 uses. Interestingly, if the reaction medium is acidified (to contain 2%HNO_3) there is a marked increase in activity of the non-treated catalyst compared to both the untreated and the 2%HNO_3 pre-treated catalysts in the absence of HNO_3. However, this effect is short lived and when the catalyst is recycled for a second use, without the further addition of HNO_3 the activity of the catalyst falls back to that of the non-treated catalyst.

These results clearly demonstrate that the beneficial effect of acid pre-treatment is sustainable for catalysts calcined at 400°C for 3 hours in air. Atomic absorption spectroscopy of these catalysts did not show any loss of Au or Pd after 4 reactions, in comparison to the fresh (dried but uncalcined) catalysts.
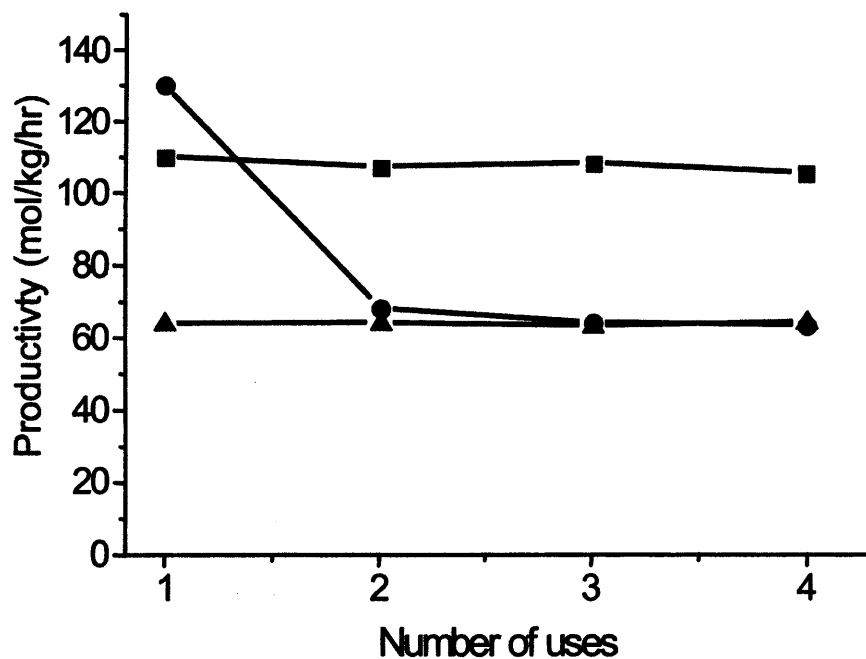
Figure 5.6 Effect of reuse on 2.5 wt%Au-2.5 wt%Pd/TiO₂ catalysts. The untreated catalyst (▲) is stable over 4 uses, but exhibits lower activity than the 2% HNO₃ treated catalyst (■). The addition of 2% HNO₃ in the autoclave with the untreated catalyst (●) shows higher initial activity which is lost after subsequent re-uses in the absence of additional acid.
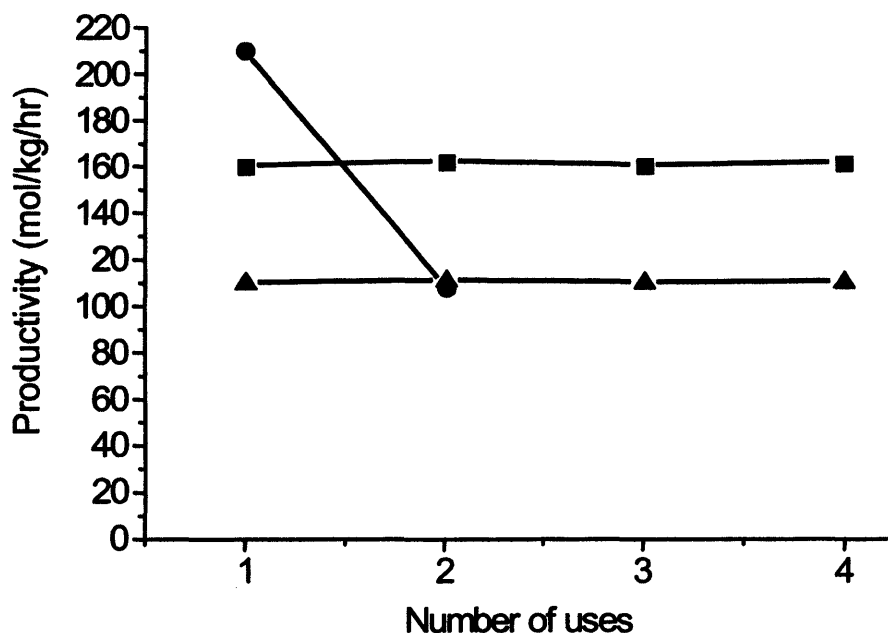
Figure 5.7 Effect of reuse for 2.5 wt%Au-2.5 wt%Pd/carbon catalysts. As with the Au-Pd catalysts (fig. 5.6) the untreated (▲) and 2% HNO_3 treated (■) catalysts are stable over 4 uses, with the latter showing a higher activity. The addition of 2% HNO_3 in the autoclave with the untreated catalyst (●) shows a higher initial activity which is lost on subsequent re-use.

5.3.2   Synthesis reaction at elevated temperatures

As previously discussed, the catalysts active for the direct synthesis of H_2O_2 are also active for the subsequent hydrogenation and decomposition of H_2O_2. Previous work undertaken within the group demonstrated that 2°C [10, 11] was the optimum temperature to undertake this reaction in the absence of stabilisers. At higher temperatures H_2 conversion is higher but the selectivity and yield to H_2O_2 is much lower, as the hydrogenation reaction becomes more facile. As the hydrogenation reaction is "switched off" with the pre-treated catalysts, the activity of the calcined 2.5wt%Au-2.5wt%Pd on pre-treated TiO_2 at higher temperatures was investigated (figure 5.8).
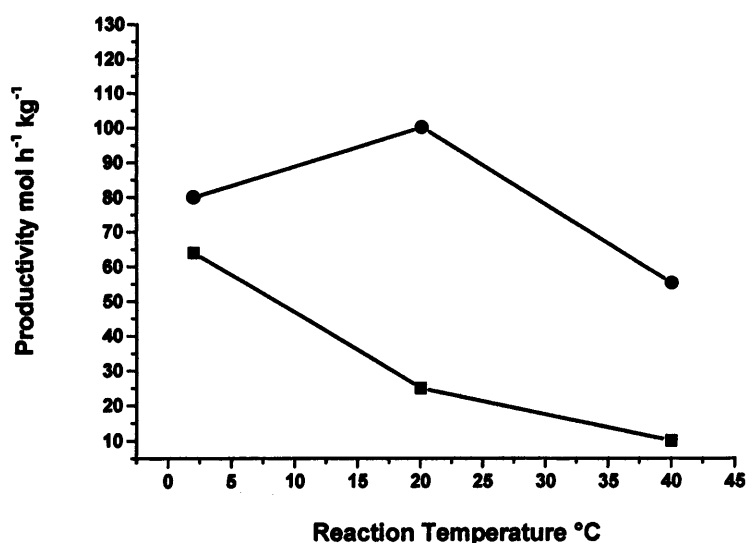
Figure 5.8 The effect of pre-treatment on the temperature dependence of catalytic activity. The untreated Au-Pd/TiO$_2$ catalyst (■) shows decreasing activity at progressively higher temperatures, in contrast to the 2%HNO$_3$ pre-treated catalyst (●), which even at 40°C shows significant activity.

The non pre-treated catalyst has much lower activity at room temperature and at 40°C exhibits almost no activity for H$_2$O$_2$ synthesis. In contrast the 2%HNO$_3$ pre-treated catalyst is more active at room temperature than at 2°C, and at 40°C has approximately the same activity (64mol/h-kg$_{cat}$) as the non-treated catalyst at 2°C

5.3.3 Reaction Profile – time on-line studies

The progress of the reaction was followed by stopping repeated experiments after different times for the 2%HNO$_3$ pre-treated 2.5wt%Au-2.5wt%Pd/G60 calcined catalysts at 2°C and at room temperature. The results, shown in figure 5.9, clearly show that for a 30 minute reaction, unlike the pre-treated TiO$_2$, the 2%HNO$_3$ treated catalyst is more active at 2°C than at room temperature. However, the initial activity of the 2%HNO$_3$ pre-treated catalyst at 25°C (900mol/h-kg$_{cat}$) was much higher than
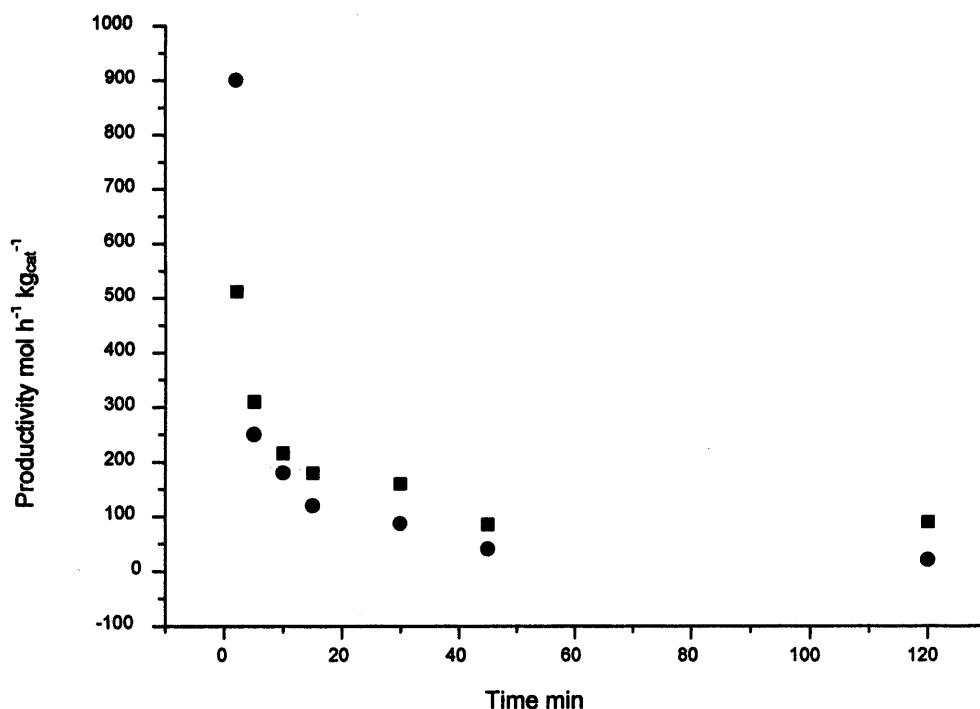
that of the same catalyst at $2^{\circ}C$ ($500mol/h$-kg_{cat})

Figure 5.9 Reaction profile for the $2\%HNO_3$ treated $2.5wt\%Au$-$2.5wt\%Pd/G60$ catalyst at $2^{\circ}C$ (■) and $25^{\circ}C$ (●)

These results led to an investigation of the initial rates (measured after 2 minutes) of all the Au-Pd acid pre-treated catalysts to date. The selectivities and rates are reported in table 5.5. These results demonstrate that for TiO_2 and carbon supported catalysts pre-treatment leads to higher activity for H_2O_2 synthesis than for the non-treated catalysts. In the case of SiO_2 supported catalysts there is no increase in initial activity for the acid pre-treated catalyst.

Table 5.5 Initial rates (after 2 minutes) and hydrogen selectivity to H_2O_2 for acid pre-treated catalysts

Catalyst	Pre-treatment	Initial Selectivity to H_2O_2 (%)	Initial Productivity (mol/ kg_{cat}-h)
2.5%Au-2.5%Pd/TiO$_2$ (P25)	None	99	202
2.5%Au-2.5%Pd/TiO$_2$ (P25)	2%HNO$_3$	99	315
2.5%Au-2.5%Pd/carbon [1]	None	99	391
2.5%Au-2.5%Pd/carbon [1]	2%HNO$_3$	99	564
2.5%Au-2.5%Pd/carbon [1,2]	2%HNO$_3$	99	900
2.5%Au-2.5%Pd/carbon [3]	2%HNO$_3$	99	197
2.5%Au-2.5%Pd/SiO$_2$[4]	None	99	278
2.5%Au-2.5%Pd/SiO$_2$[4]	2%HNO$_3$	99	267

(All catalysts were calcined in air 400°C for 3h. Standard reaction conditions as per table 5.2 were used, the productivity was measured after 2 minutes [1] Adrich G60 activated carbon [2] Reaction at 25 °C [3] Waterlink Sutcliffe Carbons Activated Carbon Grade: 207A, Mesh: 12x20 [4] Grace more details in chapter 2)

5.3.4 Experiments investigating higher whether H_2O_2 concentrations can be achieved

Up until this point, the most active catalyst for H_2O_2 synthesis at 30 minutes is the calcined 2.5wt%Au-2.5wt%Pd on 2%HNO$_3$ pre-treated G60 carbon, giving a

H_2O_2 concentration of 0.38wt%. To stay outside the lower explosive region of H_2 and O_2, diluted gases are used to prevent explosions. With 100% conversion and selectivity a concentration of 1.2wt% H_2O_2 could be achieved under standard reaction conditions. As illustrated in figure 5.10, increasing reaction length and temperature will increase H_2 conversion, but is deleterious for the selectivity. A reaction length of 30 minutes was chosen as the optimum compromise between the two, as selectivities approaching 100% can be achieved, with a yield of around 35%. In order to determine whether higher concentrations of H_2O_2 can be achieved without operating with higher H_2 and O_2 concentrations a series of top-up reactions were carried out, where after a 30 minute reaction the gases were vented and fresh gas added. The reaction was then allowed to proceed for 30 minutes, and the process repeated.
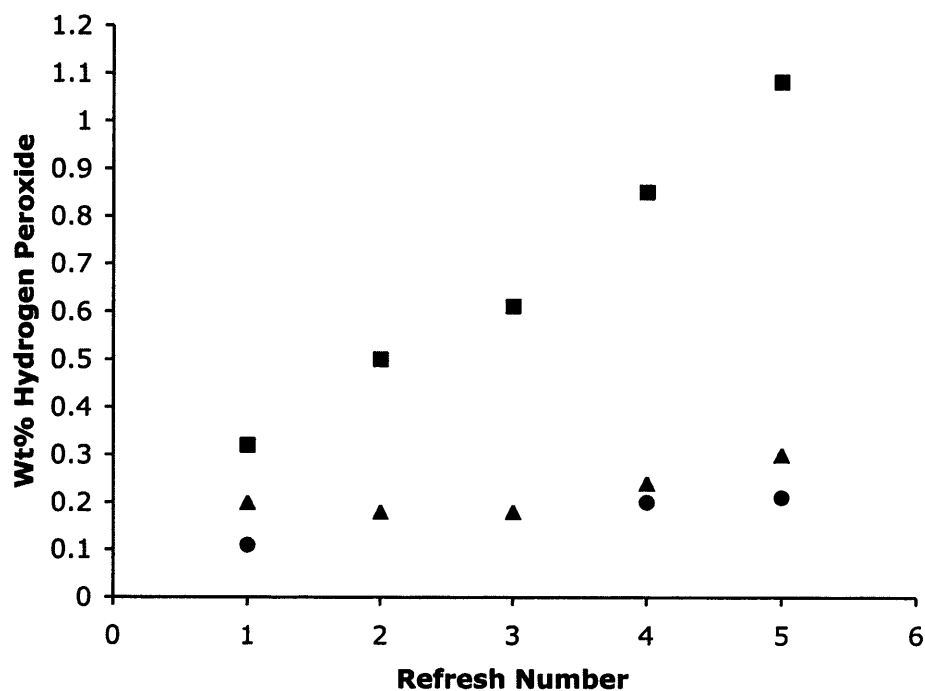

Figure 5.10 The effect of sequential experiments using gas top-up on hydrogen peroxide concentration. The acid treated Au-Pd/G60 (■) catalyst shows increasing hydrogen peroxide concentration as reactant gases are refreshed. In contrast the untreated Au-Pd/G60 (▲) catalyst and 5%Pd/G60 (●) catalyst show no increase

hydrogen peroxide concentration as the gases are refreshed, due to enhanced hydrogen peroxide decomposition for the non-treated catalysts.

These results are illustrated in figure 5.10 and demonstrate that under these inherently safe operating conditions high H_2O_2 concentrations can be achieved using the calcined 2.5wt%Au-2.5wt%Pd on 2%HNO$_3$ pre-treated G60 carbon catalyst, in comparison to the 2%HNO$_3$ Pd/carbon catalyst and the untreated Au-Pd catalyst.

5.4   Role of the support

In an attempt to elucidate the nature of the acid pre-treatment a series of decomposition experiments were conducted over the acid pre-treated catalysts, and over the bare supports after pre-treatment. The results form these experiments are summarised in table 5.6.

The results shown in table 5.6 give a fresh insight into the nature of the pre-treatment. The TiO_2 after a 3 hours treatment in 2%HNO$_3$ shows no hydrogenation of H_2O_2 in a 30 minute period, in comparison to the non-treated TiO_2 which shows 20% hydrogenation in 30 minutes. Again, after a second use the treated TiO_2 still shows no hydrogenation activity, which appears to show that the acid pre-treatment brings about a permanent change to the support. The hydrogenation activity of the TiO_2 without the acid washing maintains 20% decomposition. A similar trend is observed for the G60 carbon: after 1 use the 2%HNO$_3$ support hydrogenates 15% of the H_2O_2 present in 30 minutes; however on re-use the hydrogenation activity drops to 0%. Another point of interest in these results is the hydrogenation over the 2.5wt%Au-2.5wt%Pd catalysts (calcined 3hours in air). The Au-Pd/TiO_2 is more active for hydrogenation than the G60 equivalent, but in both cases the acid pre-treated catalyst exhibits lower hydrogenation activity than the non-treated catalysts-by a factor of 6 for the TiO_2 and 10 for the G60 carbon.

Table 5.6 Hydrogen peroxide synthesis and hydrogenation over different supports and catalysts

Support/ Catalyst	Pre-treatment	H_2O_2 Productivity (mol/h-kg_{cat})	Decomposition (%) * catalyst	Support[1]
Carbon[2]	None	110	20	40[a], 38[b]
Carbon[2]	Water	112	21	39
Carbon[2]	2%HNO$_3$	160	1.8	15[a], 0[b]
TiO$_2$[3]	None	64	30	20[a]
TiO$_2$[3]	Water	64	32	20[a], 19[b]
TiO$_2$[3]	2%HNO$_3$	95	5	0[a],0[b]

*Hydrogen peroxide decomposition over 2.5wt%Au-2.5wt%Pd catalyst or the support: H_2O_2 (0.4 wt.%) in a methanol/water solution (CH_3OH, 5.6 g; H_2O 2.9 g) reacted with 2.9 MPa H_2(5%)/CO_2 for 30 min at 2 °C.

[1] Support only, i.e. treated as stated but no addition of Au-Pd

[2] 2.5wt%Au2.5wt%Pd/G6O activated carbon (Aldrich) calcined at 400°C for 3 hours

[3] 2.5wt%Au2.5wt%Pd/TiO$_2$ (P25, Degussa) calcined at 400°C for 3 hours

[a] Hydrogenation over fresh support

[b] Hydrogenation over once-used support

5.5 Characterisation

To determine the origin of the effect of acid pre-treating the support, we have characterized representative catalysts using X-ray photoelectron spectroscopy (XPS) and scanning transmission electron microscopy (STEM).

5.5.1 XPS

The XPS survey spectra of the G60 carbon (figure 5.11) show that the acid treatment does not affect the overall chemical composition of the support surface.
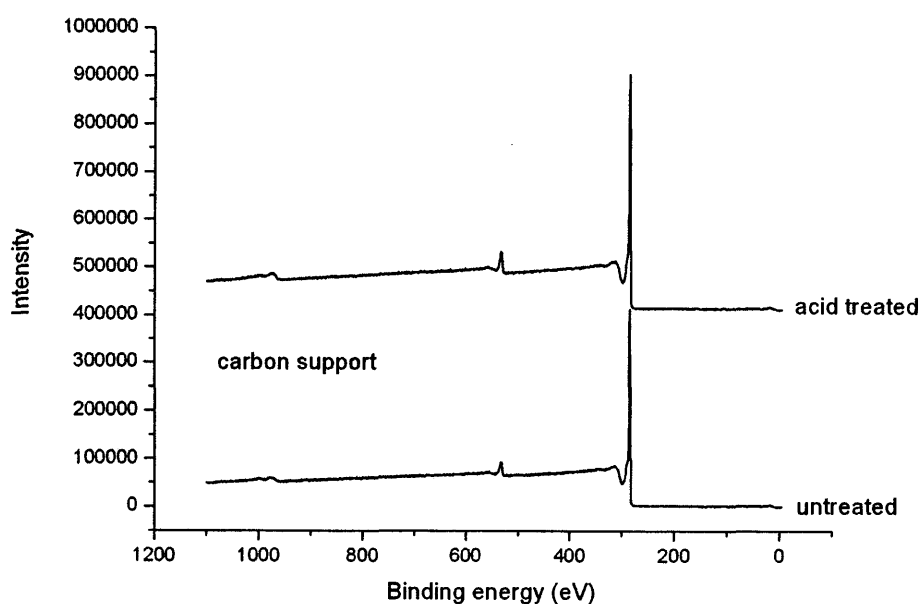

Figure 5.11 XPS survey spectra of treated and un-treated G60 carbon

However, significant differences are observed between the fresh and acid pre-treated supports after impregnation with Au-Pd followed by calcination at 400°C. The surface Pd:Au ratio (figures 5.12 and 5.13) for the calcined Au-Pd/carbon catalyst with the untreated support (Pd:Au = 3.5:1 by weight) is significantly higher than that of the acid pre-treated catalyst (Pd:Au = 1.94:1 by weight).
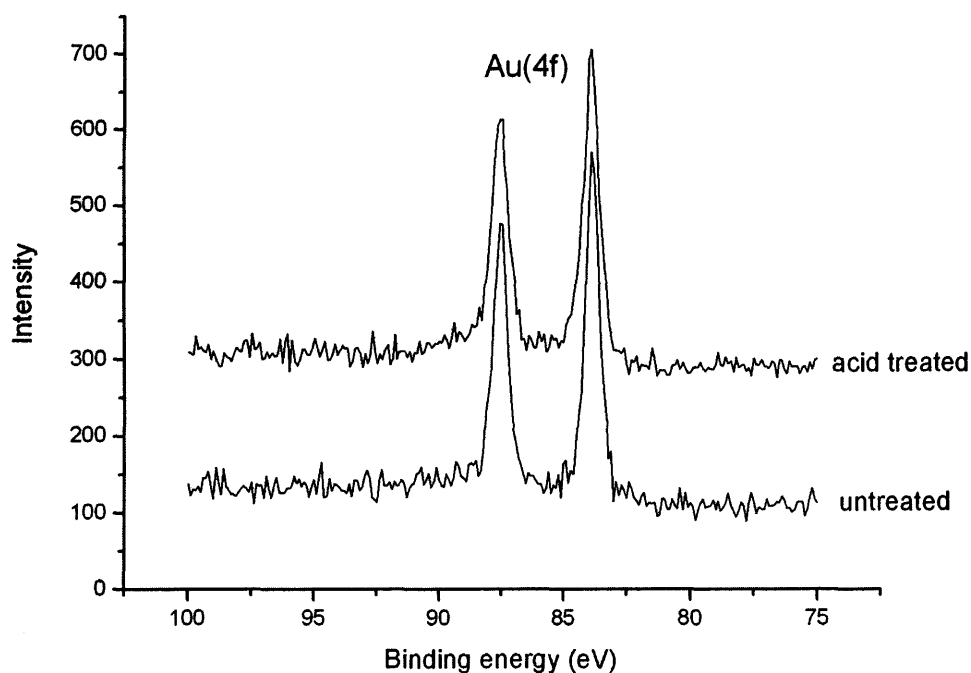
Figure 5.12 Au(4f) spectra for the untreated and acid-treated carbon supported Au-Pd catalyst

In addition, a careful examination of the O(1s) region (figure 5.14, 5.15) reveals a distinct change after acid treatment, since acid treatment leads to the disappearance of a feature at 540 eV binding energy, which has been suggested as arising from either a carboxylic or methoxy species[23].
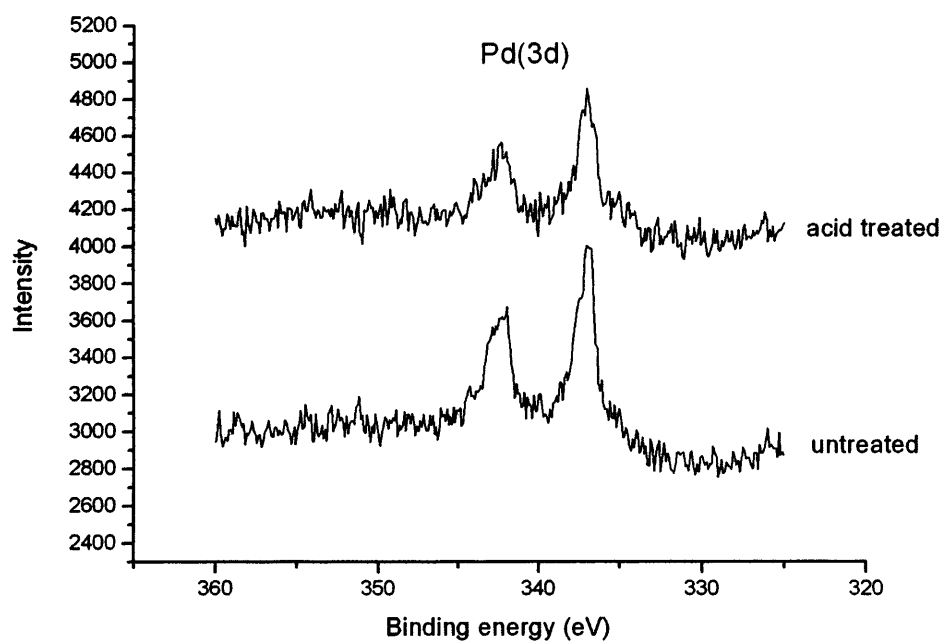
Figure 5.13 Pd(3d) spectra for the untreated and acid-treated carbon supported Au-Pd catalyst.
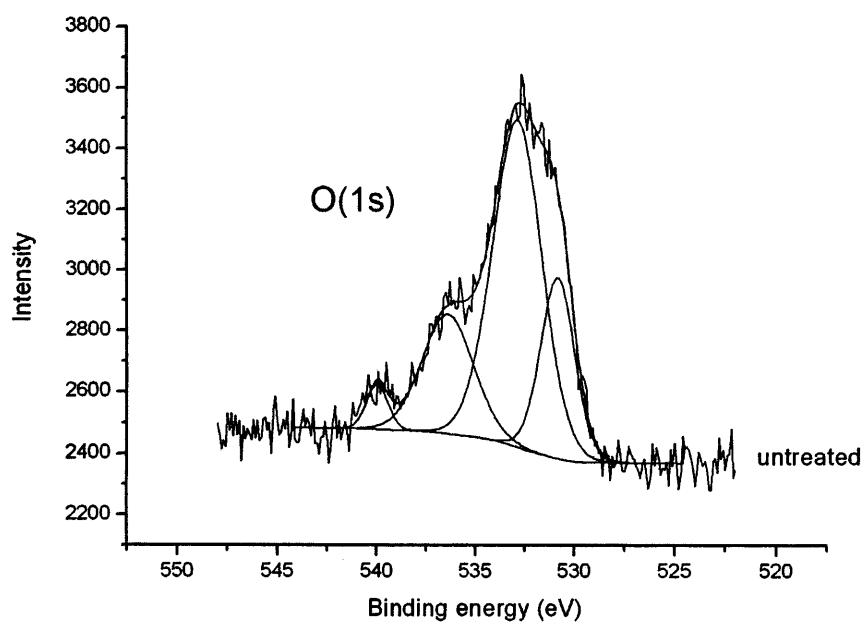

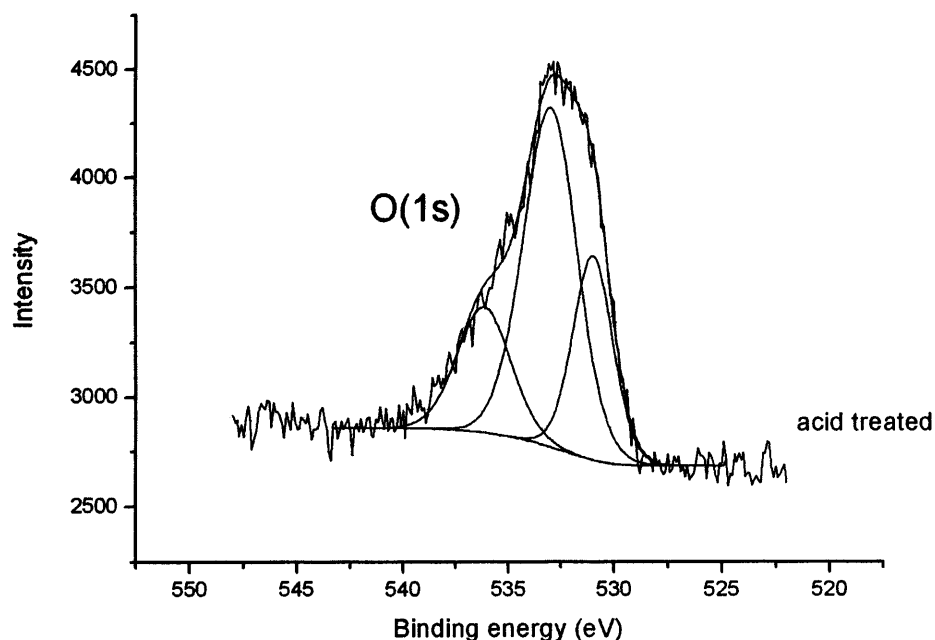Figure 5.14 O(1s) spectrum for the untreated carbon support

Figure 5.15 O(1s) spectrum for the acid treated carbon support

5.5.2 STEM analysis

STEM-annular dark field (ADF) images of the untreated Au-Pd/C sample revealed a tri-modal particle size distribution (Figure 5.16, 5.17).

The smallest particles fell in the 2-5 nm range, intermediate size particles were approximately 10-40 nm in size, while occasional particles were observed exceeding 70 nm. X-ray energy dispersive spectroscopy (STEM-XEDS) spectral images showed that the composition of the metal nanoparticles was size dependent. The intermediate size particles are clearly visible in both the Au M_2 and Pd L_α XEDS maps, indicating that they are Au-Pd alloys, whilst the smaller (2-5nm) particles are only clearly visible in the Pd L_α map. Multivariate statistical analysis (MSA) and colour overlay maps demonstrate that the intermediate scale particles are homogeneous random AuPd alloys.
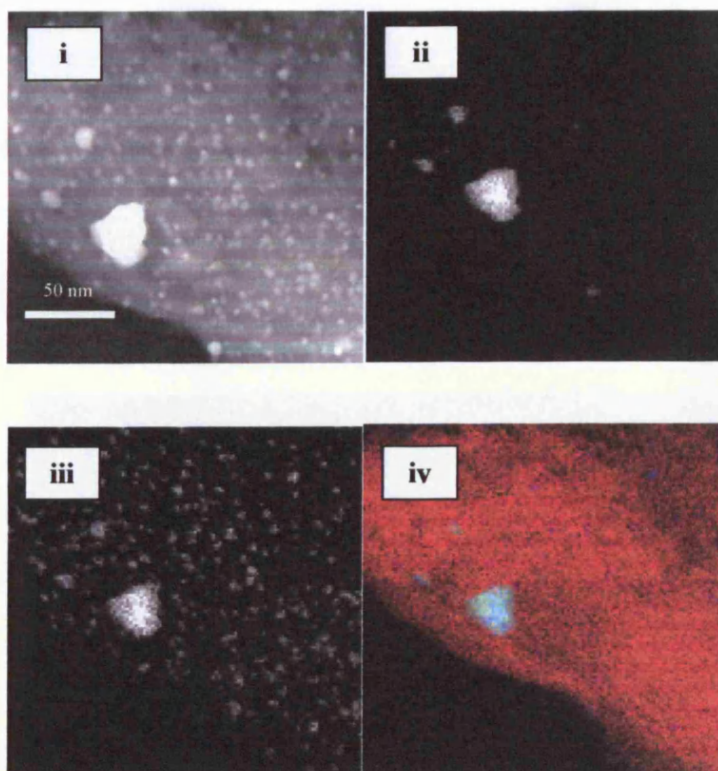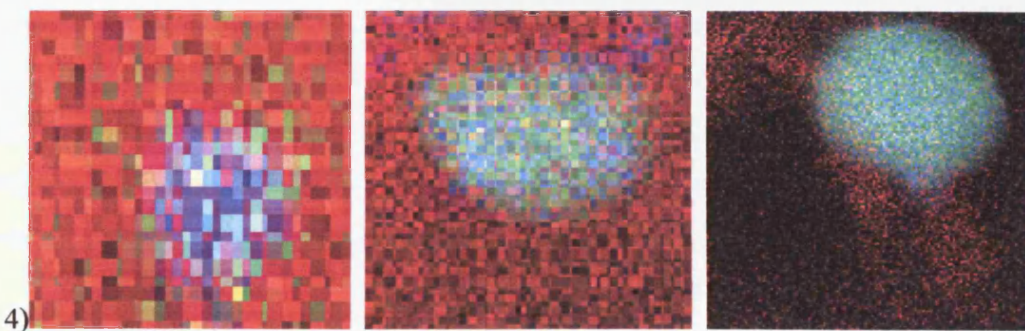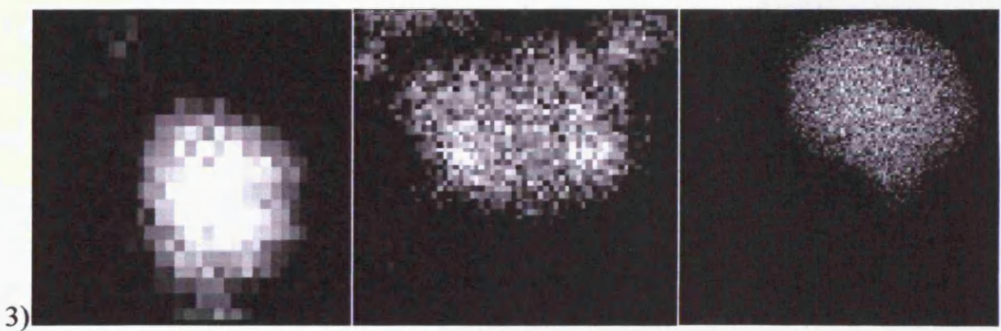
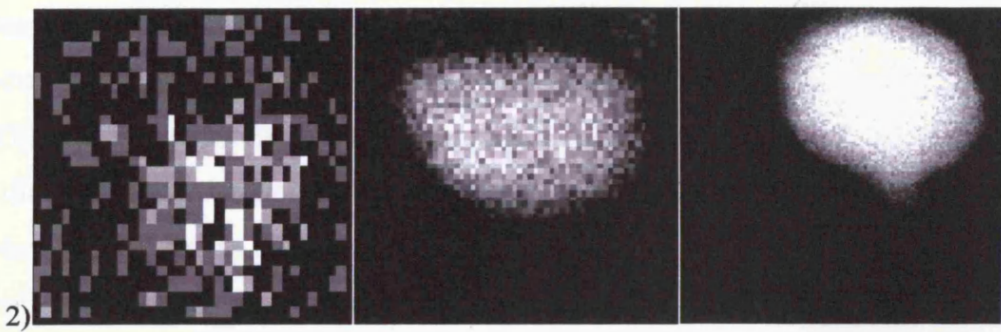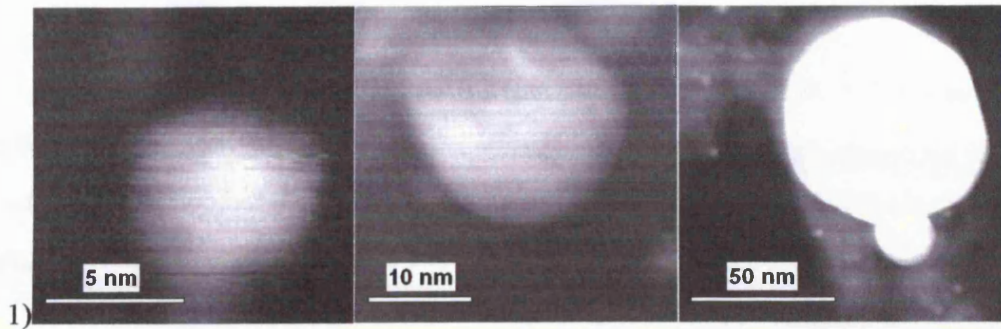Figure 5.16 Untreated Au-Pd/carbon catalyst Montage of i, STEM-ADF image, ii, Au-M_α XEDS map iii, Pd-L_α XEDS Map iv, RGB colour overlay (red = C, green = Au, and blue = Pd). Similar images were obtained for the acid pre-treated samples.

1)

2)

3)

4)

2%Au-98%Pd   **65%Au-35%Pd**   **95%Au-5%Pd**

Figure 5.17 Dependence of alloy composition on particle size in AuPd/carbon catalysts 1) STEM-ADF image 2) Au M_2 XEDS map 3) Pd-Lα XEDS map 4) RGB colour overlay image [red = C, green = Au, and blue = Pd]. The images for the small and intermediate size particles were obtained from acid treated catalysts, and for the large particles from an untreated sample

To investigate the particle size-composition dependence further, a much higher data collection time (350ms per pixel) was employed, in order to improve the counting statistics. Figure 5.17 shows a matrix of ADF images, Au M_2 and Pd L$_\alpha$ XEDS maps, and RGB overlay for typical particles in the small (5nm), intermediate (18nm) and large (70nm) size ranges. By comparing the relative intensities of the Au M_2 and Pd L$_\alpha$ maps, it is qualitatively clear that all the particles are Au-Pd alloys, but as the particle size increases the Pd-to-Au ratio decreases. The colour (Pd-blue, Au-green, C-red) overlay images also reflect this trend since they show a gradual change of colour from blue to green with increasing particle diameter. Quantitative analyses show the small, intermediate and large particles to have compositions of 98:2, 35:65 and 5:95 expressed in wt%Pd: wt%Au. The intermediate size particles are the closest to the nominal Au:Pd (1:1) composition, whereas the smallest particles are in fact a very dilute alloy of Au in Pd. Simple estimates based on a hemispherical Au-Pd particle of 5nm diameter and 98wt% Pd:2wt% Au composition suggest it would contain approximately 1900 Pd and 40 Au atoms.

In contrast, the acid pre-treated AuPd/C sample exhibited only the small (2-5nm) and intermediate (10-50nm) size AuPd alloy particles of similar composition and morphology (*i.e.* random homogeneous alloy) to those observed in the untreated sample. Furthermore no Au-Pd particles greater than 50nm were found.

5.6   Discussion

5.6.1   Catalyst preparation and stability.

Acid pre-treatment of titania, carbon and silica supports prior to metal impregnation of Au and Pd leads to an increase in H_2O_2 synthesis and H_2 selectivity, in comparison to catalysts prepared in the same way without pre-treatment. The beneficial effect of washing the support in $2\%HNO_3$ was investigated-higher HNO_3 concentrations did not further activate the catalyst, an Au-Pd catalyst pre-treated in 60% HNO_3 has the same activity as the $2\%HNO_3$ pre-treated catalyst. Acid pre-treatment in other acids (HCl, H_3PO_4) also induce this beneficial effect, although not to the same extent as HNO_3. An Au-Pd catalyst prepared with carbon pre-treatedwith $2\%NH_4OH$ was much less active for H_2O_2 synthesis, indicating that it is the acid that is important. In order to determine whether the increased activity was a "nitrate effect"; (this is observed with CO oxidation[12]), the standard G60 carbon was washed with 2% NH_4NO_3 then impregnated with Au and Pd. This catalyst had the same activity as the untreated catalyst, suggesting that the increase in activity was not due to nitrate promotion. The precise manner in which the support is pre-treated is also vital for the promoted activity of the catalysts-addition of HNO_3 during the impregnation step did not result in an increase in activity, and addition of HCl was deleterious. Treatment of the catalyst after metal deposition in-situ during the reaction resulted in a catalyst that was extremely active for its first use, however without further addition of acid in the reaction the activity of the catalyst falls to that of an untreated catalyst. AAS of the G60 support showed significantly lower Na and K levels in the support after acid washing. Doping the support with Na and K did not result in a less active catalyst-indicating that the removal of these species was in no way beneficial.

The acid treated catalysts were analysed by STEM analysis to attempt to identify the nature of the pre-treatment. This analysis showed that the treated TiO_2 catalysts adopt a core-shell structure, where a Pd-rich shell surrounding an Au-rich core was found after calcination at 400°C, as does the untreated catalyst. However,

the carbon supported catalysts exist as random alloys, in direct contrast to similar sized Au-Pd particles supported on TiO$_2$. Hence the enhancement in activity observed with acid pre-treatment is not due to the specific morphology of the Au-Pd alloys.

A significant difference found in the number distribution of small and intermediate size particles is illustrated in the histograms presented in Figure 5.18. Acid pre-treatment of the support improves nanoparticle nucleation for the Au-Pd catalyst and favours the formation of a significantly greater fraction of small 2-5nm particles at the expense of the intermediate and large particles. This is consistent with the increased surface Au content determined from XPS (figure 5.12).
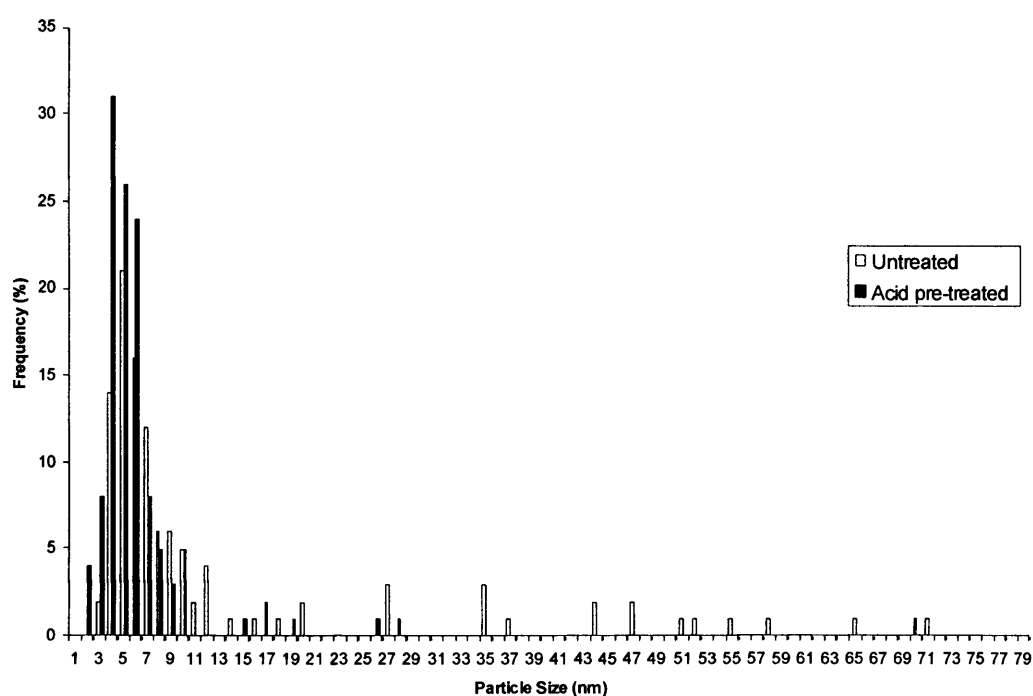

Figure 5.18 Particle size distribution of alloy particles for the untreated and acid pre-treated Au-Pd/carbon catalysts from STEM.

Figure 5.18 clearly shows that the tendency for acid pre-treatment to shift the Au-Pd particle size distribution towards the lower end of the size scale. Occasionally particles of 50-100nm diameter were observed in the untreated sample, which have

been omitted from this histogram; these large particles were not observed with the pre-treated catalyst.

Similar quantitative analyses were completed for the Au and Pd only catalysts, the results of which are shown in figure 5.19. The most striking difference between these histograms is the acid pre-treatment shifts the Au particle size distribution towards the lower end of the size scale, **which is not seen for the Pd only catalysts**.

On the basis of this it seems that the beneficial effect of acid pre-treatment is to enhance the gold dispersion in the bimetallic alloy particles by generating smaller Au-Pd nanoparticles. This hypothesis as strengthened by the fact that there is a similar effect for pure Au/carbon catalysts where the acid pre-treatment decreases the average Au particle size (figure 5.19), in contrast to the Pd catalyst where no such dispersion effect is observed (figure 5.19) which is consistent with the lack of enhancement in the catalytic performance (Table 5.1).

From these observations it seems that the smaller Au-Pd particles observed after acid washing result in the catalyst being highly active for H_2O_2 synthesis, due to the smaller particles being less active for H_2O_2 hydrogenation. This is further illustrated by increased activity of the 2.5wt%Au-2.5wt%Pd/TiO_2 catalyst being more active at room temperature than at 2°C, in comparison to the untreated catalyst which is less active at elevated temperatures. The effect of the acid pre-treatment seems to be to stabilise the H_2O_2 as its produced, so it is not subject to further hydrogenation. Another point, which illustrates the ability of the catalyst to stabilise H_2O_2 *in-situ*, is the gas top-up experiments shown in figure 5.10. It is clear from these data that the acid pre-treated catalyst has the ability to produce more concentrated H_2O_2 solutions than the untreated catalyst, due to the stabilising nature of the catalyst.
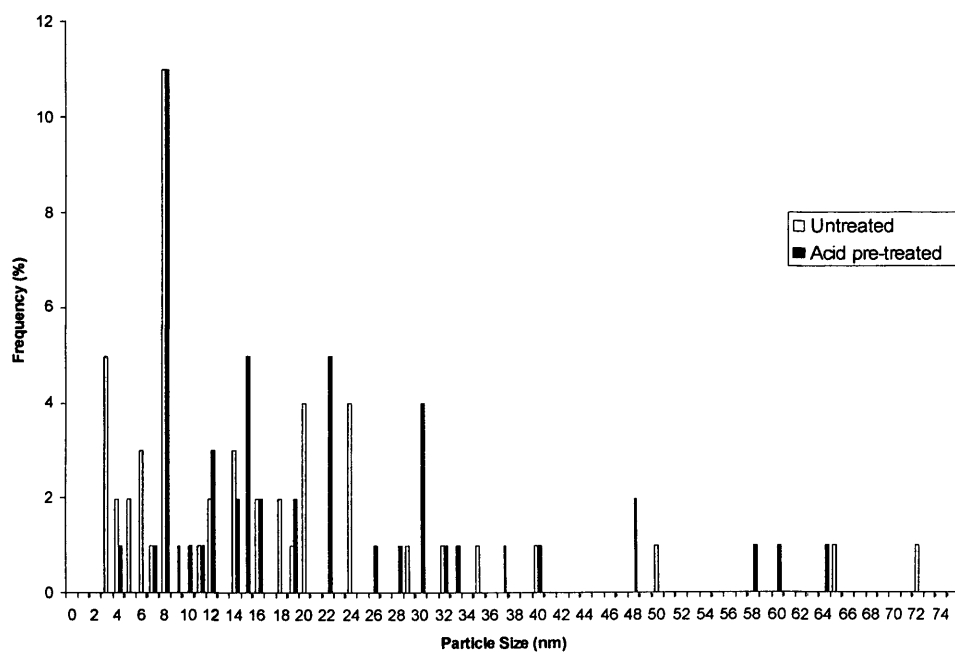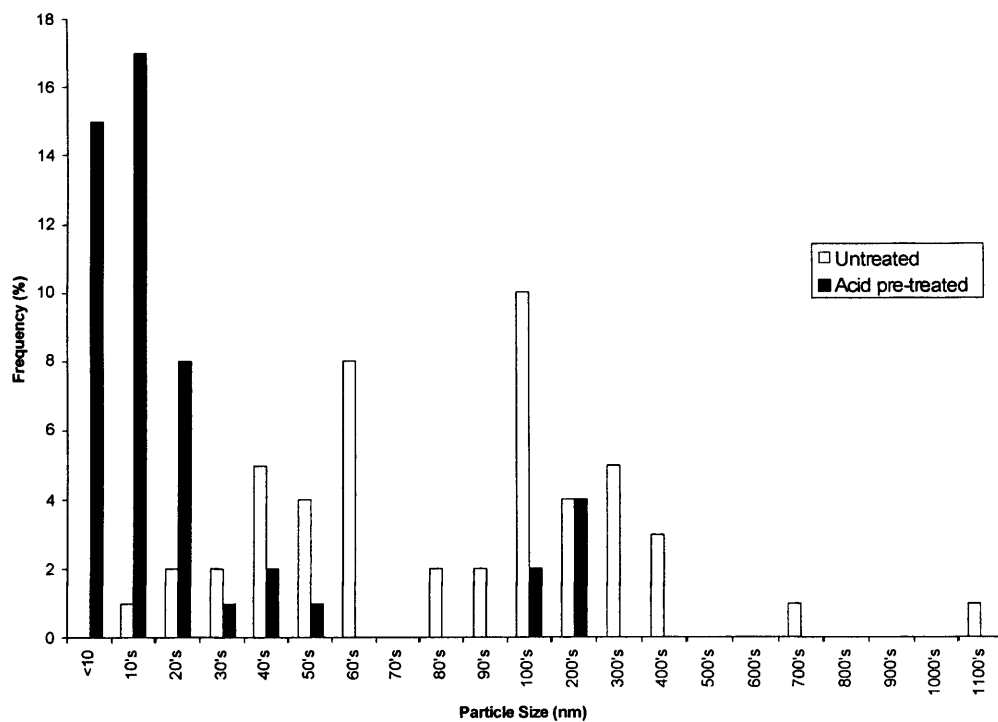
Figure 5.19 Particle size distribution of Au (top) and Pd (bottom) particles for the untreated and acid pre-treated monometallic carbon supported catalysts

Another point that needs to be addressed is why the acid pre-treatment results in more active catalysts. It is possible that the acid pre-treatment leads to the formation of sites that the Au and Pd will preferentially nucleate on during calcination, leading to a higher dispersion of smaller particles. Alternatively, the pre-treatment blocks sites active for hydrogenation which is consistent with the data for hydrogenation over bare supports-both the acid pre-treated TiO_2 and G60 carbon show much less hydrogenation activity than the untreated supports.

Acid pre-treatment of supports in the preparation of supported Au-Pd catalysts provides a general enhancement in the H_2O_2 yield by a factor of *ca.* 6 compared with comparable Pd-only catalysts. The catalysts are fully stable and re-usable without any significant loss of catalyst performance. The acid pre-treatment stabilizes H_2O_2 with respect to subsequent hydrogenation, and enhances the synergy observed between Au and Pd in the alloy nanoparticles. In this way higher reaction temperatures can be used and the rates and selectivities obtained are markedly higher than those observed for the current commercial indirect process[13] or any previously reported catalysts for the direct process [4, 8, 14],[10, 11, 15-20]-13. These results could provide the basis for the development of a new green technology for the synthesis of this important commodity chemical using intrinsically safe non-explosive conditions.

5.7   Conclusions

Acid pre-treatment of support prior to metal impregnation was explored for the synthesis of Au, Au-Pd and Pd catalysts for the direct synthesis of H_2O_2 from H_2 and O_2 in a stirred autoclave.

I)   Pre-treatment of a supports prior to metal impregnation leads to highly active and selective Au-Pd catalysts for H_2O_2 synthesis

II)   This increase in activity is not affected by HNO_3 concentration, low concentrations (2%) can be used to good effect.

III)   Pre-treatment with HCl and H_3PO_4 also leads to more active catalysts, whereas washing with NH_4OH is deleterious.

IV)   Doping with NO_3, K or Na does not bring about an increase in activity.

V)   Pre-treating SiO_2 brings about synergy for Au-Pd catalysts not seen without this pre-treatement.

VI)   Pre-treated catalysts are less active for H_2O_2 hydrogenation than the untreated catalysts, as are the treated bare supports.

VII)   Au-Pd pre-treated catalysts can be used to obtain higher H_2O_2 concentrations than untreated Au-Pd or treated Pd catalysts due to increased stability of H_2O_2 *in situ.*

VIII)   Acid pre-treatment coincides with a decrease in Au-Pd particle distribution and higher dispersion, which is also seen for Au only catalysts but not Pd only catalysts.

5.8 References

[1] V. R. Choudhary, C. Samanta, P. Jana, (Council of Scientific & Industrial Research, India). Application:US, **2006**, p. 10 pp.

[2] G. Paparatto, G. De Alberti, R. D'Aloisio, (ENI S.p.A., USA; Polimeri Europa S.p.A.). Application:WO, **2002**, p. 27 pp.

[3] H. A. Huckins, (Princeton Advanced Technology, Inc., USA). Application: US, **1997**, pp. 9 pp.

[4] J. Van Weynbergh, J. P. Schoebrechts, J. C. Colery, (Interox International S.A., Belg.). Application: WO, **1992**, p. 19 pp.

[5] http://www.chemie.de/news/e/44266/.

[6] B. Bertsch-Frank, I. Hemme, L. Von Hippel, S. Katusic, J. Rollmann, (Degussa-Huels AG, Germany). Application:DE, **2000**, p. 10 pp.

[7] B. Bertsch-Frank, T. Balduf, C. Becker-Balfanz, I. Hemme, J. Rollmann, R. Schuette, W. Wildner, (Degussa-Huels A.-G., Germany). Application: DE, **1999**, p. 8 pp.

[8] J. K. Edwards, B. E. Solsona, P. Landon, A. F. Carley, A. Herzing, C. J. Kiely, G. J. Hutchings, *Journal of Catalysis* **2005**, *236*, 69.

[9] B. E. Solsona, J. K. Edwards, P. Landon, A. F. Carley, A. Herzing, C. J. Kiely, G. J. Hutchings, *Chemistry of Materials* **2006**, *18*, 2689.

[10] P. Landon, P. J. Collier, A. F. Carley, D. Chadwick, A. J. Papworth, A. Burrows, C. J. Kiely, G. J. Hutchings, *Physical Chemistry Chemical Physics* **2003**, *5*, 1917.

[11] P. Landon, P. J. Collier, A. J. Papworth, C. J. Kiely, G. J. Hutchings, *Chemical Communications (Cambridge, United Kingdom)* **2002**, 2058.

[12] B. Solsona, M. Conte, Y. Cong, A. Carley, G. Hutchings, *Chemical Communications (Cambridge, United Kingdom)* **2005**, 2351.

[13] H. T. Hess, *Kirk-Othmer Concise Encyclopedia of Chemical Technology, 4th Edition, Vol. 13*, Wiley, **1995**.

[14] J. K. Edwards, B. Solsona, P. Landon, A. F. Carley, A. Herzing, M. Watanabe, C. J. Kiely, G. J. Hutchings, *Journal of Materials Chemistry* **2005**, *15*, 4595.

[15]   H. Henkel, W. Weber, US, **1914**.

[16]   B. Zhou, L.-K. Lee, (Hydrocarbon Technologies, Inc., USA). Application: US, **2001**, p. 11 pp.

[17]   L. Gosser, (du Pont de Nemours, E. I., and Co., USA). Application: JP JP, **1988**, p. 17 pp.

[18]   V. R. Choudhary, C. Samanta, A. G. Gaikwad, *Chemical Communications (Cambridge, United Kingdom)* **2004**, 2054.

[19]   D. P. Dissanayake, J. H. Lunsford, *Journal of Catalysis* **2003**, *214*, 113.

[20]   D. P. Dissanayake, J. H. Lunsford, *Journal of Catalysis* **2002**, *206*, 173.

Chapter Six

Chapter 6 : General Discussion, Conclusions and Future Work

6.1   General discussion and conclusions

It is clear from the work outlined in the preceding chapters that the direct synthesis of hydrogen peroxide form hydrogen and oxygen using supported Au, Pd and Au-Pd catalysts is a complex one, and the conclusions listed at the end of chapters 3 – 5 reflect this.

In the case of Al_2O_3, Fe_2O_3 TiO_2 and activated carbon supported catalysts the formation of hydrogen peroxide is higher using supported Au-Pd catalysts than the Pd only catalysts. This discovery is unprecedented, as the majority of the literature dealing with the direct synthesis reaction lean towards the use of Pd catalysts. The Au-Pd catalysts described previously all display higher selectivity towards H_2O_2 than the corresponding Pd catalysts, which follows with the observation previously that Au catalysts are very good for selective oxidation reactions. Thus, combination of Au with Pd (supported Pd generally display high conversion to H_2O_2 but are relatively unselective) leads to the formation of very active, selective catalysts. The nature of this phenomenon is relatively complex, as with the oxide supported catalysts a core-shell structure forms on calcination (consisting of a Pd shell surrounding an Au core) and this initially was thought to be responsible for the synergistic effect. However, the synergy is also observed for carbon supported Au-Pd catalysts, and in this case the Au-Pd exists as a homogenous alloy.

The SiO_2 catalyst initially did not display this synergy for Au-Pd catalysts, and STEM images showed that the Au-Pd system was very complex. The highly dispersed Pd found on the silica could be responsible for this observations, however it is not clear from the studies carried out why the Pd particles segregated in this manner. As detailed in chapter 5, silica pre-treatment with a dilute acid led to Au-Pd catalysts more active than the Pd analogue. Indeed, this acid pre-treatment led to an increase in activity for Au-Pd catalysts supported on TiO_2 and activated carbon. The hydrogenation activity (H_2O_2 + H_2 → H_2O_2) of the pre-treated catalysts was much lower than the untreated catalysts, suggesting that the acid poisons the sites

responsible for H_2O_2 hydrogenation. STEM analyses of the pre-treated catalysts showed that there is a change in particle size distribution – with smaller Au-Pd particles in the pre-treated samples. This indicates is that these smaller particles are either more active for the direct synthesis of H_2O_2 or less active for their decomposition. However, as the acid pre-treated supports are less active for hydrogenation than the untreated there must indeed be a chemical change in the support, which has not been observed in the characterisation techniques employed thus far.

Another question that arises from the studies carried out is why different oxides produce catalysts, with identical Au-Pd loadings, that have markedly different activity. This may be explained by looking at the iso-electric point (IEP) of the support. When the IEP of the support is plotted against Au-Pd catalyst activity an interesting trend is observed – catalysts with lower IEP have higher activity for H_2O_2 synthesis. This is shown in figure 6.1
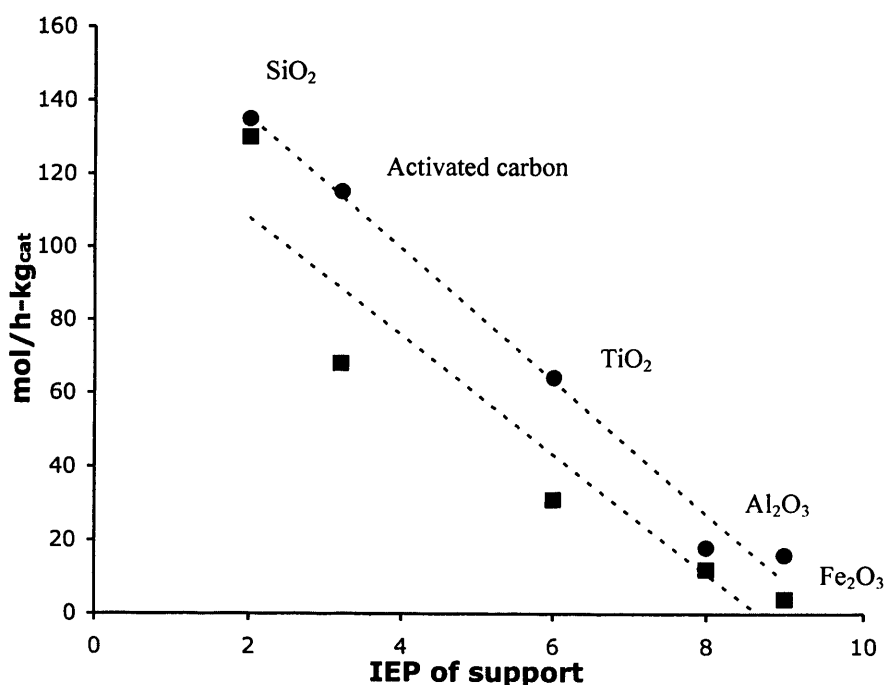

Figure 6.1 Effect of the isoelectric point of the support on the corresponding 2.5wt%Au-2.5wt%Pd (●) and 5wt%Pd (■) catalyst activity for H_2O_2 synthesis.

IEP determined from literature values[1-3]. Catalysts calcined in air at 400°C and tested for H_2O_2 synthesis under the standard reaction conditions detailed in chapter 2.

From these results it is very clear that there is a correlation between the IEP of the support and the activity of the resultant catalyst, for Au-Pd and Pd catalysts. The preparation activity testing for the catalysts is identical. Although the isoelectric points of the resulting catalyst has not been determined, the preparation method is unlikely to have altered this property to a great extent. Hence, I consider that there are two possible explanations for this trend in activity.

1   The impregnation preparation for all catalysts is in aqueous $HAuCl_4$, at a pH lower than that of any of the supports (pH~0). In this highly acidic medium, all of the supports have a net positive charge as support-OH_2^+ species form on the surface. Anions present in the reaction medium (Cl^-) will hence be attracted to the support surface. As all of the metal is incorporated into the catalyst (AAS) the activity could scale with chlorine content on the surface. This could be determined by quantitave XPS analysis of the surface species.

2   The pH of the reaction medium is constant (7) for all of the synthesis reactions. Hence, *in situ* the catalysts will have either a net positive charge or negative charge depending on their isoelectric points. The Au-Pd catalysts displaying the highest activity for H_2O_2 synthesis (TiO_2, carbon, titania) all have low isoelectric points and will thus display a net negative charge on the surface during the synthesis reaction at pH 7. This net negative charge could have a stabilisation effect on H_2O_2 formed, possibly preventing H_2O_2 decomposition.

If acid pre-treatment changes the isoelectric point of the support, the origin of the increased activity may lie in either of these observations.

Systematic studies also showed that direct synthesis reaction is influenced by the reaction conditions under which the synthesis is achieved. Long reaction times (>30 mins) led to a drastic decrease in catalytic activity as hydrogen peroxide

decomposition becomes prevalent. However, at short reaction lengths (2 minutes) the activity of the catalyst can be as high as 900mol/h-kg$_{cat}$ and these high initial activities can be utilised for the in-situ oxidation of a suitable substrate like benzyl alchohol.

Another factor influencing the formation of H$_2$O$_2$ is the composition of the solvent. Initial experiments using water showed that the activity of several different catalysts was the same, indicating diffusion limitations within the system. However, observations using varying catalytic masses indicated that the water system was not mass transport limited, rather the solubility of the gases is much lower in water as opposed to water : methanol.

6.2 Future work

a) Diversification of the preparation method

The particle size distribution of Au nano-crystals in a supported gold catalyst is highly dependant on the method by which it was prepared. This research has been primarily focussed on the optimisation and study into the direct reaction using Au-Pd catalysts prepared by impregnation, which results in large particle sizes. Utilising methods like sol gel immobilisation and deposition precipitation and investigating the Au-Pd particle size dependence on catalyst activity would be useful in elucidating whether the large (60nm) Au-Pd particles observed on Al$_2$O$_3$ or the small Au-Pd particles (10nm) on acid pre-treated carbon are responsible for the synthesis. This would help with the design of active catalysts if this reaction were to be industrialised, and may also lead to the development of active catalysts with lower Au and Pd loadings.

b) *In-situ* utilisation of hydrogen peroxide produced

The Au-Pd/TiO$_2$ catalysts have been shown to be effect for the *in-situ* oxidation of benzyl alcohol to benzaldehyde. This could be a very effective way of utilising the H$_2$O$_2$ and maintaining the high initial rates of formation of the catalyst.

c) Further investigation in to the nature of the support pre-treatment

Although it is clear from the STEM of the pre-treated catalysts that the acid washing of the support leads to a size decrease in the average Au-Pd particle, the reasons for this are still unclear. Quantitiave XPS analysis may help to elucidate the role of chloride ions in the catalytic activity.

6.3   References

[1]   K. Bourikas, C. Kordulis, A. Lycourghiotis, *Environmental Science and Technology* **2005**, *39*, 4100.

[2]   S. Kittaka, *Journal of Colloid and Interface Science* **1974**, *48*, 327.

[3]   M. A. Fraga, E. Jordao, M. J. Mendes, M. M. A. Freitas, J. L. Faria, J. L. Figueiredo, *Journal of Catalysis* **2002**, *209*, 355.

Chapter Seven

Chapter 7 : Appendix

7.1   List of publications arising from this work

[1]   G. J. Hutchings, S. Carrettin, P. Landon, J. K. Edwards, D. Enache, D. W. Knight, Y.-J. Xu, A. F. Carley, Topics in Catalysis 2006, 38, 223.

[2]   G. Li, D. I. Enache, J. Edwards, A. F. Carley, D. W. Knight, G. J. Hutchings, Catalysis Letters 2006, 110, 7.

[3]   G. Li, J. Edwards, A. F. Carley, G. J. Hutchings, Catalysis Today 2006, 114, 369.

[4]   B. E. Solsona, J. K. Edwards, P. Landon, A. F. Carley, A. Herzing, C. J. Kiely, G. J. Hutchings, Chemistry of Materials 2006, 18, 2689.

[5]   D. I. Enache, J. K. Edwards, P. Landon, B. Solsona-Espriu, A. F. Carley, A. A. Herzing, M. Watanabe, C. J. Kiely, D. W. Knight, G. J. Hutchings, Science (Washington, DC, United States) 2006, 311, 362.

[6]   J. K. Edwards, B. Solsona, P. Landon, A. F. Carley, A. Herzing, M. Watanabe, C. J. Kiely, G. J. Hutchings, Journal of Materials Chemistry 2005, 15, 4595.

[7]   J. K. Edwards, B. E. Solsona, P. Landon, A. F. Carley, A. Herzing, C. J. Kiely, G. J. Hutchings, Journal of Catalysis 2005, 236, 69.